NASA CONTRACTOR REPORT

NASA CR-2774
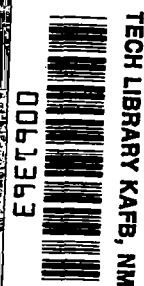
N.A.S.A. CR-2

PREDICTION OF LIGHT AIRCRAFT HORIZONTAL TAIL ONSET FLOWS - A REVIEW AND ANALYSIS

Delbert C. Summey and Frederick O. Smetana

Prepared by
NORTH CAROLINA STATE UNIVERSITY
Raleigh, N.C. 27607
for Langley Research Center

NATIONAL AERONAUTICS AND SPACE ADMINISTRATION • WASHINGTON, D. C. • APRIL 1977

0061363

1. Report No. NASA CR-2774	2. Government Accession No.	3. Recipient

4. Title and Subtitle PREDICTION OF LIGHT AIRCRAFT HORIZONTAL TAIL ONSET FLOWS- A REVIEW AND ANALYSIS	5. Report Date APRIL 1977
	6. Performing Organization Code

7. Author(s) Delbert C. Summey and Frederick O. Smetana	8. Performing Organization Report No.
	10. Work Unit No. 505-10-11-03

9. Performing Organization Name and Address Department of Mechanical and Aerospace Engineering North Carolina State University Raleigh, North Carolina	11. Contract or Grant No. NSG 1077
	13. Type of Report and Period Covered Contractor Report

12. Sponsoring Agency Name and Address National Aeronautics and Space Administration Washington, DC 10546	14. Sponsoring Agency Code

15. Supplementary Notes

Langley Technical Monitor - Harold L. Crane   Topical Report

16. Abstract

Analytical methods presented in the literature for the determination of onset flow in the vicinity of the horizontal tail of light aircraft are reviewed. The theoretical basis of the two computer programs (WASH and WAKE) are then developed in detail. WASH calculates the location of wake-sheet streamlines behind the wing, and upwash and downwash angles ahead of and behind the wing, respectively. WAKE computes two-dimensional velocity profiles along the wake streamlines given the upper and lower surface velocity profiles at the wing trailing edge. Comparisons with experiment indicate good agreement for wake location, downwash angles, and two-dimensional velocity profiles at low to moderate angles of attack. Also included is a discussion on the adptation of the results of the two programs to predict the total onset flow at the tail.

17. Key Words (Suggested by Author(s)) Onset flow at horizontal tail Wake location, and velocity profiles Downwash angles WAKE and WASH computer programs	18. Distribution Statement Unclassified - Unlimited Subject Category 02

19. Security Classif. (of this report) Unclassified	20. Security Classif. (of this page) Unclassified	21. No. of Pages 128	22. Price* $5.75

TABLE OF CONTENTS

LIST OF FIGURES

LIST OF FIGURES (Continued)

NOMENCLATURE

A_n —   constants used to represent the Γ distribution in the downwash section.

$\bar{a}$ —   vector from a vortex filament to a point in space.

b   —   wing span in downwash section or wake width in boundary layer section.

C_D —   wing drag coefficient.

C_L —   wing lift coefficient.

c   —   wing chord.

c_d —   wing section drag coefficient.

c_ℓ —   wing section lift coefficient.

c_1 —   eddy viscosity parameter in boundary layer solution.

D   —   total drag.

d   —   cylinder diameter in boundary layer section.

d_o —   profile drag per unit wing span.

$f(\xi, \eta)$ —   function of ξ and η which will appear as the unknown in the transformed boundary layer equations.

H   —   turbulent boundary layer form factor.

h   —   cylinder length in boundary layer section or perpendicular distance from the point of interest to vortex filament in downwash section.

$\bar{\ell}$ —   vector having direction of infinitesimal vortex filament.

m   —   streamwise index in boundary layer finite difference solution.

m_o —   wing section lift curve slope.

n   —   normal index in boundary layer finite difference solution.

q   —   dynamic pressure.

T   —   unknown in finite difference boundary layer recursive relation.

t   —   wing thickness.

NOMENCLATURE (Continued)

U   — freestream velocity in boundary layer section.

u   — induced freestream velocity component in the downwash section or velocity component parallel to streamline direction in boundary layer section.

V   — freestream velocity vector in downwash section.

v   — induced spanwise velocity vector in downwash section or normal velocity.

W   — total velocity induced at a point by a vortex.

w   — induced total velocity vector in general downwash section or induced vertical velocity component.

x   — freestream coordinate in downwash section or streamline coordinate in boundary layer section..

y   — spanwise coordinate in the downwash section or normal coordinate in boundary layer section.

z   — vertical coordinate in the downwash section.

α — angle of attack.

Γ — strength of the bound vortex at any wing section.

ϵ — downwash angle in downwash section or eddy viscosity in boundary layer section.

ζ — nondimensional wake width.

η — nondimensional normal coordinate in boundary layer section or normalized loss of wake dynamic pressure.

Λ — sweep angle.

ξ — nondimensional distance behind wing trailing edge.

ρ — density of air.

τ — turbulent shearing stress.

ψ — two-dimensional stream function.

∞ — subscript denoting freestream conditions.

INTRODUCTION

The primary function of an aircraft's horizontal tailplane is to balance the pitching moment which arises when the lift force developed by the wing is not applied through the airplane's center of gravity. Control of the airplane in the vertical plane is accomplished by varying this balancing moment so that the wing seeks a new equilibrium lift. The size of the horizontal tail thus determines the allowable c.g. travel as well as the lift coefficient which can be generated at any time. One does not gain a higher degree of control capability, however, without accepting at the same time a performance decrement resulting from the higher drag of the larger surface.

Since the advent of the airplane, designers have pondered the problem of positioning and sizing the horizontal tail to achieve both good aircraft performance and acceptable longitudinal stability and control. Their problem is compounded by the passage of the wing through the air ahead of tail. This produces (1) a downward inclination or downwash in the air approaching the tail, and, if the tail is directly in the wing wake, (2) a lower velocity at the tail due to the wing drag force. If the tail is sized assuming the onset flow to be freestream but is instead immersed in the wing wake, it will be unable to generate the expected trim moment. Thus, to maintain control capability one must either locate the tail such that it never encounters such momentum deficiencies or else increase its size proportional to the kinetic energy deficiency actually encountered. The latter course entails a performance penalty. Because of the non-linear response of the tailplane to onset flow angle, it is important to know the local flow direction everywhere in the tail region as well as those areas where momentum deficiencies exist. One would like to predict the wake location and the velocity deficit in the region of the horizontal tail to facilitate the process of positioning and sizing.

As part of its program to provide technical support to the light aircraft industry and to aeronautical education in general, the National Aeronautics and Space Administration funded the present study at North Carolina State University. This work seeks to provide rigorous, easy-to-use methods (which now means computer programs) to predict the downwash and velocity profiles in the vicinity of the horizontal tailplane as well as detailed descriptions of the methods used, their historical antecedents, and some worked out examples. The study is thus analogous to previous studies (Ref. 1,2,3,4) which treat riding and handling qualities, aircraft performance, and wing and body lift and drag in a similar fashion.

As will become evident from the literature review, the procedures for estimating downwash angle and wake position are better-defined than those for estimating wake velocity profiles. The downwash calculation is usually approached by replacing the wing with a series of horseshoe vortices representing both the wing lift and the vorticity shed by the wing. The downwash is a result of the interaction of the flow due to these horseshoe vortices with the freestream flow. It is most intense in a curved plane emanating from the trailing edge of the wing. The locus of this plane is usually obtained by integrating the local downwash angle from the wing trailing edge to some downstream point of interest. More rigor may be added to this method by permitting the trailing vortices to deflect both spanwise and vertically so that their paths become streamlines. These streamlines then define the wake centerline position. This approach permits both upwash ahead of the wing and downwash behind to be calculated with a greater degree of accuracy than does the more conventional straight vortex method. The downwash computer program presented in this report employs the deflected vortex approach.

Since the purpose of the present work is to provide a rigorous yet relatively simple method for determining the <u>onset flow in the immediate neighborhood of the horizontal tail</u>, it is not necessary to continue the calculation beyond this region to the point where the trailing vortices rollup into the familiar vortical flow patterns observed far downstream of the aircraft. While the method employed herein can treat the inviscid flow aspects of this region satisfactorily, other simpler methods are entirely adequate for developing the essential features of this "far field" problem; further, the method used here to determine the viscous dissipation present about the wake centerline is valid only in regions of quasi-planar flow, certainly not in vortical flow regions. For this reason also, no attempt should be made to extend the calculation downstream beyond the region of the horizontal tail.

The perceptive reader will note that no mention is made in the ensuing pages of the obvious contributions of the fuselage, both viscous and inviscid to the character of the flow field downstream of the wing. While the downwash method used does include a treatment of the effects of fuselage interference on the wing lift distribution, it does not include the effect of diminishing fuselage size as one moves aft on the downwash field nor the effects of the rapidly growing boundary layer on the aft fuselage. These were regarded as small perturbations whose determination would be excessively difficult given presently available analytical tools; for this reason they are not included. The user must therefore consider this fact in applying the results to new design situations.

Another contribution which has been neglected in the computation is the modification in the wing's downwash field due to the upwash field of the horizontal tail. Since the upwash angles are inherently smaller than the downwash angles and since the tail lift is generally less than 1/5 the wing lift, this contribution has been neglected.

2

The method used herein is based on the lifting line representation of the wing; it is therefore applicable only to situations where the wing is of moderate-to-high aspect ratio, unswept, and relatively lightly loaded (the fuselage does not cover a very significant portion of the wing area). Situations where these conditions are not satisfied will usually demand a much more complex lifting surface treatment.

Another consequence of the lifting line representation is that the induced field in the immediate neighborhood of the wing is distorted by the concentration of the wing's bound vortices along a single line instead of being distributed over the whole surface. Thus the downwash and upwash angles in this region may be excessive while at greater distances they will be indistinguishable from those obtained from a lifting surface representation. Since, the region of interest in light aircraft is located more than 1.5 wing chords downstream of the wing's trailing edge, a lifting line representation should be quite adequate.

The variation in flow velocity as one moves vertically across the wing plane of symmetry is usually approximated by empirical relations derived from experimental data given the wing section drag coefficient and the distance behind the wing trailing edge. A more exact approach solves the two-dimensional boundary layer equations, using a finite difference technique, for the wake flow and then applies this solution along various streamlines displaced spanwise as given by the wake position procedure above. The result is a quasi-three-dimensional solution. The starting conditions for the integration are the viscous velocity profiles on both upper and lower wing surfaces. This approach is used here to determine the vertical variation in flow magnitude.

The work presented here begins with a two-part review of the pertinent literature dealing with the determination of (1) downwash angles and wake sheet location, and (2) velocity profiles in the wing wake. General theory and discussion of results sections are then presented for both the downwash (WASH) program and the velocity profile (WAKE) program. User instructions, program listings, and sample outputs of both programs are given in the appendices.

LITERATURE REVIEW

DOWNWASH AND WAKE POSITION

In order to estimate the lift and drag forces experienced by an aircraft's horizontal tail, it is imperative that the magnitude and direction of the local onset flow be known. The disturbance produced by the wing is the major contributer to non-uniform horizontal tail onset flows. Dwinnell (Ref. 5) points out that a wing generating a lifting force must have a pressure differential from the lower to the upper surface with the higher pressure on the lower surface. At the wing tips the air tends to flow laterally from the lower to the upper surface in an attempt to remove this differential. This lateral or spanwise flow is from wing tip to wing root on top and from wing root to wing tip on the bottom (see total velocity vectors in Figure 1). The air immediately aft of the wing trailing edge is given a swirling motion due to the
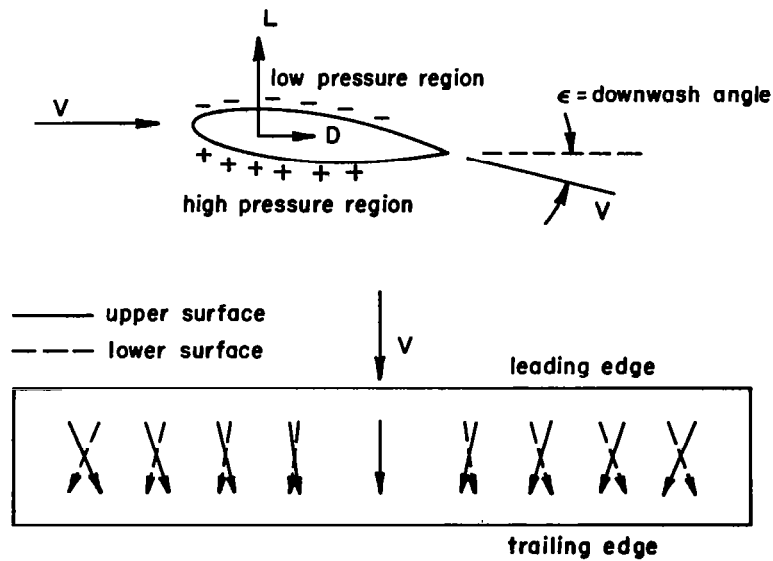

Figure 1. Side and planform views of flow over a wing (bound and trailing vortex patterns not shown in sketch).

shearing of the transverse velocity components on the upper and lower surfaces. These swirls or vortices, more predominant at the wing tips, are referred to as trailing vortices, and they tend to give the air behind the wing an average downward inclination, usually called downwash (see Figure 1 for definition of downwash angle). The spanwise variation of the downwash is a function of the wing planform shape.

The circulation theory developed in the late 1800's and early 1900's to account for lift in an inviscid fluid proved to be very useful in estimating downwash. In 1878 Lord Rayleigh showed that the swerving flight of a "cut" tennis ball could be explained best in general terms by comparing it to the case of a cylinder placed in an inviscid uniform stream. By imposing a circulatory flow upon the cylinder, the cylinder developed a force normal to the direction of the uniform stream (a lift force), directly proportional to the strength of the circulatory flow. In 1910 Joukowski showed that when a cylindrical body of arbitrary cross section moves with a velocity V in a fluid whose density is ρ and there is a circulation of magnitude Γ around it, a force normal to the velocity is produced equal to the product ρVΓ per unit length of the cylinder. Joukowski made the assumption that the flow must leave the sharp trailing edge of airfoil-like bodies smoothly. Using this hypothesis, usually referred to as the Kutta-Joukowski condition because Kutta reached the same assumption independently somewhat earlier, the problem of lift became purely mathematical: one has only to determine the amount of circulation so that for zero vertex angle at the trailing edge, the velocity of the flow leaving the upper surface is equal to that leaving the lower surface. For finite vertex angles the trailing edge must be a stagnation point.

Although the work of Rayleigh and Joukowski was concerned with wings having infinite aspect ratios (no spanwise flow), the circulatory flow idea was extended to wings with large aspect ratios and little or no sweep by Prandtl in his now well-known Lifting-Line Theory. von Karman (Ref. 6) summarizes Prandtl's theory in the following way: (a) the wing is replaced by a lifting line perpendicular to the flight direction; (b) the lifting line is assumed to consist of a bound vortex with circulation variable in order to account for the fact that the lift may change along the span; (c) in accordance with the change in circulation along the span, free vortices are born and extend downstream; however, (d) the flow produced by the vortex system is considered as a small perturbation of the fundamental stream relative to the wing, and therefore (e) it is assumed that the free vortices approximately follow the original direction of the streamlines parallel and opposite to the flight direction; (f) the flow in the immediate neighborhood of a wing section is determined by the two-dimensional solution given by Kutta and Joukowski.

In the lifting line theory the wing surface is replaced by a line vortex of varying strength, called the bound vortex. A sheet of trailing vortices extends from the lifting line downstream to infinity. The perturbation in the flow field due to an infinitesimal segment of each vortex is found from the Biot-Savart Law (expressed here following Reference 7 in Vector notation).

$$\bar{w} = \frac{\Gamma}{4\pi} \frac{d\bar{\ell} \times \bar{a}}{|\bar{a}|^3} \qquad (1)$$

where $\bar{w}$ = induced velocity vector at a point in the flow field
         Γ = strength of the vortex whose segment is being considered
         $\bar{d\ell}$ = vector having the direction and length of the infinitesimal
                vortex filament
         $\bar{a}$ = the vector from the vortex filament to the point

the local value of Γ on the bound vortex is determined from

$$\Gamma(y) = \frac{Vc\, C_\ell(y)}{2}$$ (2)

where C_ℓ is the section lift coefficient of the wing
         V is the free stream velocity
         c is the wing chord

The strength of a particular trailing vortex is determined by the change in
the Γ of the bound vortex which occurred as one moved outboard from the
spanwise position where the previous trailing vortex was shed. All of the
vorticity on the wing must eventually be shed downstream. The flow direc-
tion in the field downstream (or upstream for that matter) of the lifting
line is then a sum of the contributions of all the trailing vortices, the
bound vortex, and the free stream. The perturbation in the free stream
velocity field resulting from these contributions is most intense in a sheet
which for positive lift moves downward and to the rear from the lifting line.
In the physical situation which this model represents this sheet is essentially
the center of the wing wake. From equation (2) it is evident that the greater
the wing lift the greater the vortex strength; thus it is reasonable to expect
that the greater the wing lift the greater will be the downward deflection of
the wake centerline as it moves aft.

   Attention will now be directed to ways of evaluating the Γ distribution
over the wing since it is essential for downwash calculations. Reference 8
notes that the main problem of lifting line theory is the determination of the
spanwise distribution of air loads on wings from the fundamental equation of
the theory. Its simplest form relates the absolute and effective angles of
attack,

$$\alpha_a = \alpha_o - \alpha_i$$ (3)

where α_a = absolute angle of attack

         α_o = effective angle of attack

         α_i = induced angle of attack.

9

The effective angle of attack may be expressed in terms of Γ by writing the section lift equation as

$$\rho V \Gamma = \rho V^2 \, c \, m_o \, \alpha_o / 2 \qquad \text{or} \qquad \alpha_o = \frac{2\Gamma}{m_o \, Vc}$$

where ρ = density of air
m_o = section lift curve slope.

Now the induced angle of attack may be written as $- \tan^{-1}(\frac{w}{V}) \approx - w/V$ and since w can be expressed in terms of Γ, then the only unknown in the fundamental equation is Γ. Using the Biot-Savart Law the downwash velocity $w_{y_o y}$ at the point y_o on the bound vortex, induced by a vortex behind the wing at the point y may be written as

$$w_{y_o y} = \frac{d\Gamma}{4\pi} \frac{1}{y_o - y} \, . \tag{4}$$

Replacing $d\Gamma$ by $(d\Gamma/dy)dy$ and noting that the downwash at y_o resulting from all the trailing vortices may be obtained by integrating $w_{y_o y}$ from $- b/2$ to b/2 (b is the wing span), then

$$w_{y_o} = + \frac{1}{4\pi} \int_{-b/2}^{b/2} \frac{d\Gamma/dy}{y_o - y} \, dy \, . \tag{5}$$

The fundamental equation can now be written in the form

$$(\alpha_a)_{y_o} = (\frac{2\Gamma}{m_o \, Vc})_{y_o} + \frac{1}{4\pi V} \int_{-b/2}^{b/2} \frac{d\Gamma/dy}{y_o - y} \, dy \tag{6}$$

where the subscript refers to the variable evaluated at the point y_o.

Probably the best known procedure for solving the fundamental equation is given by Glauert in Reference 9. The first step is to invoke the following substitutions:

$$y = b/2 \cos \theta \tag{7}$$

and

$$\Gamma = Vb \sum_{n=1}^{\infty} A_n \sin n\theta \,. \tag{8}$$

The sine series rather than the cosine series is chosen for Γ because the boundary conditions of $\Gamma = 0$ at both wing tips ($\theta = 0$ and $\theta = \pi$) are automatically satisfied for all values of A_n. The constants A_n are found by determining the values necessary to force the flow over the wing to be tangent to the mean camber surface. It can then be shown that the fundamental equation can be written as

$$\sum_{n=1}^{\infty} [A_n \sin n\theta(\mu n + \sin \theta)] = \frac{\mu}{2} \alpha_a \sin \theta \tag{9}$$

where $\mu = m_o c/(4b)$.

The above equation is valid for any spanwise station (θ between 0 and π), and in general μ and α_a will be functions of θ. The problem has been reduced to one of determining the values of the coefficients A_n which will satisfy the above equation at every desired value of θ along the span of the wing in question. If a 5 term series is desired for Γ then equation (9) must be applied at 5 spanwise stations yielding 5 equations in the 5 unknown A_n's. Once the A_n's have been obtained then Equation 8 will yield Γ for different spanwise positions.

As an alternative to solving Equation 9 at several spanwise stations, the computer programs given in Reference 4 are quite useful. Programs are presented to (1) calculate the lift, drag, and moment coefficients of conventional airfoils (two-dimensional) and (2) given the wing planform shape and airfoil characteristics for the root and tip sections, extend these two-dimensional characteristics to three dimensions. By using a lifting line theory, the three-dimensional extension yields local lift, drag, and moment coefficient information at several spanwise stations along the wing span. The section lift coefficients may be used directly in Equation 2 to compute the strength of the bound vortex.

With the foregoing as background, attention will now turn to literature specifically treating the calculation of downwash. Two 1939 NACA Reports have become classics in the field: NACA TR-648 (Ref. 10) and NACA TR-651 (Ref. 7). The latter presents methods for predicting important wake parameters in terms of the distance behind the airfoil trailing edge and the profile drag coefficient for plain and flapped wings. The methods were based on a correlation of extensive experimental measurements of downwash angles and wake characteristics. Downwash was computed in the wing chord plane using the Biot-Savart equation

11

operating on a vortex system made up of a bound vortex at the wing quarter-chord and a planar vortex sheet extending straight behind the quarter-chord line to infinity. It is pointed out that the wing wake coincides with the trailing vortex sheet because of their common origin at the trailing edge and their equal freedom to move in the induced velocity field behind the wing. The vertical displacement of the vortex sheet can therefore be approximated by integrating the downwash angle in the streamwise direction from the trailing edge to some specified distance downstream. Silverstein, Katzoff, and Bullivant used the idea of superposition to obtain maps of constant downwash angles behind the wing. First, using a planar vortex system, downwash angles were calculated at several points in the plane of symmetry to yield a contour map similar to that of Figure 2. This map was then distorted in the vertical plane to account for the vertical displacement of the vortex sheet. The distorted contour map is also shown in Figure 2. Using this procedure, which neglects spanwise curvature of the wake sheet as well as vortex roll-up effects, agreement with experimental data is good at distances typical of to the tail plane locations.

In NACA TR-648 (Ref. 10) Silverstein and Katzoff prepared downwash charts to make the methods presented in TR-651 more readily useable in design activities. Included in the report are curves of the lift and drag of flapped airfoil sections and charts for finding the contribution of the different types of flaps to the total wing lift. The downwash charts are for elliptical wings and wings of taper ratios 0.1, 0.2, 0.3, and 0.5, with aspect ratios of 6, 9 and 12, having flaps covering 0, 40, 70 and 100 percent of the wing span. These charts may be used without a prior knowledge of the material in TR-651. Although written some 35 years ago, these reports are still the basis of current downwash predictions for light aircraft.

The interest in high speed flight led to some new downwash investigations in the late 40's and early 50's. In Reference 11 a study was made in the Langley 7- by 10-foot wind tunnel to determine downwash angles behind wings of various sweep angles and aspect ratios. Although the emphasis was on sweep effects, downwash characteristics were also measured for some unswept wings. The results are displayed graphically as curves of constant downwash angles. In 1954 an experimental investigation was conducted by Tolhurst (Ref. 12) to define the downwash field and vortex sheet shape behind a large-scale wing-fuselage combination incorporating a 63° swept-back wing of aspect ratio 3.5. Data is presented for 9 vertical-transverse planes behind the wing for 3 angles of attack at a Reynolds number of 6.1 million. A comparison of these experimental results with theory showed that an acceptable approximation to the downwash distribution within the distance surveyed could be obtained if the vortex sheet were assumed to be flat and the spanwise vorticity distribution were assumed to be that of the wing. Rogers (Ref. 13) studied the application of two-dimensional vortex theory to the prediction of flow fields behind wings of wing-body combinations at subsonic and supersonic speeds. The wing trailing vortex was represented initially by line vortices distributed to approximate the spanwise distribution of circulation along the trailing edge of the exposed wing panels; however, a bound wing vortex was not included.
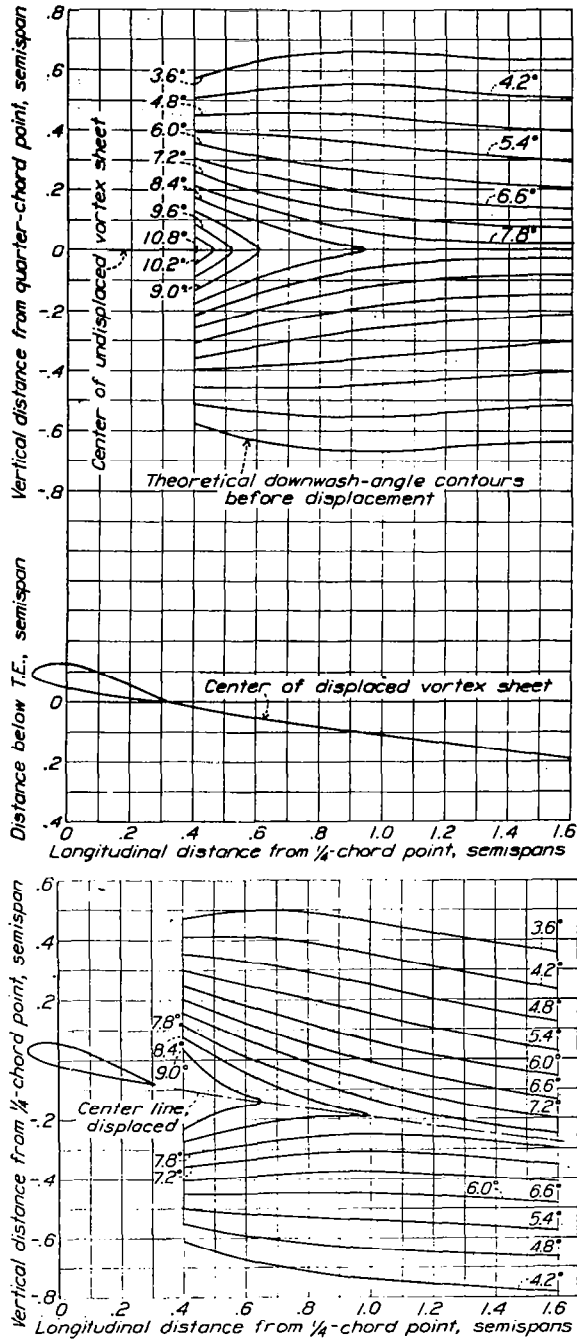
Figure 2. Example of downwash calculation procedure (Ref. 7) in the plane of symmetry for a USA 45 airfoil at $C_L = 1.175$.

The afterbody was represented by corresponding image vortices within the body. Two-dimensional line-vortex theory was then used to compute the induced velocities at each vortex, and the resulting displacement of each vortex was calculated by means of a numerical stepwise integration procedure. The displacement of each vortex independently permits inclusion of both the roll-up phenomenon and the spanwise wake-sheet curvature. Rogers found that this method predicted vortex paths at high speeds with reasonable facility and accuracy.

In 1970 Butter and Hancock presented a method (Ref. 14) for calculating the shape of the trailing vortex system behind a swept wing at low speed. The authors were concerned about the two-dimensional approaches which omit the main wing bound vortex; they believed that when C_L is large the wing circulation effects are significant. A method was therefore proposed which would include the effect of the main wing bound vorticity and the three-dimensional pattern of trailing vorticity. The wing is replaced by a single lifting-line bound vortex which represents the circulation distribution around the wing while the trailing sheet is approximated by a number of discrete line vortices. Starting with a nearly planar system (i.e., bound vorticity on the wing and trailing vorticity streamwise as in Figure 3) and using a step-by-step process, working downstream aft of the wing trailing edge, the vertical and spanwise displacements of the trailing sheet are determined. To calculate the position of the ith vortex at station 1, δx behind the 3/4-chord line (station 0), the sidewash and downwash velocities, (v_i and w_i) due to all the other vortices are calculated at $\delta x/2$. The change in vertical and spanwise position (δz and δy) for the ith vortex from station 0 to station 1 is then given by

$$\delta y = v_i \delta x/V \qquad \text{and} \qquad \delta z = w_i \delta x/V \qquad (10)$$

This procedure is used to obtain the new position of each vortex at station 1. Downstream of station 1 each vortex extends to infinity using the y and z coordinates at station 1. Once the locations are established at station 1, the remainder of the stations downstream may be analyzed in a similar manner. Butter and Hancock found that the principal factors governing the accuracy of the results are the downstream step-size and the number and position of the vortices chosen to represent the trailing vortex sheet. They note that if too many trailing vortices are taken numerical difficulties may arise; induced velocities calculated at a point between two such vortices will be given by the difference of two large velocities of opposite sign. When compared with experimental results, the downwash angles were found to be too large near the trailing edge due to the concentrated nature of the bound vortex; however, further downstream agreement was good.

In Reference 15 Labrujere presents a method for calculating the vortex location behind a thick lifting wing. The flow around a wing in uniform onset flow is determined with the aid of a source distribution on the surface of the

14
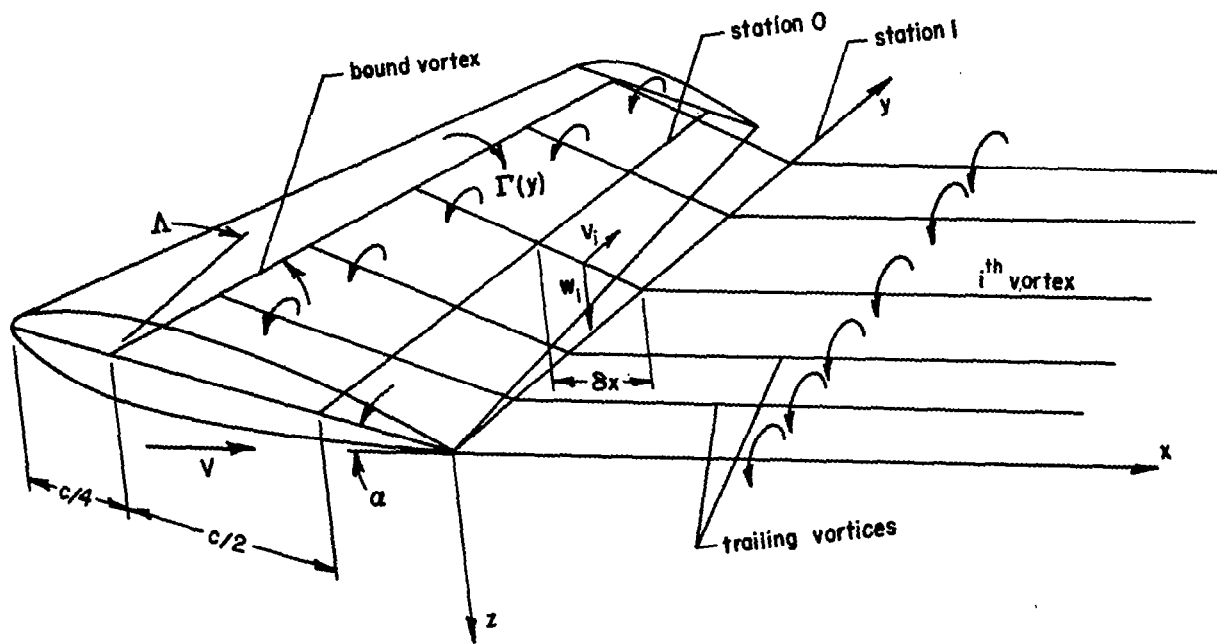
Figure 3. Coordinate system and wing placement for the method presented in Reference 14.
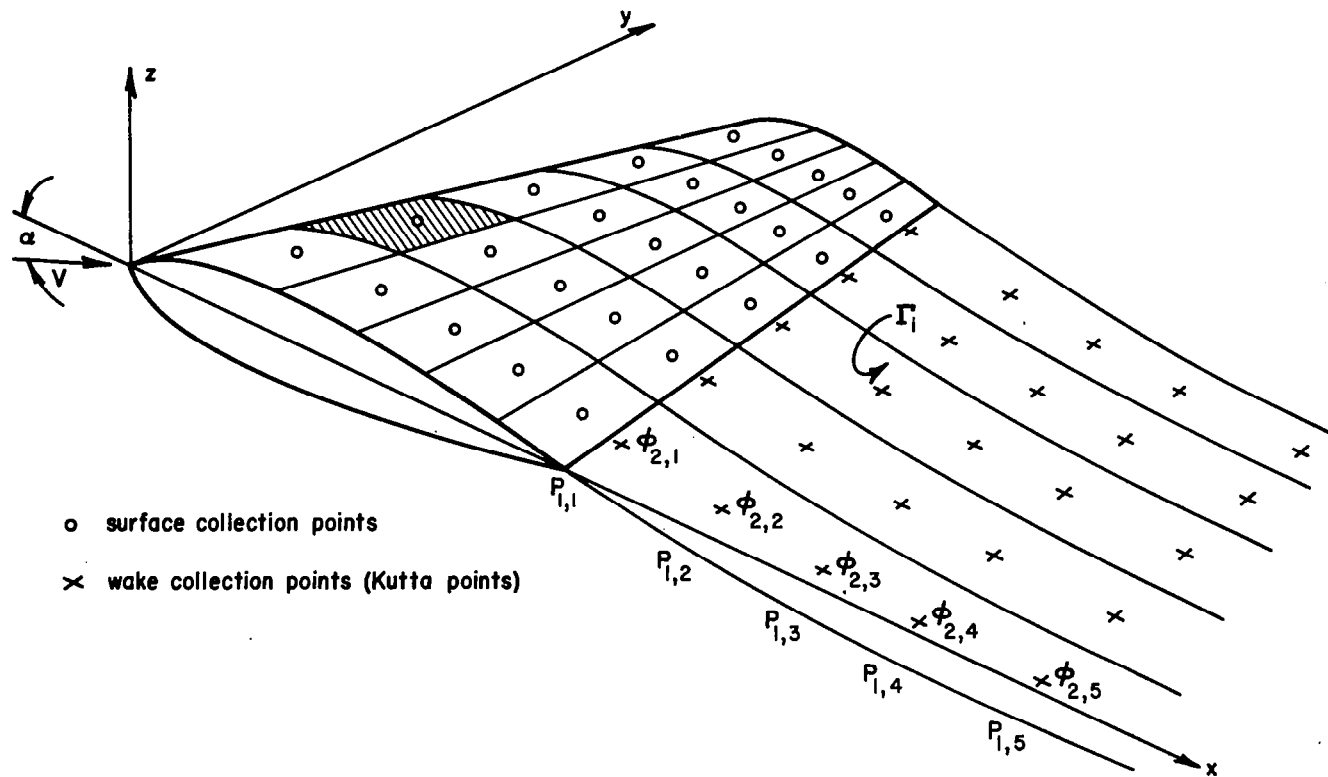
Figure 4. Representation of wing and wake by a source distribution on the wing surface and discrete vortices inside and behind the wing (Ref. 15).

wing and a vortex distribution on its camber surface and wake. The wing and camber surface are divided into a number of strips whose edges are formed by lines y = constant and which are each subdivided in a number of quadrilateral panels. Along the periphery of each camber panel a line vortex is located (see Figure 4). The strengths of these "singularities" are determined by imposing the boundary condition of tangential flow to the wing surface at a number of surface points and the condition of tangential flow to the trailing vortex sheet at a number of "Kutta points" noted in Figure 4. Since the position of the vortex sheet and the strength of the singularities are related "non-linearly", an iterative procedure is required in order to determine the shape of the sheet as well as the singularity distributions for a given wing and at a given angle of attack. Although only a limited comparison with experimental results was made using this method, the agreement was good.

Comparing Labrujere's technique with that of the previous reference, there are three reasons why the Butter and Hancock method is preferred as the basis for further work: (1) Labrujere combines the problems of the flow over the wing and the flow in the wake, solving them simultaneously; for a large number of panels both on the wing and in the wake this requires both more computer storage and a longer execution time than is required for the two problems independently (necessary in the Butter and Hancock approach). (2) The iterative nature of Labrujere's method may necessitate several executions unless the initial estimate of the wake shape is accurate. (3) Although Butter and Hancock's method may be used iteratively to improve accuracy, they found that for step sizes of a quarter semispan and smaller, subsequent iteration did not significantly affect the position of the trailing vortices.

In the last few years the interest in trailing vortex sheets has turned to the far field problem. At large distances behind the wing, vortex roll-up has occurred, and the hazard of one aircraft flying into the vortex core of another aircraft has spurred interest in trying to analytically predict the shape and velocities of a rolled vortex pair as well as the dissipation of this vortex pair with time. References 16, 17, and 18 cover the topic very well and discuss the pertinent work which has been done to the present time.

17

WAKE VELOCITY PROFILE

While an inviscid theory is acceptable for predicting the location and inclination of the wing wake, the estimation of actual velocities requires a viscous analysis. The velocity deficit behind a wing is a function of the wing drag, a viscous phenomenon caused by the shear forces which the wing introduces in the fluid. The only really correct way to attack the problem is to solve the full, time-dependent Navier-Stokes equations of motion in three-dimensions over a substantial region. With present computers and computational techniques, computers will have to grow in storage size and speed by one or two orders of magnitude in order to obtain an accurate solution to the problem in the space of a few hours.

Boundary layer theory, which has been a valuable tool in solving for the viscous flow over airfoils and even bodies at zero or small angles of attack (Refs. 19 and 4), has also been applied to the flow in jets and wakes. Boundary layer theory consists of simplifying the Navier-Stokes equations so that they are applicable in the viscous flow near the surface of a body or in a wake. For the flow over a body the region where viscous effects are dominant is usually very thin compared to the body size. The equations are simplified by estimating the order of magnitude of each term and neglecting those which are small compared with the other terms. As might be expected, these simplified equations are much easier to solve, yet they retain the correct physical description of the flow in most cases. The conventional way of approaching the wake problem is to assume that the flow downstream of the trailing edge can be described by the boundary layer equations which are then solved by a momentum integral or finite-difference method. The remainder of this section will review some of the pertinent literature on the determination of wake velocity profiles.

Two-dimensional wakes were probably first investigated by H. Schlichting in his thesis presented to Goettingen University in 1930. In his general text, Boundary Layer Theory (Ref. 20), he notes that a wake is formed behind a solid body which is being dragged through a fluid at rest or behind a solid body which has been placed in a stream of fluid. The velocities in a wake are smaller than those in the main stream and the velocity losses in the wake amount to a momentum loss in the fluid due the body drag. The spread of the wake increases as the distance from the body is increased, and the differences between the velocity in the wake and that outside become smaller. A wake is a free turbulent flow (not confined by solid walls) and therefore of boundary layer nature. This means that (1) the region of space in which a solution is being sought does not extend far in the transverse direction, as compared with the main flow direction, and (2) the transverse gradients are large. The problem can therefore be studied using the two-dimensional, steady, boundary layer equations given below:

$$u \frac{\partial u}{\partial x} + v \frac{\partial u}{\partial y} = \frac{1}{\rho} \frac{\partial \tau}{\partial y} \qquad \text{(x-momentum equation)} \qquad (11)$$

$$\frac{\partial u}{\partial x} + \frac{\partial v}{\partial y} = 0 \qquad \text{(continuity equation)} \qquad (12)$$

where x and u are the coordinate and velocity along the wake centerline, y and v are the coordinate and velocity normal to the wake centerline, ρ is the density of the fluid, and τ is the turbulent shearing stress (see Figure 5).
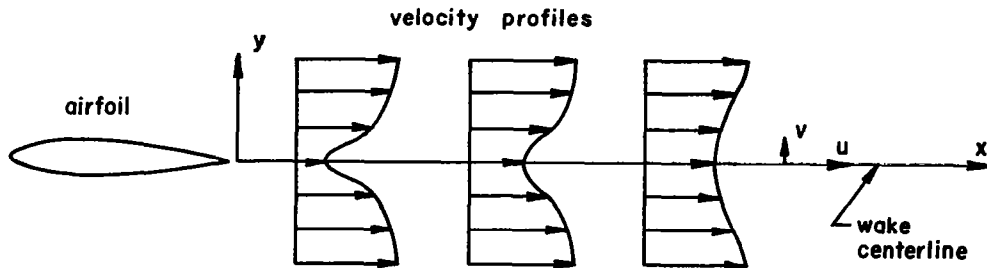
Figure 5. Sample velocity profiles in an airfoil wake.

The pressure gradient term has been dropped from the x-momentum equation because, from a certain distance behind the body on downstream, the pressure remains essentially constant in the y-direction. This assumption is not necessarily true near the airfoil trailing edge. To integrate Equations 11 the turbulent shearing stress must be expressed in terms of the main flow parameters. One of the simpliest and most widely used wake flow models for τ is that given by Prandtl in Equation 13.

$$\tau = \rho\varepsilon \frac{\partial u}{\partial y} = \rho c b (u_{max} - u_{min}) \frac{\partial u}{\partial y} \qquad (13)$$

where b denotes the width of the wake, c is an empirical constant, and ε is the virtual kinematic viscosity or eddy viscosity, assumed constant over the whole wake width. Schlichting points out that experience has shown that for two-dimensional turbulent wakes, the wake width increases as $\sqrt{x}$ while the centerline velocity decreases as $1/\sqrt{x}$.

As noted in Reference 20 Goertler and Reichardt investigated the two-dimensional wake behind a circular cylinder. Goertler found that if he assumed:

(1) $u_1 = U - u$ which at large distances from the body is small compared to U, the freestream velocity,

(2) the drag on the cylinder is obtained by applying the momentum theorem far downstream so that

$$D = h\rho \int_{y=-\infty}^{y=+\infty} u_1(U - u_1)dy \qquad (14)$$

where D is the drag on the cylinder of height or length h,

(3) that the second term of Equation 11 is small compared to the first,

then, by integrating the simplified version of Equation 11

$$\frac{u_1}{U} = \frac{1}{4\sqrt{\pi}} \frac{UC_Dd}{\varepsilon_o}^{1/2} (\frac{x}{C_Dd})^{-1/2} e^{(-\eta^2/4)} \qquad (15)$$

where: C_D = cylinder drag coefficient

ε_o = constant eddy viscosity

d = cylinder diameter

x = distance downstream behind the cylinder

η = nondimensionalized y-coordinate = $y\sqrt{\dfrac{U}{\varepsilon_o x}}$.

Upon comparison with experimental measurements made by Schlichting, Goertler evaluated the constant in Equation 13 with the relation

$$\varepsilon_o = (0.047)(2b_{1/2} u_{1_{max}})$$

where: $b_{1/2}$ = half the wake width halfway between $u_{1_{max}}$ and $u_{1_{min}}$ at some x-station

$u_{1_{max}}$ = the maximum value of u_1 in the wake at that x-station.

Using similar assumptions and a slightly different eddy viscosity model, Reichardt arrived at the following expression for u_1:

$$\frac{u_1}{U} = \frac{\sqrt{10}}{18(.18)} (\frac{x}{C_Dd})^{-1/2} \left\{1 - (y/b)^{3/2}\right\}^2 . \qquad (16)$$

21

Schlichting (Ref. 20) notes that the two solutions for the wake velocity actually do not differ much one from the other.

While the above work was concerned with the wake of a circular cylinder, in 1939 Silverstein, Katzoff, and Bullivant (Ref. 7) generalized the available experimental results so that velocity profile and wake width information behind airfoils could be predicted in terms of the downstream distance and the profile drag coefficient. The profile drag of an airfoil may be approximately equated to the loss of momentum in the wake by the relation:

$$d_o = \rho \int_{-\infty}^{\infty} u(U - u) dy \qquad (17)$$

where d_o is the drag per unit span. At distances behind the wing comparable with tail-plane location, where the static pressure in the wake has reached that of freestream, experimental investigations have shown that Equation 17 may be approximated in coefficient form by the more elementary expression:

$$c_{d_o} = \frac{1}{c} \int_{-b/2}^{b/2} (1 - \frac{q}{q_o}) dy \qquad (18)$$

where, $c_d = $ section profile drag coefficient
$q/q_o = $ ratio of dynamic pressure in the wake to that in the free-stream
$b = $ wake width
$c = $ wing chord.

The wake may be completely described by the width b, the loss of dynamic pressure at the wake center Δq, and the shape of the wake profile. As an aid in generalizing the results, the following nondimensional ratios were adopted:

$$\eta = \frac{\Delta q}{q_o} = (1 - q/q_o)$$

$$\zeta = \frac{1}{2} (\frac{\text{wake width}}{\text{wing chord}}) = \frac{b}{2c}$$

$$\xi = \frac{\text{distance behind trailing edge of wing}}{\text{wing chord}} = \frac{\ell}{c} .$$

Using Prandtl's proportionality relations

$$\zeta \sim \xi^{1/2} c_{d_o} \qquad \text{and} \qquad \eta \sim \frac{c_{d_o}^{1/2}}{\xi^{1/2}} \qquad (19)$$

the available experimental data was used to find the proportionality constants which should be used in Equations 19. It was found that:

$$\zeta = 0.68 \, c_{d_o}^{1/2} \, (\xi + 0.15)^{1/2} \qquad (20)$$

$$\eta = \frac{2.42 \, c_{d_o}^{1/2}}{\xi + 0.3} \qquad (21)$$

fit the data very well. The equation for η was found to vary with $1/\xi$ rather than $1/\xi^{1/2}$ as mentioned previously. The authors point out that discrepancy is probably associated with the high values of η near the trailing edge of the experimental data used for correlation; in Prandtl's formulation η was assumed small. For a complete wake description, the shape of the profile must also be defined. The profile shape was found to be closely approximated by either of the following empirical relations:

$$\frac{\eta'}{\eta} = \left[1 - \left(\frac{\zeta'}{\zeta}\right)^{1.75} \right]^2 \qquad (22)$$

or

$$\frac{\eta'}{\eta} = \cos^2\left(\frac{\pi\zeta'}{2\zeta}\right) \qquad (23)$$

where η' = relative loss in dynamic pressure
ζ' = distance from wake centerline ($\zeta' \le \zeta$).

The profiles given above are assumed symmetric about $\zeta' = 0$ and for ξ values in the vicinity of the tail plane this is not a bad approximation even for unsymmetric airfoils.

In TR-648 (Ref. 10) Silverstein and Katzoff made the methods presented in TR-651 easily adaptable to design by preparing charts for determining the velocity profile at the horizontal tail. Over the years both TR's have been very valuable in predicting tail plane velocity profiles for light aircraft.

23

In 1947 an investigation of free turbulent mixing was presented by Liepmann and Laufer in Reference 21. The investigation examined the various ways turbulence had been modeled up to that time and discussed the physical significance of the models using experimental measurements of the mean velocity, the intensity and scale of turbulent fluctuations, and the turbulent shear in a two-dimensional mixing zone. The authors decided that the assumptions of constant mixing length and constant exchange coefficients (as in Equation 13) across the wake width were, strictly speaking, incorrect. Measurements of the field fluctuating velocities in a turbulent mixing zone show that both the mixing length and exchange coefficient vary across the mixing region, contrary to the assumptions made by Prandtl and others. They concluded that if only the mean-velocity distribution of a turbulent flow problem is desired, it usually can be obtained by dimensional considerations, assuming a reasonable curve (e.g., an error function in the case of a mixing region), and determining one constant from experiment. (This agrees with the methods already presented from References 20 and 7). Also, for an understanding of turbulent flow in general, a study of various mean-velocity distributions is of little use; the field of turbulent fluctuations must be studied in detail probably requiring a knowledge of the diffusion of turbulent energy. The constant exchange coefficient as presented in Equation 13 can therefore be used in a turbulence model with good success if only mean velocity profiles are desired; but for any deeper understanding of turbulence, the microstructure must be investigated more fully.

The subject of eddy viscosity models is treated to some extent in References 22 and 23. Elassar and Pardolfini, using a multilevel linear difference scheme examined four eddy viscosity models and evaluated the constants in these models by comparing calculated velocity profiles with experimental data in the similarity region. The thrust of the report is directed toward high-speed compressible flow, and all the models are more complex than Equation 13. In Reference 23 similarity solutions of the boundary layer equations in wakes with tailored pressure gradients were obtained. Experimental data was used to obtain a value for the constant eddy viscosity and the agreement between theory and experiment is described as good. While both of these reports are valuable in a general nature, it would be desirable to have viscosity constants evaluated using data obtained in the wake behind an airfoil. References 24 and 25 indicate that boundary layer solution procedures are being applied to high-speed turbulent mixing layers using more elaborate viscosity models than that given in Equation 13. These same techniques should be readily adaptable to low speed turbulent mixing and could be very useful if computer storage requirements and execution times are not excessive.

In order to improve upon the turbulent wake prediction methods, more experimental data are necessary for wake profiles at several stations behind an airfoil rather than at the tail-plane location only. References 26 and 27 are very helpful in this respect in that they present two-dimensional velocity profiles in the wakes of symmetrical Joukowski and Piercy airfoils respectively.

24

An 11.8 percent thick Joukowski airfoil was tested at angles of attack of 0 and 6 degrees for a Reynolds number of 0.42 million. Velocity profiles were measured at stations of 0.0005, 0.0025, 0.01, 0.25, and 0.5 chord lengths behind the airfoil trailing edge. A similar investigation on the 12 percent thick Piercy airfoil, with wires on the leading edge to force transition, yielded velocity profiles at 0.0005, 0.0025, 0.01, 0.25, and 0.4 chord lengths. In addition to the profiles, the drag coefficient and other boundary layer information was also measured.

A recent report by Goradia and Lilley (Ref. 28) also present some experimental data for profile measurements behind a modified NACA 0015 airfoil at several angles of attack. The report describes a procedure developed by the authors to improve two-dimensional drag predictions for single and multi-element airfoils by describing the airfoil wake using regions of similarity. Although correlations are given for only two or three airfoils and the computer program is not provided, the procedure seems to have improved the drag predictions given in CR-1843 (Ref. 29). Experimental data, taken in connection with this work is presented in both tabular and graphical form; however, the tabular data, particularly at stations near the airfoil trailing edge, indicate profiles which fail to return to freestream velocity at the upper and lower edge.

While the data given in the three references cited above are valuable, they were taken in the wake of symmetrical airfoils. More data is obviously needed, particularily for unsymmetric airfoils, but the lack of data is due in part to the high cost of wind tunnel testing and the difficulty of measuring wake velocities accurately.

A review of the literature revealed several papers concerning the effect of flow curvature on the formulation and solution of the two-dimensional boundary layer equations. Murphy (Ref. 30) formulated the boundary layer equations with curvature and indicated that even for laminar flow these equations are at their simplest more complex than the no-curvature case. Williams (Ref. 31) obtained a solution for a free jet flowing off a step only by assuming a curvature function which made the boundary layer equations similar (the streamwise coordinate did not appear explicitly). One encounters similar increases in solution complexity when treating three-dimensional boundary layers. Although the problem can be formulated, the computer storage requirements and execution times required with present machines and methods are excessive. Add to this the complexity of curvature and it is understandable why attention is still directed toward solving the simplified problem. Solution to such a problem, hopefully, preserved the qualitative aspects of the physical situation even though it cannot duplicate it quantitatively in all respects.

PROGRAM FOR DOWNWASH AND

WAKE POSITION CALCULATIONS

GENERAL THEORY

For many years the vertical displacement of the wake centerline location and downwash behind wings has been calculated using a bound vortex and a finite number of trailing vortices. The spanwise curvature of the trailing vortices and their roll-up may be included in the calculation by allowing the vortices themselves to be deflected in both the vertical and spanwise directions (Ref. 13 and 14). Analyses have also been conducted by representing the wing and vortex sheet as a single vortex lattice and using an iterative solution procedure with boundary conditions of no flow normal to the vortex panels to determine the wake location (Ref. 15). Because of the paneled wake procedure (lattice) achieves only a slight improvement in wake location at a large increase in computer cost , the WASH program presented here uses a method similar to those given in References 13 and 14. For simplification the x, y, and z coordinates are non-dimensionalized by the wing semispan, and a unity freestream velocity is assumed since only ratios of induced velocities to freestream velocity are required to estimate the downwash and sidewash angles.

The first step in computing the downwash characteristics and wake position is that of representing the wing by a bound vortex at the wing quarter-chord and by a trailing vortex system running aft from the quarter-chord line. The symmetric half-wing is placed in the coordinate system shown in Figure 6. The root chordline is in the xz-plane at $y = 0$, with the origin at the trailing of the wing root. The root chordline has an incidence, α, with the negative x-axis.
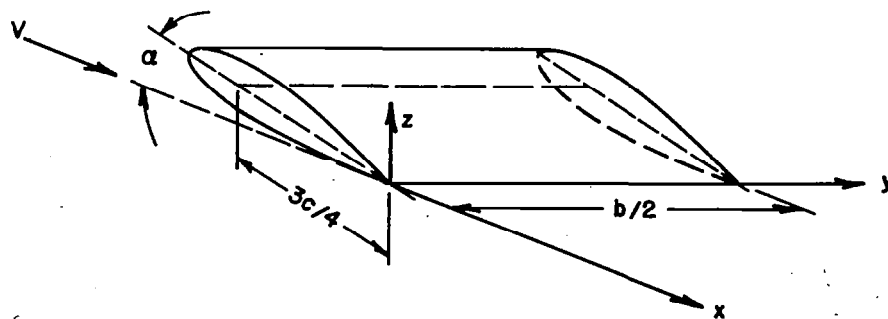
Figure 6. Definition of coordinate system and wing placement used in WASH program.

The analysis will be limited to unswept wings; therefore, the x and z coordinates of the wing quarter-chord are given by

$$x_b = -\frac{3c \cos \alpha}{2b} \qquad \text{and} \qquad z_b = \frac{3c \sin \alpha}{2b}$$

where (x_b, y_b, z_b) = the coordinates of the bound vortex normalized by the semispan
  b = wing span
  $c \doteq$ wing root chord
  α = wing angle of attack.

The strength of the bound vortex is calculated using Equation 2 once the section lift coefficient distribution is known. Although the WASH program was designed to use the output of the three dimensional aerodynamic characteristics program given in Reference 4, any procedure may be used to calculate the section lift coefficients. The lift coefficients at 10 different normalized spanwise stations must be read into the WASH program. The specification for both is ordered from positive wing tip to wing root[*] (see Figure 7).
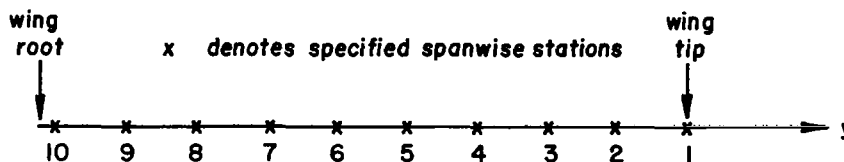
Figure 7. Ordering scheme for spanwise station and section lift specification.

Recall of course that the wing and its flow field is being represented by a system of horseshoe vortices. The initial streamwise position of the various trailing vortices is defined by assuming the vortices are shed at stations midway between the 10 specified y values on each semi-span, i.e., on each half of the lifting line. In carrying out the computations, advantage can be taken of the assumed symmetry in the loading and the geometry. In this fashion, the section lift coefficients as well as the input y stations and the positions of the shed vortices for the negative y axis can be defined. A schematic of the

---

[*] The root value for y cannot be zero; it may be a very small number, but because of the technique used for estimating the bound vortex contribution, the value must be non-zero.

20 stations at which the section lift coefficients are specified and the 18 shed vortex stations for the entire wing is given in Figure 8.

x **denotes specified spanwise stations for complete wing**

I **denotes shed vortex stations for complete wing**
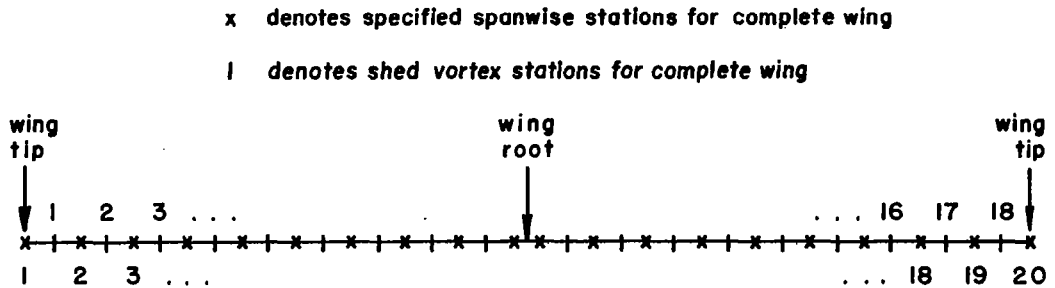
Figure 8.   Reordered specified spanwise stations and shed vortex stations for complete wing.

Once the bound vortex strength is calculated using Equation 1 at the specified y stations, the strength of the shed vortices is computed by the change in Γ from one station to the next. Thus, for the right half of the wing the trailing vortex system is similar to that given in Figure 9.
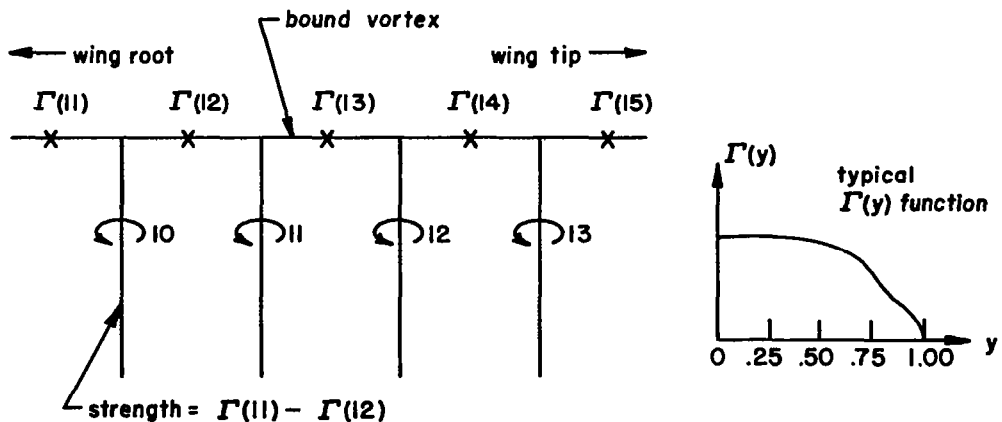
Figure 9.   Example of indexing procedure used for the trailing vortex system on the right half of the wing with a typical $\Gamma(y)$ distribution.

Each initial trailing vortex is made up of two straight line segments, one from the bound vortex to the trailing edge and another from the trailing edge to infinity in the x-direction parallel to the freestream (see Figure 10).
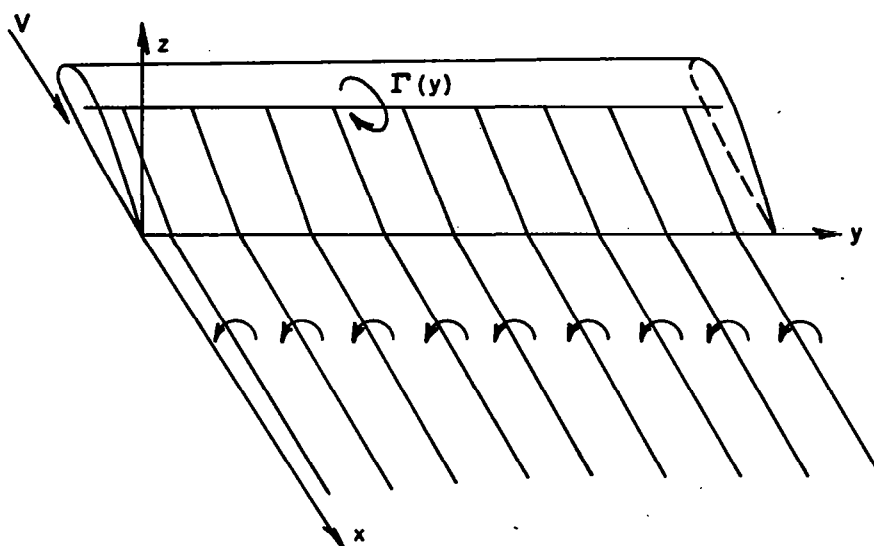
Figure 10. Example of initial approximation of trailing vortex system.

The net velocity induced by the vortex system at a point in the vicinity of the wing is computed by summing the contributions from the bound vortex and every straight line segment of each trailing vortex. The velocity induced at a point due to a vortex is defined by the Biot Savart law (Equation 2). An alternate form of this equation for straight line filaments is given in Reference 5 as

$$dW = \frac{\Gamma}{4\pi} \frac{\sin \theta \, d\ell}{r^2} \tag{24}$$

where
dW = total velocity induced at a particular point by a filament $d\ell$
Γ = strength of the vortex filament
r = distance to increment of filament at the point the velocity is induced
θ = angle between the length r and the filament.

The contribution of the bound vortex is calculated by integrating Equation 24 from the negative wing tip to the positive tip. Expressing $\sin \theta$ and r in terms of the x, y, and z coordinates, and noting that $d\ell$ becomes dy, the induced velocity at a point (x, y, z) due to the bound vortex is written as

$$W_b = \int_{-1}^{1} \frac{\Gamma(y_o) \, b/2 \, \sqrt{(x - x_b)^2 + (z - z_b)^2} \, dy_o}{4\pi[(x - x_b)^2 + (y - y_o)^2 + (z - z_b)^2]^{3/2}} \tag{25}$$

where all coordinates are non-dimensionalized by the semispan. Equation 25 may be solved numerically, or if a functional form is known for $\Gamma(y_o)$, it may be integrated in closed form. In order to use the closed form technique, two successive specified values of $\Gamma(y)$ for the bound vortex were fitted using the cubic spline given in Reference 33 matching first and second derivatives at the end points. The cubic spline fit is of the form

$$\Gamma(y) = A_{1j}y^3 + A_{2j}y^2 + A_{3j}y + A_{4j} \tag{26}$$

where $y_j \le y \le y_{j+1}$, $j = 1, 2, \ldots, 19$.

Note that for each of the 19 intervals the cubic coefficients depend on the interval (y_j, y_{j+1}) in which the spanwise station lies, but they are constant in a given interval. It is this variation of the coefficients that gives the spline fit its remarkable curve fitting properties. Using the cubic representation Equation 25 is integrated (Ref. 34) in each of the 19 intervals yielding the total velocity induced by the bound vortex at the point (x, y, z). This total velocity is divided into a freestream component, u, and a vertical or downwash component, w, by the relation given below:

$$u_b = W_b(x - x_b)/\sqrt{(x - x_b)^2 + (z - z_b)^2}$$

$$w_b = W_b(z - z_b)/\sqrt{(x - x_b)^2 + (z - z_b)^2} \tag{27}$$

w and W are defined as positive in the negative z direction, and u is positive in the positive x direction. Since the bound vortex is always parallel to the y-axis, there is no sidewash component in W_b. The streamwise component u_b is usually very small compared with the freestream velocity.

The velocity induced by a trailing vortex is calculated by summing the effect of each straight line segment of the vortex. The total velocity induced at a point by a straight line vortex segment is also calculated using Equation 24; the evaluation is however, much simplier than the bound contribution because Γ along all segments of a trailing vortex is constant. Thus, expressing $d\ell$ and r in terms of θ, one has

$$W_t = \frac{\Gamma}{4\pi} \int_{\theta_A}^{\theta_B} \frac{\sin\theta}{h} \, d\theta \tag{28}$$

where W_t = is the total velocity induced at a point (x, y, z) by a
                vortex of length AB,

θ_A and θ_B = angles between the length r and the filament at points
                A and B respectively, and h is the perpendicular distance
                from the point (see Figure 11).
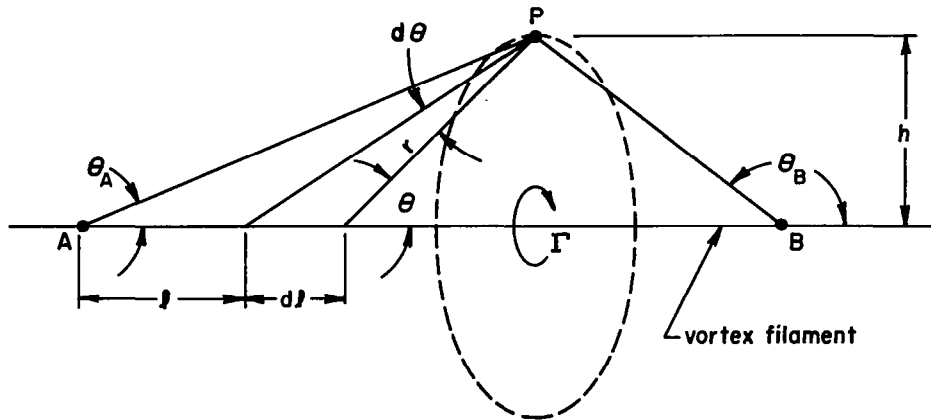
Figure 11. Nomenclature diagram for velocity induced by a straight-line
            vortex filament (Ref. 5).

Carrying out the integration indicated in Equation 28 yields

$$W_t = \frac{\Gamma}{4\pi h} (\cos\theta_A - \cos\theta_B) . \tag{29}$$

34

This total induced velocity must also be divided into its component parts: freestream, sidewash, and downwash velocities. As seen in Figure 12, the total induced velocity at P_0 due to a line vortex from P_1 to P_2 of strength Γ may be rewritten as

$$W_t = \frac{\Gamma(\cos\theta_1 + \cos\theta_2)}{4\pi \ b/2 \ d_{01} \ \sin\theta_1} \ . \tag{30}$$
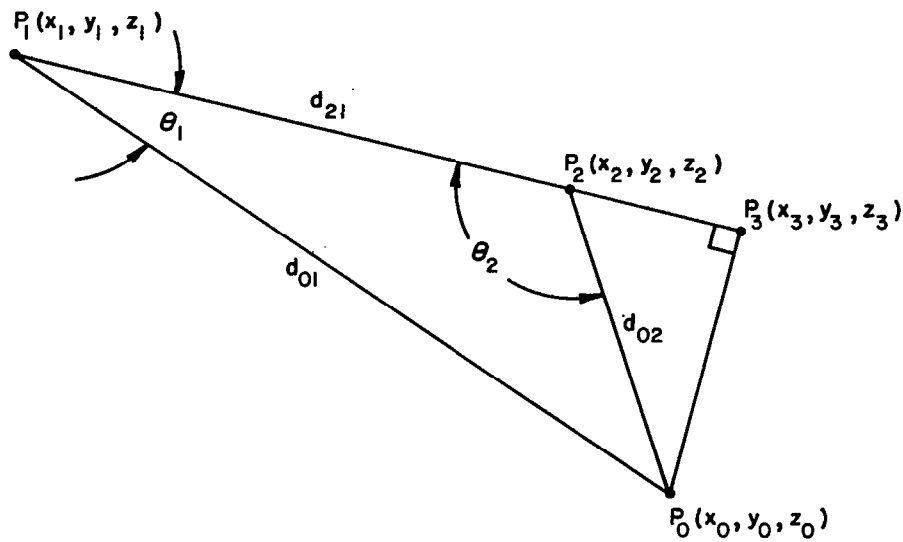
Figure 12.   Schematic for velocity induced at P_0 due to a vortex from P_1 to P_2.

The components are derived using the following relations to obtain the direction cosines:

$$d_{21} = \sqrt{(x_2 - x_1)^2 + (y_2 - y_1)^2 + (z_2 - z_1)^2}$$

$$d_{01} = \sqrt{(x_0 - x_1)^2 + (y_0 - y_1)^2 + (z_0 - z_1)^2}$$

$$d_{02} = \sqrt{(x_0 - x_2)^2 + (y_0 - y_2)^2 + (z_0 - z_2)^2} \tag{31}$$

$$\theta_1 = \cos^{-1}[(d_{21}{}^2 + d_{01}{}^2 - d_{02}{}^2)/(2d_{21}d_{01})]$$

$$\theta_2 = \cos^{-1}[(d_{21}{}^2 + d_{02}{}^2 - d_{01}{}^2)/(2d_{21}d_{02})]$$

$$x_3 = x_1 + d_{01} \cos \theta_1 \ (x_2 - x_1)/d_{21}$$

$$y_3 = y_1 + d_{01} \cos \theta_1 \ (y_2 - y_1)/d_{21} \qquad \text{(31)}$$
$$\text{Cont.}$$

$$z_3 = z_1 + d_{01} \cos \theta_1 \ (z_2 - z_1)/d_{21}$$

$$A = (y_2 - y_1)(z_3 - z_1) - (y_3 - y_1)(z_2 - z_1)$$

$$B = -[(x_2 - x_1)(z_3 - z_1) - (x_3 - x_1)(z_2 - z_1)]$$

$$C = [(x_2 - x_1)(y_3 - y_1) - (x_3 - x_1)(y_2 - y_1)] \ .$$

The components can therefore be written as

$$u_t = W_t \ A/\sqrt{R}$$

$$v_t = W_t \ B/\sqrt{R} \qquad \text{(32)}$$

$$w_t = W_t \ C/\sqrt{R}$$

where $R = A^2 + B^2 + C^2$.

In summary, the induced velocity components at a point are calculated due to (1) the bound vortex using Equations 25 and 27 and (2) a straight line segment of a trailing vortex using Equations 30 and 32. The velocity due to the entire vortex system is computed by summing the contributions from the bound vortex and each segment of the 18 trailing vortices.

The spanwise curvature in the trailing vortex system is modeled by representing each vortex by a number of straight-line segments which are free to follow the local direction of the flow. The position of these vortex segments is determined using a stepwise downstream marching procedure which will now be discussed.

As previously mentioned, the first approximation of the vortex sheet consists of the 18 trailing vortices with 2 segments each, one segment from the bound vortex to the y-axis and another from the y-axis to x = ∞ parallel to the x-axis. Since the actual vortex system behind a wing is displaced in both the y and z directions, the following procedure is used to compute the position of each trailing vortex at a length Δx behind the trailing edge. Noting Figure 13 and considering vortex #10 at station #2, the v and w induced velocity components due to all the other vortices are calculated halfway between stations #2 and #3 (x = Δx/2) using the y and z coordinates at station #2. The changes in spanwise and vertical position of vortex #10 in moving from station #2 to #3 is approximated by Equations 10 as

$$\Delta y = v\Delta x$$

$$\Delta z = w\Delta x \ .$$
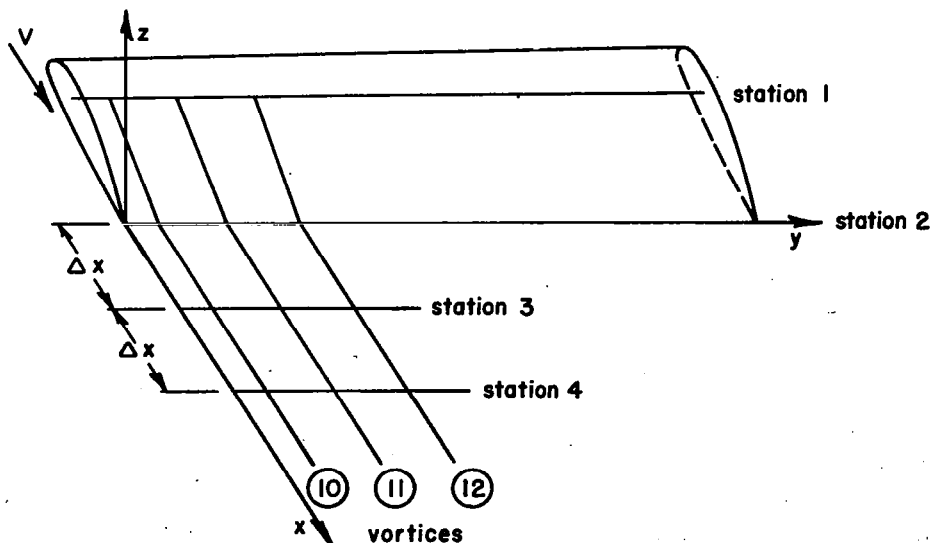
Figure 13. Schematic of downstream stepwise technique used in WASH program.

37

The position of the vortex at station #2 was (0, y(vortex #10), 0) and the
position at #3 becomes (Δx, y(vortex #10) + Δy, Δz). A similar procedure is
used to calculate the position of the other 17 trailing vortices at station
#3. Downstream of station #3 the trailing vortices are assumed to go to
infinity in the streamwise direction. After the position is determined at
station #3 the procedure is reapplied at stations #4, #5, etc. until the
vortex sheet is traced as far downstream as desired. The WASH program prints
the coordinates of each vortex as well as the total vortex length from the
trailing edge at each downstream station. The procedure discussed above is
equivalent to that used in Reference 14 where it was found that for stepsizes
as large as .25 semispans an accurate wake location was predicted. Butter
and Hancock did note that numerical difficulties were sometimes encountered
when more than 5 spanwise stations for the half-wing were used; however, the
WASH program using double precision arithmetic utilizes 9 spanwise stations
without numerical difficulty as long as the specified y stations are approx-
imately evenly spaced. An example of a wake sheet calculated using the above
procedure is given in Figure 14. The two views of this wake sheet were
plotted using the PLOT program of Reference 4. The WASH program will punch a
data set which may be read directly into the PLOT program; the data set
requires only the addition of view cards at the rear defining the type of view
desired.

Once the location of the trailing vortex sheet is determined then both
downwash and upwash angle may be computed behind and ahead of the wing
respectively using the bound vortex and the new vortex sheet. The WASH
program is designed to calculate, at the user's option, three basic sets of
information:

(1) downwash and sidewash angles in a plane behind the wing at a con-
stant x-station (a negative value for the x-station yields upwash
angles ahead of the wing) indicating the variation with y and z,
(2) downwash angles in the y = 0 plane of symmetry for 1.75 semispans
downstream with z varying from .5 semispans above and below a user
specified z-station,
(3) upwash angles in the y = 0 plane of symmetry for 0.5 semispans
upstream with z varying from .25 semispans above and below the
leading edge z coordinate.

For each option presented above, a grid of coordinates, at which the
downwash information is calculated, must be established. The first option
was originally designed to compute the downwash in any x = constant plane at
all the grid points determined by y varying from 0 to 1.1 semispans in steps
of .05 semispans with z ranging from .25 semispans above and below a specified
z station in steps of .05 semispans. This required calculating downwash and
sidewash angles at 253 points. Numerical difficulties were usually encountered
at one or more of the grid points because of the grid points being located
very near a vortex segment. The vortex velocities by definition are unbounded
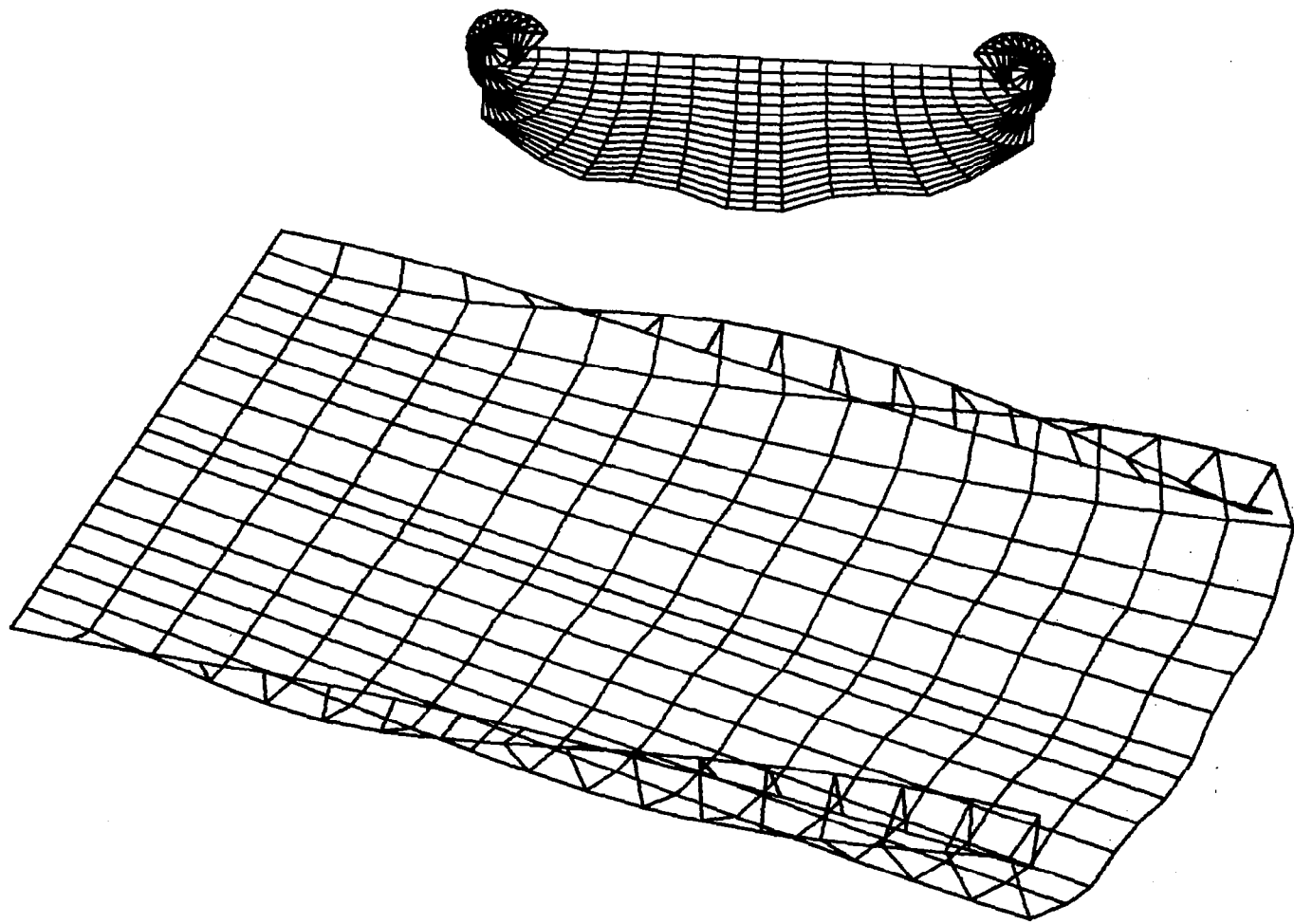
Figure 14.   Sample of wake sheet end view and orthographic projection.

at the vortex center; thus, unrealistic velocities may be predicted if the grid point is too near a vortex segment. To correct this difficulty an attempt was made to determine an optimum distance to a filament such that the filament's contributions would be included or excluded depending on whether the distance to the filament was greater or less than the optimum. While this procedure was successful in producing reasonable values of downwash angle, it does not guarantee a smooth variation in downwash in either the y or z direction since the downwash at one of two closely-spaced points may include the contribution from a filament while the downwash computed at the other point may not.

To insure a smooth variation, the following procedure is used. The user-specified x-station at which the downwash information is required must be a multiple of the stepsize; for upwash calculations any negative x-station ahead of the wing leading edge may be used. The y and z coordinates for the 6 most inboard vortices on the positive y-axis are used to establish a new grid system. Using the y coordinate at one of the six vortices as constant, the total flow angularity (vector sum of downwash and sidewash angles) and the sidewash and downwash angles are calculated for z ranging from .25 semispans above and below the z coordinate of that vortex. This procedure is also carried out for the other five most inboard vortices yielding a grid system similar to that given in Figure 15.
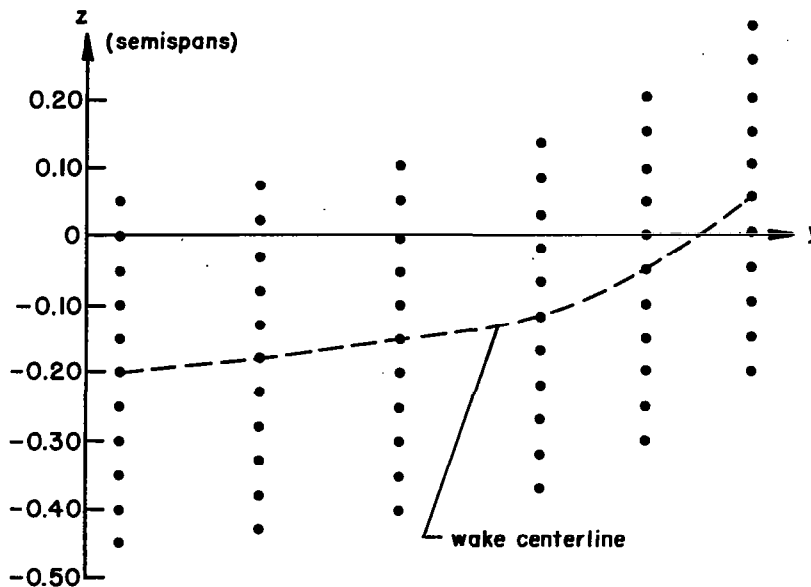
Figure 15. Example spacing for downwash calculations using NXORY=1 option (spanwise variation).

40

The numerical difficulties encountered because of the contribution of the vortex segment to the field in its immediate vicinity are eliminated by (1) excluding, for example, the contribution of vortex 11 when calculating the flow angles above and below the z coordinate of vortex 11, and (2) calculating downwash above only the six most inboard vortices which, for x-distances comparable to horizontal tail locations, have not rolled-up and therefore do not pass above or below another vortex trace. The exclusion of vortex 11 when determining the flow angles above and below it will not affect the downwash; however, the sidewash will be in error. Since the downwash and not sidewash is the quantity which the program is designed to predict, the error in sidewash is tolerated. The option discussed above is produced when the input variable NXORY is specified as 1 and STAT is read as the desired x-station in semispans. A detailed description of these and the other necessary input variables is given in the User Instructions section of Appendix A.

Option number two in the WASH program computes the downwash angles in the plane of symmetry, y = 0. The grid is specified by varying x from .25 to 1.75 semispans behind the trailing edge in steps of .05, and z ranging from .5 semispans above and below a midpoint z-value specified as the variable STAT. As above, numerical difficulties were encountered in some cases using this option because the most inboard shed or trailing vortex on a half-wing may be too close to some of the grid points. To remedy the problem in general, the downwash angles were calculated using only the 8 most-outboard vortices on both sides of the y = 0 plane, and the WASH program is written in this fashion. However, if the user desires to include the effect of the inboard vortex, the DO LOOP parameter may be changed from 8 to 9 on card PLA 110 of the WASH program. Inasmuch as the computations are made in the plane of symmetry, only half the wing need be analyzed to compute the downwash, and the sidewash is identically zero. This downwash information is computed in the plane of symmetry when the variable NXORY = 2 and STAT is the desired midpoint value of z in semispans.

If NXORY = 3, then upwash information is calculated in the plane of symmetry. The grid points at which upwash is computed are established by x ranging from the wing leading edge value of x at the wing root to .5 semispans ahead of the leading edge in steps of .05 semispans, and z varying from .25 semispans above and below the leading edge z coordinate. The upwash is calculated using all 18 trailing vortices without numerical difficulty. It should be pointed out however that the upwash values at the leading edge are excessively large because of the proximity to the bound vortex at the wing quarter-chord.

The WASH program is made up of a mainline, four subroutines, and a function subroutine. The mainline is the control center for reading and writing the specified and calculated information as well as the coding responsible for tracing the position of the vortex system downstream. The mainline calls the following subroutines: (1) SPLINE to obtain a spline fit of the bound vortex strength versus semispan distance, (2) WB which computes

the induced velocity components at a point due to the bound vortex using the function WBB, (3) WTRAIL to calculate the induced velocity components at a point due to a straight-line trailing vortex segment, and (4) PLANE to determine the downwash information in the plane specified by the user. The mainline contains the coding responsible for tracing the shed vortices downstream using a maximum of 18 steps behind the trailing edge. Using this deflected vortex system the downwash information is calculated at each of the grid points given by subroutine PLANE for the user specified plane of interest.

The program listing, sample data set, and sample output are presented along with User Instructions in Appendix A. The next section of this report presents a brief discussion of results obtained by running the program for several test cases, some of which are compared with experimental data.

42

DISCUSSION OF PROGRAM RESULTS

Results given by the WASH program were compared with two separate examples of USA 45 wings (Ref. 7) at different angles of attack, and, in addition, a sample calculation of the wake sheet location and downwash at the tail was obtained for the ATLIT (Advanced Technology Light Twin) aircraft. The theoretical section lift distribution taken from Reference 7 and given in Figure 16 served as the basis of the calculations in the WASH program. Figures 17 and 2 show the experimental lines of constant downwash angle in the plane of symmetry behind the wing and the angles predicted in Reference 7, respectively. The results of the WASH program are given in Figure 18. Reference 7, notes that the theoretical downwash of Figure 2 along the wake centerline at large distances (two semispans) appears to be approaching a value of 7.8°, while the experimental value is less than 6.6°. Reference 7 indicates that the theoretical value given in Figure 2 is too large because the method did not include spanwise curvature. The WASH program, which includes spanwise curvature, gives a value closer to the experimental result in the vicinity of the horizontal tail location. Near the wing trailing edge the theoretical method of Reference 7 over-predicts the downwash angles while the WASH program underpredicts it as compared with the experimental value. It should be noted that some difference between theory and experiment may be attributed to the fact that the Γ distribution is theoretical rather than experimental.

The experimental Γ distribution given in Figure 19 for the USA 45 airfoil was inserted in the WASH program to compare the spanwise variation in downwash with experimental values presented in Figure 20. The WASH program results are presented in Figure 21. A comparison of these two figures indicate that the total flow angular deviations computed by WASH are smaller in general than the experimental values; also, Figure 20 depicts positive sidewash angles both above and below the wake centerline while WASH predicts positive below and negative above as would be expected by vortex theory.

The wake sheet is given for each USA 45 Γ distribution discussed above in Figures 22 and 23. Each wake sheet figure was obtained by executing the plot data set from the WASH program in the PLOT program of Reference 4. While both distributions are for the same airfoil section, an examination of Figures 16 and 19 gives an indication of how wake sheet shape is affected by the section lift distribution.

NASA is currently supporting the development of the ATLIT aircraft to investigate the potential of new aerodynamic techniques for improving the performance of light twin engine aircraft. A three-view of the ATLIT is given in Figure 24 and a perspective view is given in Figure 25. A contributer to this program, N. C. State University, is currently involved in both a performance prediction and a flight evaluation program for the ATLIT, the results of which should be published as a NASA Contractor's Report early in 1977. In conjunction with this program, it was decided to analyze the ATLIT wing using the WASH program to find the downwash characteristics at the horizontal tail

in the plane of symmetry. The section lift coefficient distribution of the wing with fuselage was obtained by the methods given in Reference 4. The nacelles were neglected for this test case. The program input data set is given in Figure A-2. Figure A-3 gives typical program output: tabulated data for the spanwise variation of the downwash and sidewash in the plane of the horizontal tail, the downwash in the plane of symmetry, and the upwash ahead of the wing for a wing lift coefficient of 1.22. The wake sheet plot (Figure 26) indicates that the high wing aspect ratio (ten) yields relatively low values of downwash in the vicinity of the horizontal tail. Figure 27 is included to show the variation of upwash ahead of the wing in the plane of symmetry along with the downwash variation behind the wing. The excessively large upwash angles at the leading edge are due to the nearness of the bound vortex at the wing quarter-chord.

The cases presented above, although limited in number, show good agreement with experimental data. These test cases also indicate the type of information yielded by the WASH program; to the extent that interference effects from the fuselage and horizontal tail can be neglected, the program fulfills the design objectives of defining both the wake sheet location in the vicinity of the horizontal tail and the downwash distribution in both the spanwise and freestream directions. The program's capability for computing upwash ahead of the wing has also been demonstrated.

44
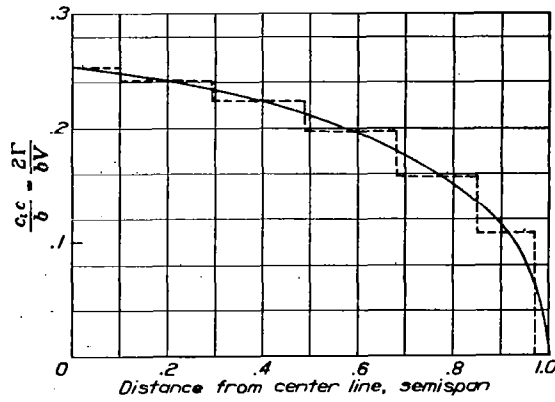
Figure 16. Theoretical $\Gamma(y)$ distribution for the 3.66 m USA
45 tapered wing with $C_L = 1.175$ (Ref. 7).
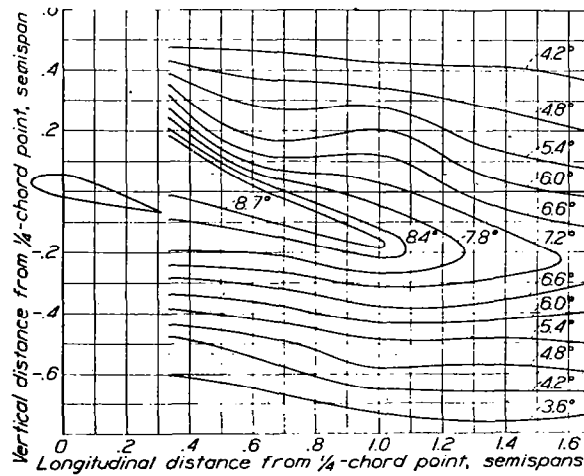
Figure 17. Experimental downwash angle contours in the plane of symmetry
behind a 3.66 m USA 45 tapered wing with $C_L = 1.175$ (Ref. 7).
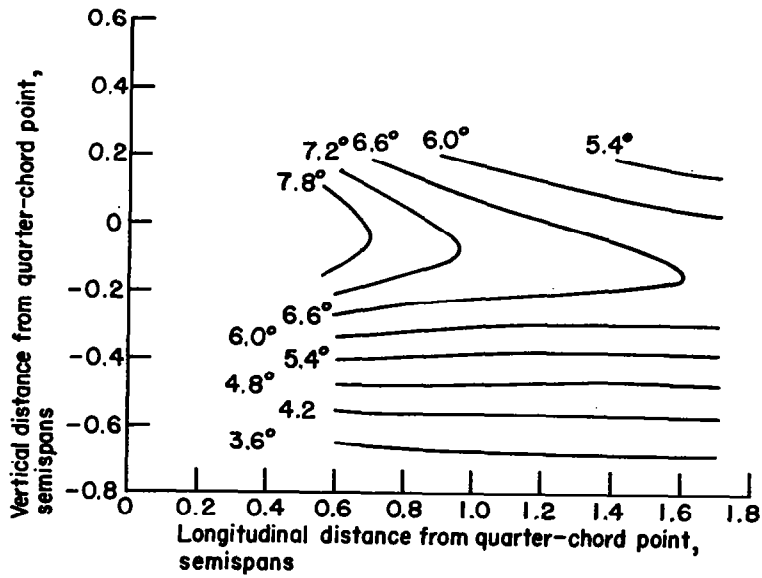
Figure 18.   Downwash angle contours in the plane of symmetry behind a
3.66m USA 45 tapered wing at C_L = 1.175 using WASH program.
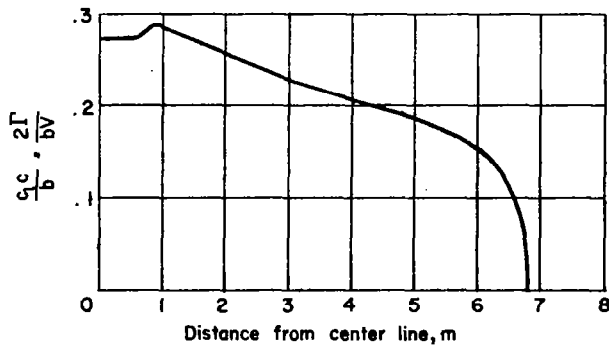
Figure 19.   Experimental span load distribution for the USA 45 wing
at C_L = 1.35 (Ref. 7).
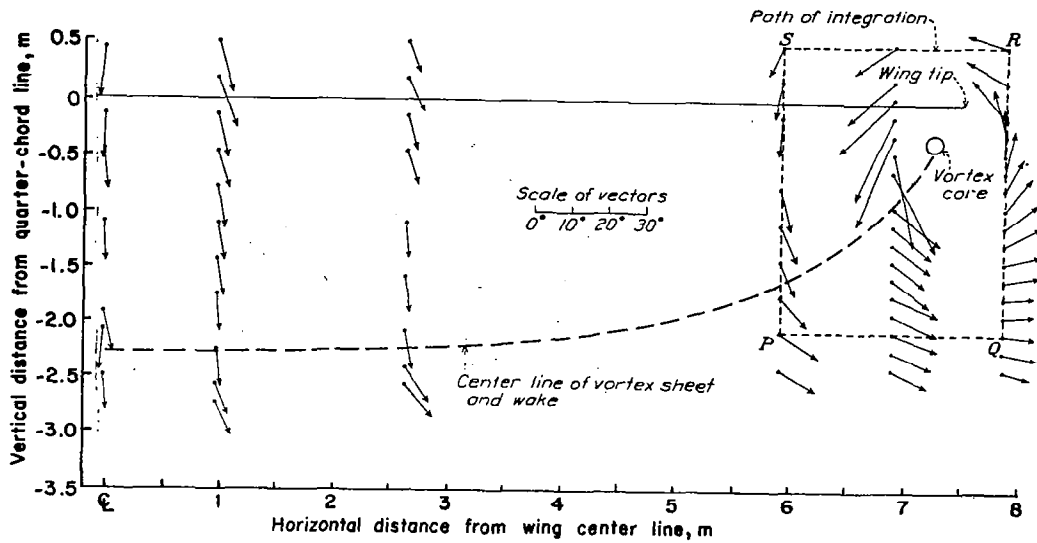
Figure 20. Experimental air flow 7.92m behind c/4 line of USA 45 wing at
C_L = 1.35 with vectors denoting deviation from freestream (Ref. 7).
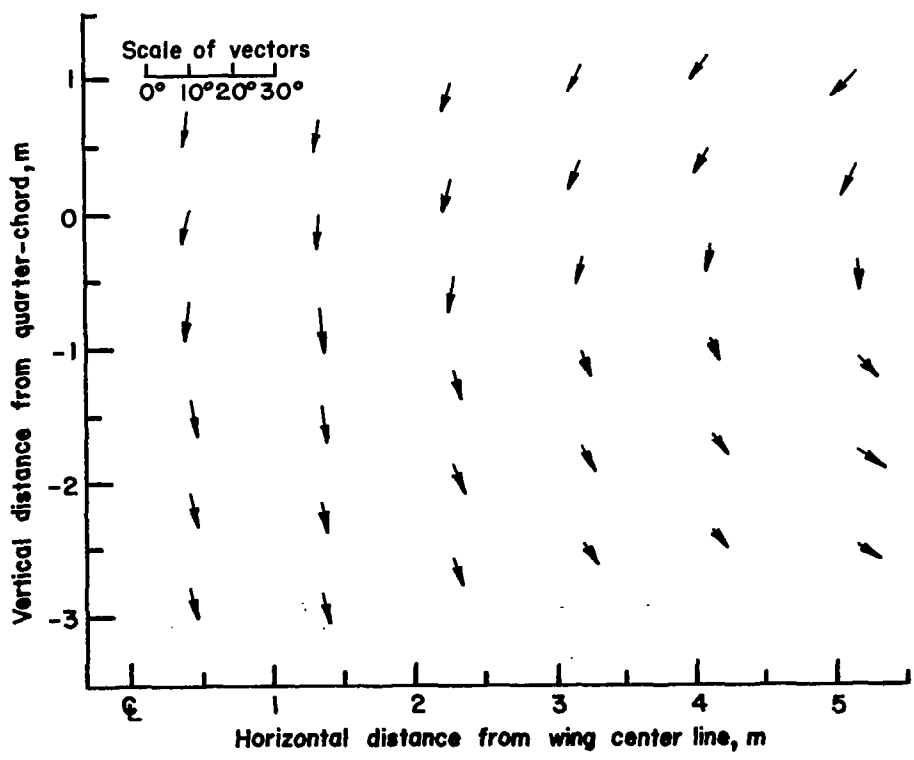
Figure 21. Air flow 7.92m behind c/4 line of the USA 45 wing at C_L = 1.35 using
WASH program with vectors denoting deviation from freestream.

47
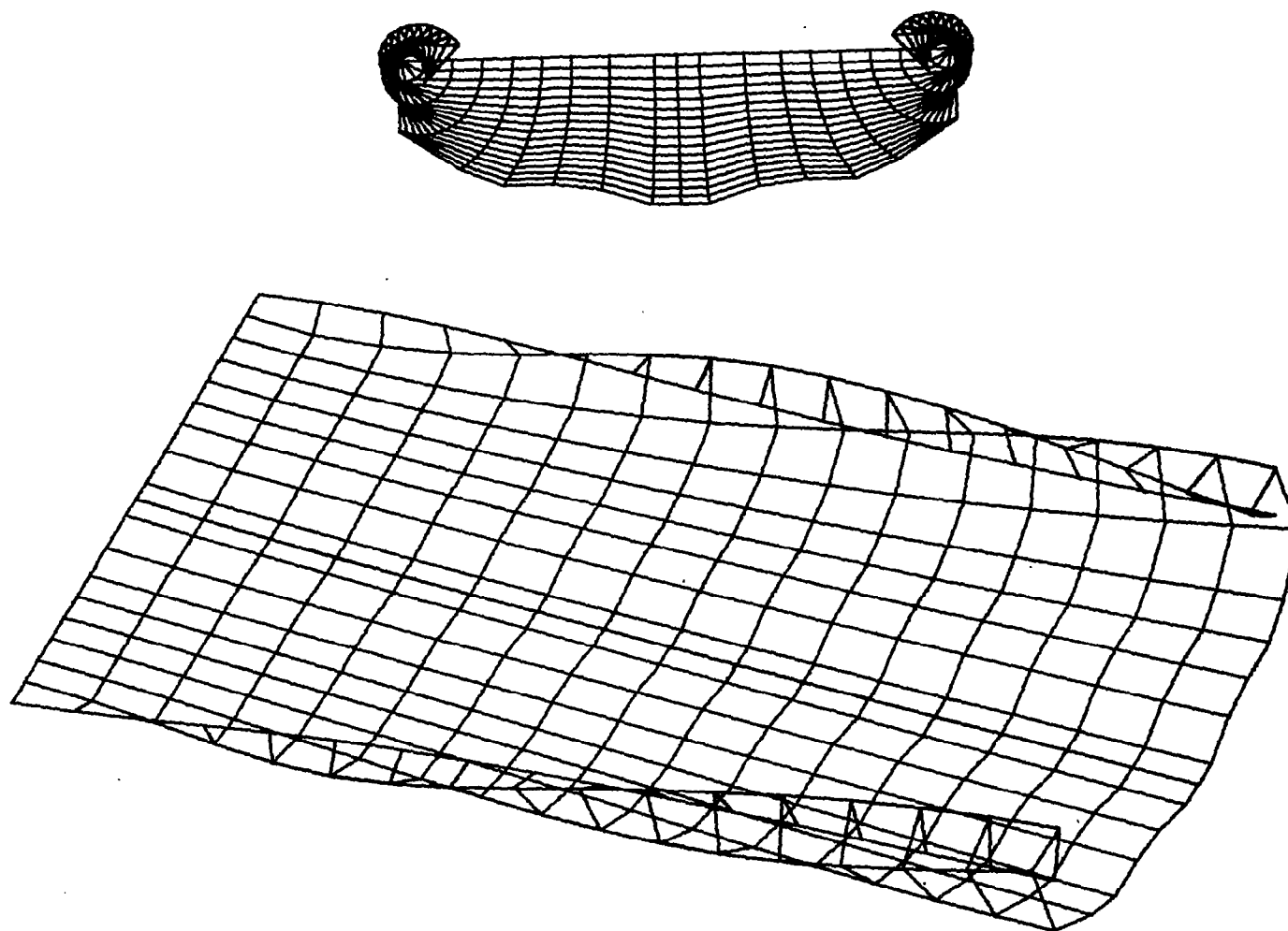
Figure.22. Wake sheet end view and orthographic projection of the USA 45 wing at C_L = 1.175 (Γ distribution taken from Figure 16).
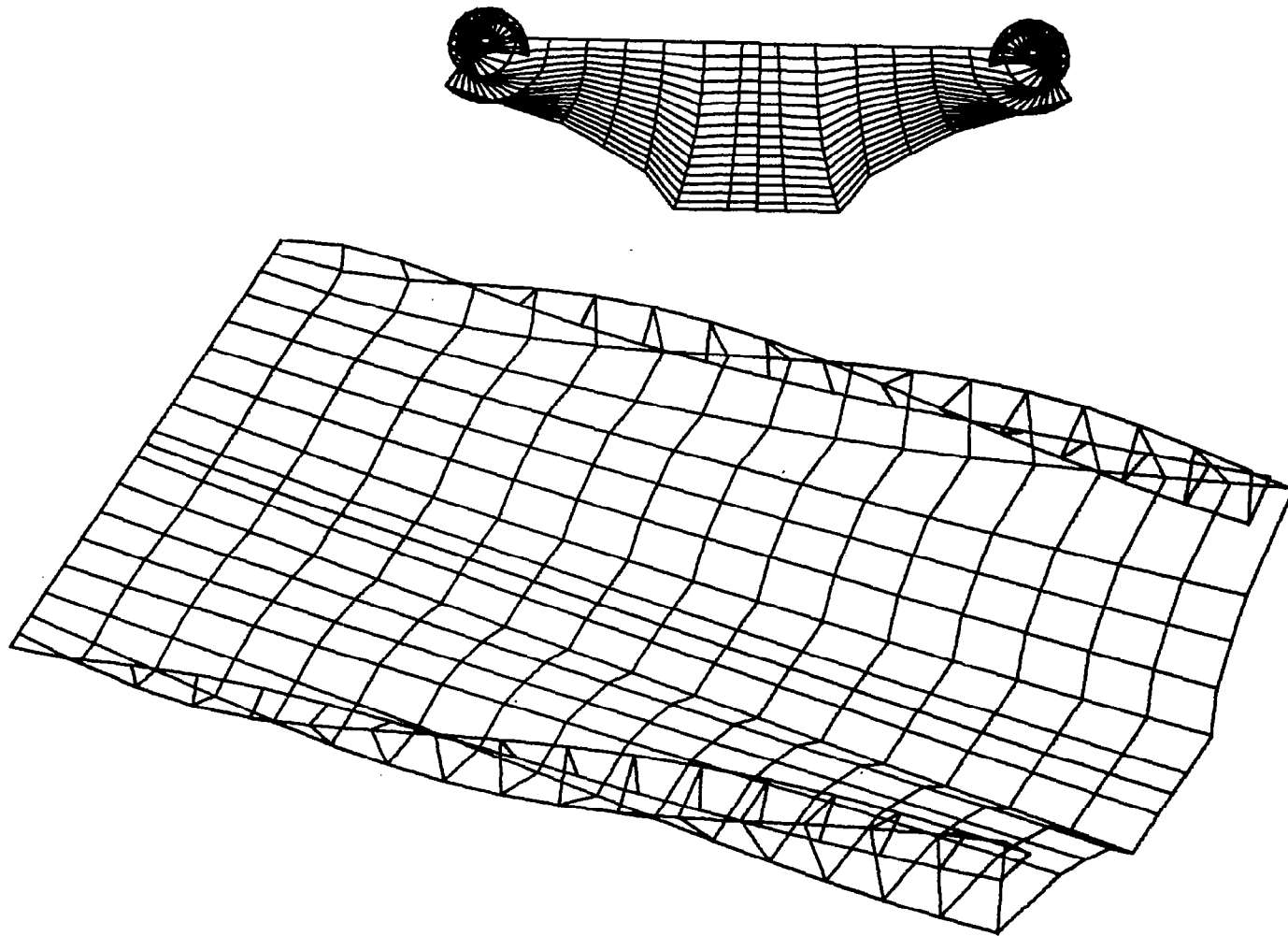
Figure 23. Wake sheet end view and orthographic projection of the USA 45 wing at C_L = 1.35 (Γ distribution taken from Figure 19).
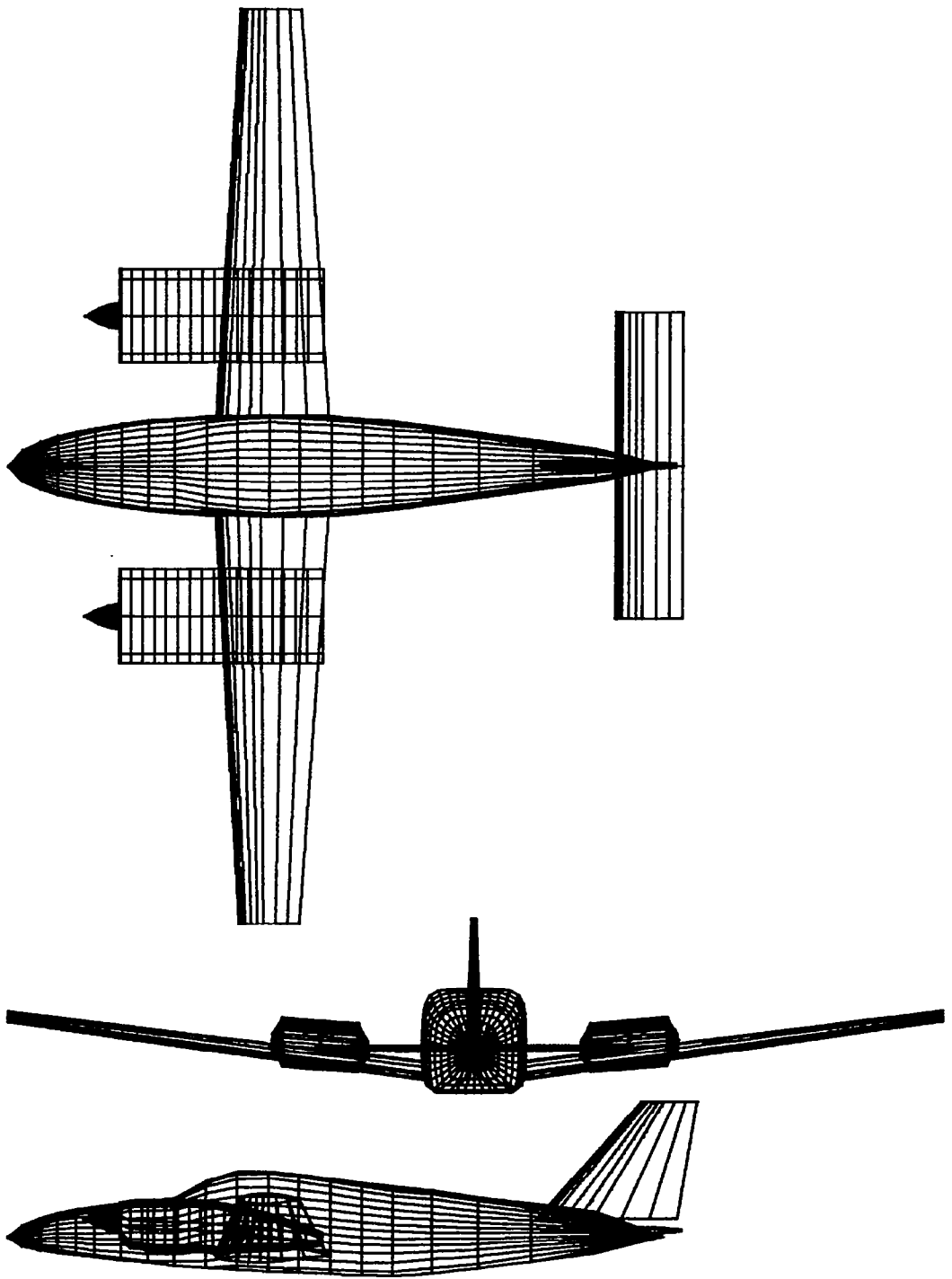
Figure 24.   Plotted 3-view of ATLIT aircraft.
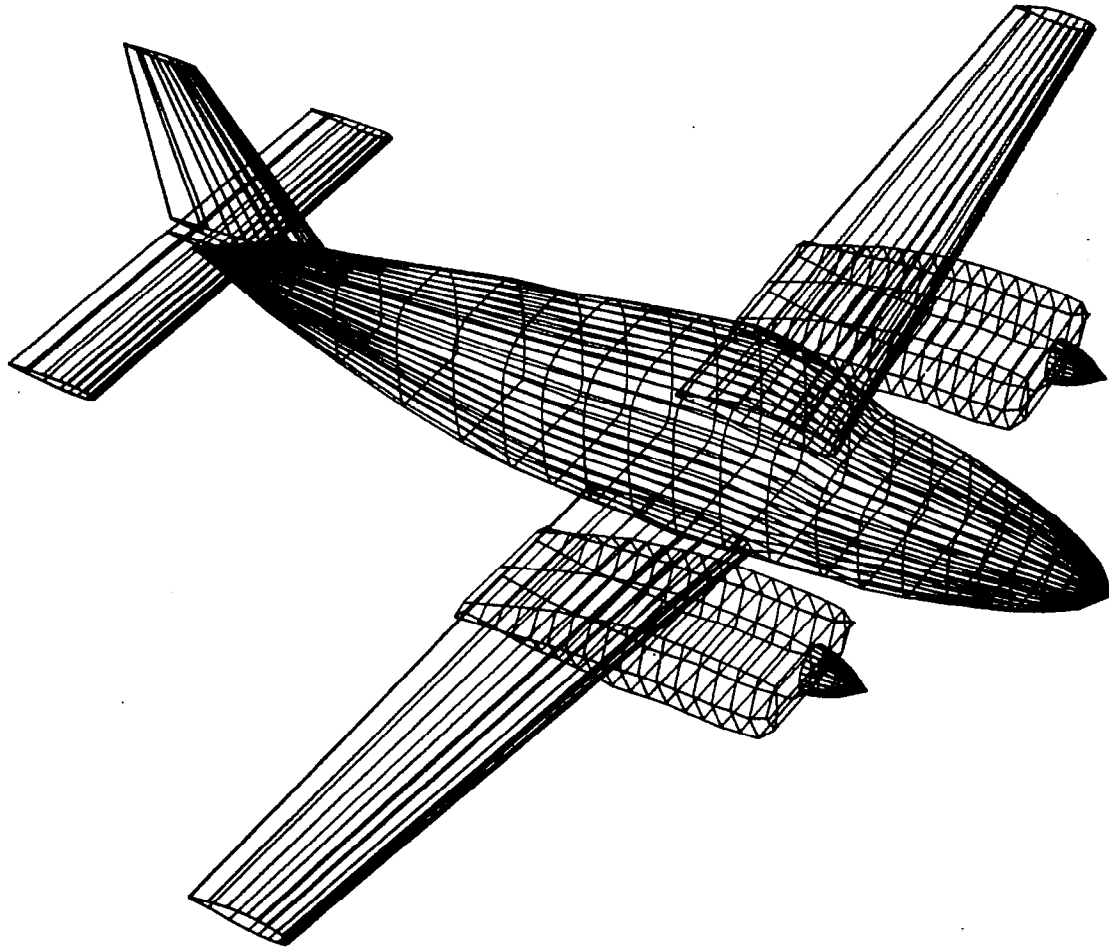
Figure 25. Perspective view of the ATLIT aircraft.
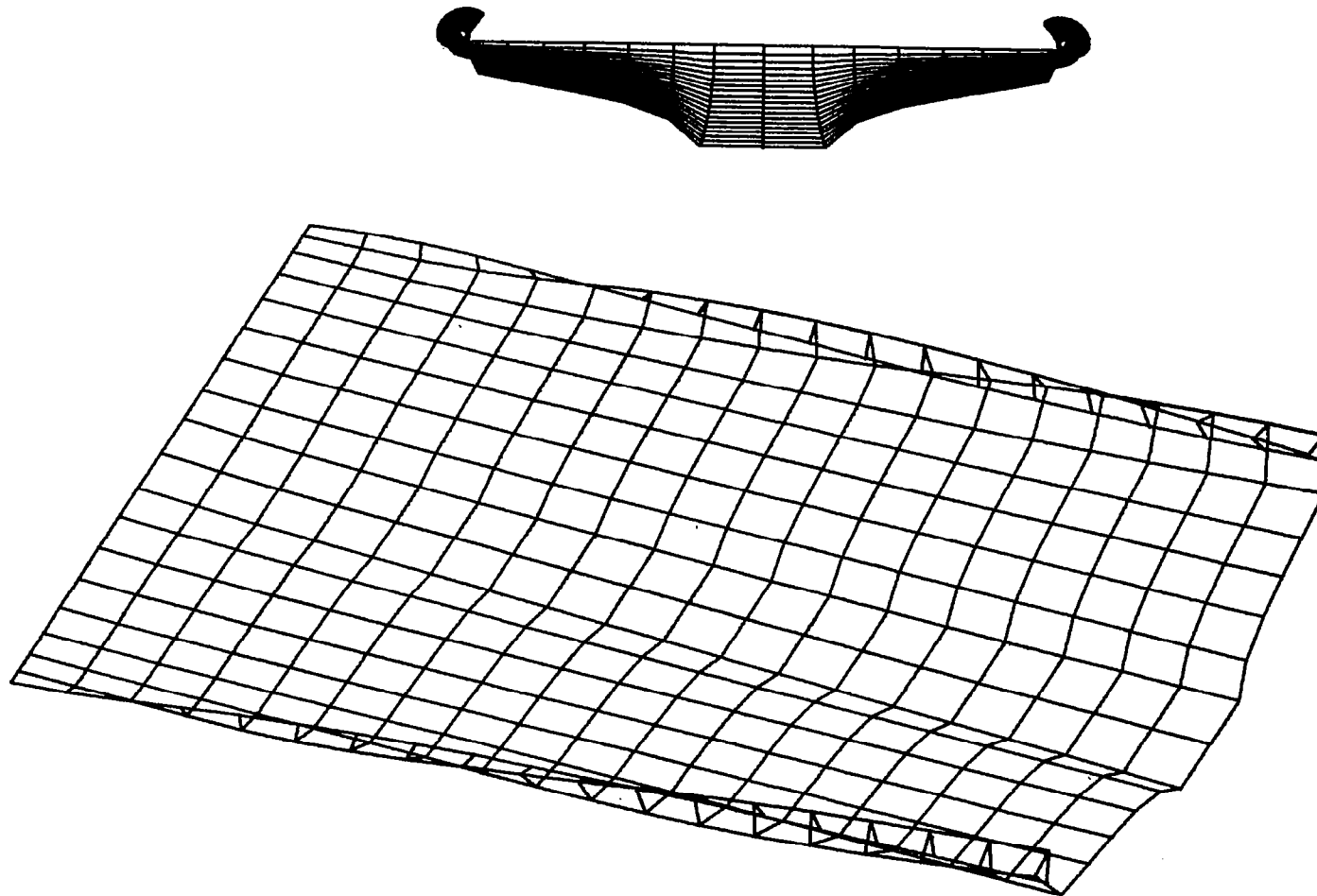
Figure 26. Wake sheet end view and orthographic projection of the ATLIT wing at $C_L = 1.22$.
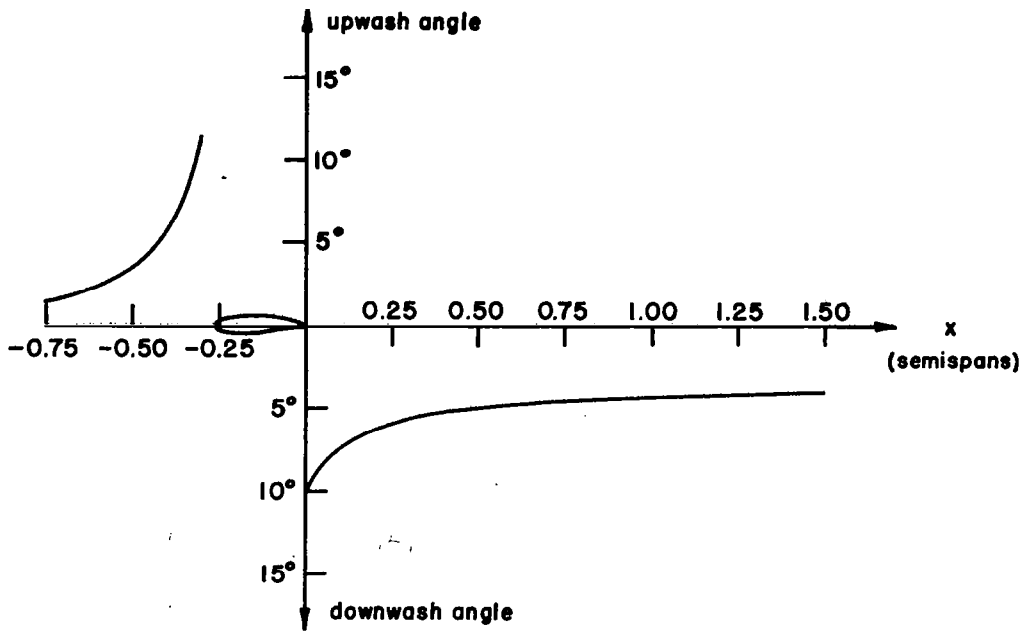
Figure 27.   Upwash and downwash angles in the plane of symmetry of the
            ATLIT wing at C_L = 1.22.

53
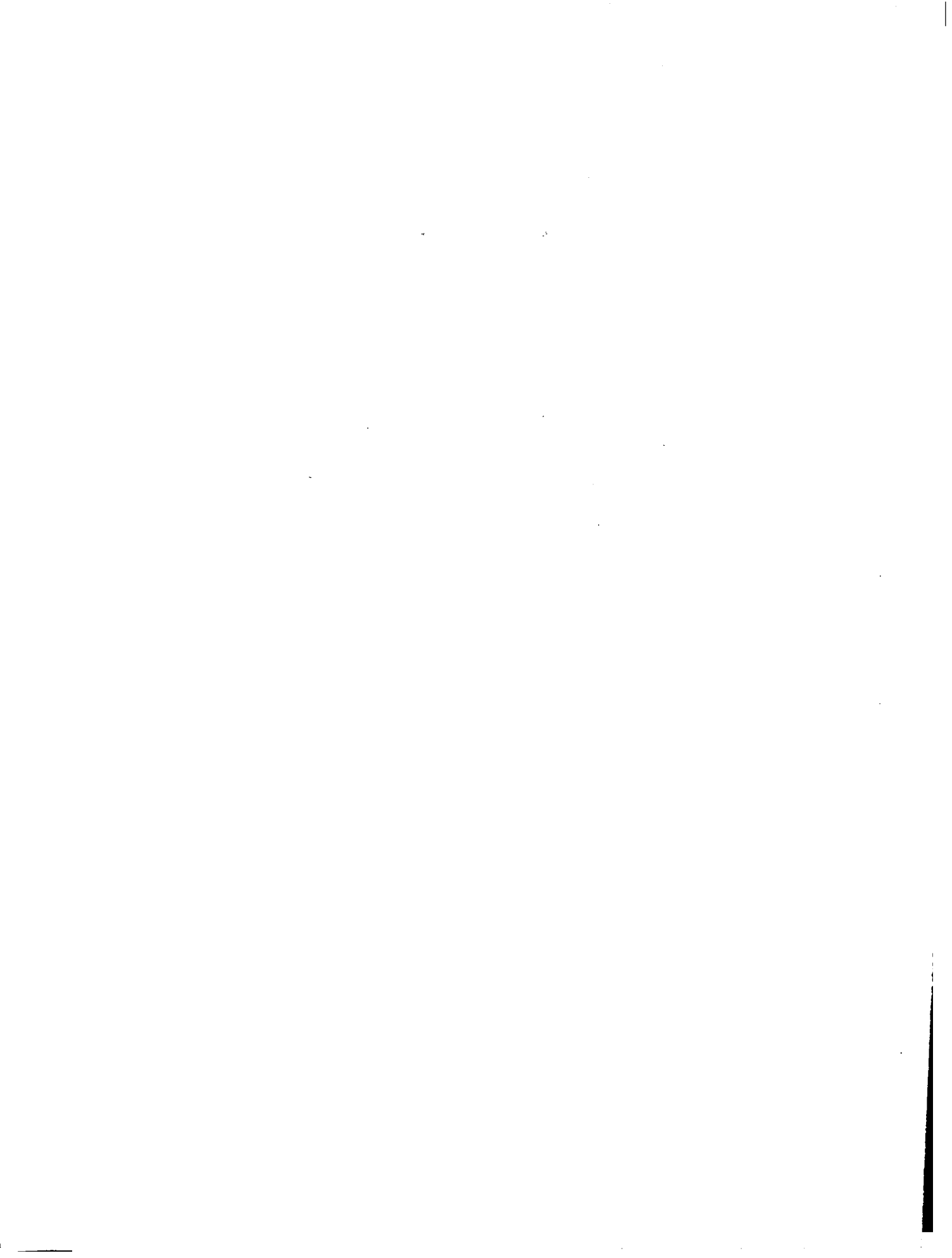
PROGRAM FOR VELOCITY

PROFILE CALCULATION
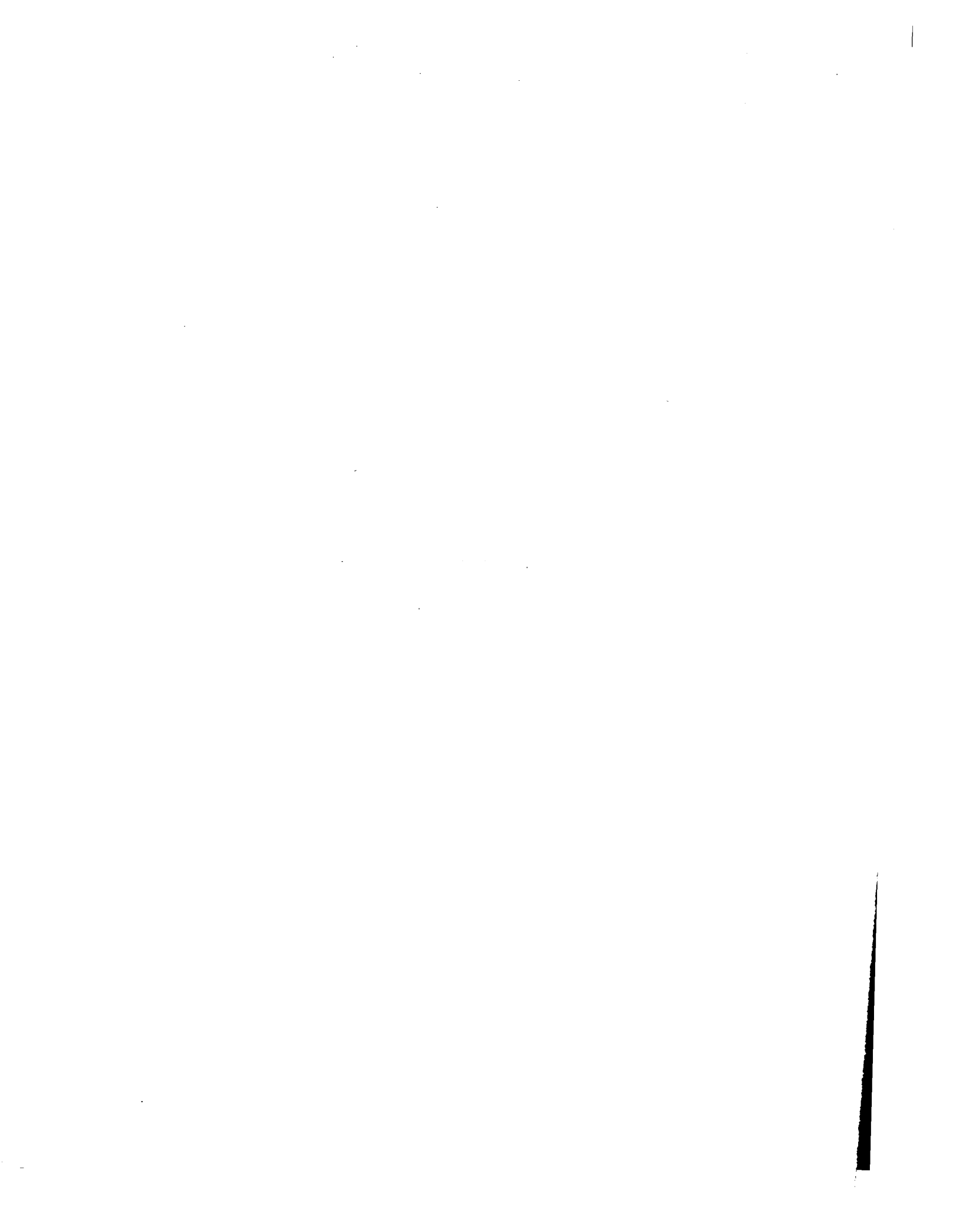
GENERAL THEORY

Once the location of the wake sheet centerline has been established using the WASH program, a viscous solution behind the wing may be obtained by solving the two-dimensional boundary layer equations along wake streamlines defined by the shed vortex paths. This same technique was applied to boundary layer solutions over arbitrary bodies with good success in Reference 4, and the results should be reasonable in this application as long as (1) the spanwise flow is small compared to the freestream flow, and (2) the streamline curvature is not large. These conditions of course are violated as one moves downstream from the wing tip and the vortices begin to roll-up. However, for streamlines which pass near the horizontal tail the conditions for the use of two-dimensional boundary layer analysis are usually satisfied quite well. Thus, this approach should be adequate for the purpose of this study which is to determine the magnitude and direction of the flow in the vicinity of the horizontal tail. The WASH program permits only nine shed vortices to the half-wing; thus, probably no more than the three most inboard vortex traces will pass inboard of the tail tip section.*

As noted in the literature review, the inclusion of curvature in the boundary layer equations greatly increases the complexity. In order to determine whether or not curvature effects should be included in the analysis results from several executions of the WASH program were examined. When vortices for typical cases of spanwise lift distributions were traced downstream, it was found that while the inboard vortex streamlines were deflected in the vertical and spanwise directions, the curvature of these streamlines was small due to the relatively slow rate of change of downwash and sidewash angles (see Figures 14 and 26) along a given vortex path. Since the curvature of the inboard vortices is small, it should not play a dominant role in a boundary layer solution near the horizontal tail. Consequently, the curvature terms in the boundary layer equations were neglected, greatly simplifying the solution process.

In order to find the flow velocities along streamlines in the vicinity of the horizontal tail including the effects of fluid viscosity, the computer program WAKE was written. Given an initial velocity profile at the airfoil trailing edge[++], the nonsimilar two-dimensional boundary layer equations are solved using a finite difference method with even stepsize in the transverse direction and unequal stepsize in the streamwise direction. The remainder of this section will be concerned with a discussion of the WAKE program theory.

The boundary layer equations (Equations 11 and 12) are written in a form more amenable to numerical solution through use of both the stream function ψ (defined by $u = \frac{\partial \psi}{\partial y}$ and $v = -\frac{\partial \psi}{\partial x}$) which automatically solves Equation 11, and a proper scaling of the x and y variables. The scaling variables η and ξ and the stream function ψ were assumed to be of the form

---

* Because of typical span loadings, the third vortex out from the fuselage will probably be positioned at around 0.4 semi-spans, a location which should be further outboard than the tip of the horizontal tail plane on most light aircraft.

++The computer program providing this initial velocity profile is given in Ref. 4.

57

$$\eta = \frac{y}{\sqrt{100c_d t x}} \quad \text{and} \quad \xi = \frac{x}{c} \qquad (33)$$

and

$$\psi(x,y) = U_\infty \sqrt{100c_d t x}\ f(\xi,\eta) \qquad (34)$$

where
c = wing chord
t = wing thickness
c_d = wing section drag coefficient
U_∞ = freestream velocity
ξ = nondimensional distance downstream of the trailing edge
η = nondimensional, scaled y coordinate normal to the x-direction
$f(\xi,\eta)$ = function of ξ and η which will appear as the unknown in the transformed boundary layer equations.

Since the continuity equation is identically satisfied by the definition of the stream function, it is necessary only to solve the momentum equation given by Equation 12 and rewritten, using Equation 13, as

$$u\frac{\partial u}{\partial x} + v\frac{\partial u}{\partial y} = \epsilon\frac{\partial^2 u}{\partial y^2}\ . \qquad (35)$$

Introducing the definition of the stream function and replacing x and y by the scaled variables, Equation 35 becomes

$$\{U_\infty f'\}\{U_\infty(\frac{\partial f'}{\partial \xi}\frac{1}{c} + f''\frac{\partial \eta}{\partial x})\} - U_\infty\sqrt{100c_d t x}\ \{\frac{f}{2x} + \frac{\partial f}{\partial \xi}\frac{1}{c} + f'\frac{\partial \eta}{\partial x}\}\{\frac{U_\infty}{\sqrt{100c_d t x}}\ f''\}$$

$$= \frac{\epsilon\ U_\infty}{100c_d t x}\ f''' \ , \qquad (36)$$

where the primed quantities denote derivatives with respect to the variable η. Simplifying the above equation, one has

$$\frac{f'}{c}\frac{\partial f'}{\partial \xi} - (\frac{f}{2x} + \frac{\partial f}{\partial \xi}\frac{1}{c})f'' = \frac{\epsilon}{U_\infty(100c_d t x)}\ f''' \ , \qquad (37)$$

or, multiplying by x and rearranging,

58

$$\frac{\varepsilon}{100c_d\dagger U_\infty} \, f''' + \frac{1}{2} \, ff'' - \xi\{f'\frac{\partial f'}{\partial \xi} - f''\frac{\partial f}{\partial \xi}\} = 0 \, . \qquad (38)$$

Equation 38 must therefore be solved at every ξ station (non-similar solution) downstream in order to obtain the velocity as a function of η. It is a third order partial differential equation in f requiring the three boundary conditions:

$$u(x,y\rightarrow\infty) = U_\infty \rightarrow u(\xi,\infty) = U_\infty \rightarrow f'(\xi,\infty) = 1$$

$$u(x,y\rightarrow-\infty) = U_\infty \rightarrow u(\xi,-\infty) = U_\infty \rightarrow f'(\xi,-\infty) = 1 \qquad (39)$$

$$v(x,y=0) = 0 \rightarrow f(\xi,0) + 2\xi \, \frac{\partial f}{\partial \xi}\bigg|_{\xi=0} = 0 \, .$$

Equation 38 together with the boundary conditions given in Equations 39 is solved in the WAKE program by the finite difference technique described below. Let $f' = T$; then

$$T'' + \frac{c_1 f}{2} \, T' - c_1\xi\{f'\frac{\partial T}{\partial \xi} - T'\frac{\partial f}{\partial \xi}\} = 0 \, , \qquad (40)$$

where $\quad c_1 = 100c_d\dagger U_\infty/\varepsilon.$

Simplify Equation 40 to read

$$T'' + \alpha_1 T' + \alpha_2 \, \frac{\partial T}{\partial \xi} = 0 \, , \qquad (41)$$

where

$$\alpha_1 = c_1(\frac{f}{2} + \xi \, \frac{\partial f}{\partial \xi}) \qquad \text{and} \qquad \alpha_2 = - \, c_1\xi f' \, . \qquad (42)$$

Equation 41 has, through this process, been converted into a second order "linear" equation in T with supposedly known coefficients. This equation is solved by assuming a solution to evaluate the α's and then, using an iterative process, T is computed numerically and the α's are corrected after each iteration until convergence is attained. Consider the grid system shown in Figure 28. If the solution is known at some station m for all n, then using central and backwards difference formulas, the solution is constructed at the station m + 1 for all n. The derivatives are approximated with the following relations taken from Reference 19:

59
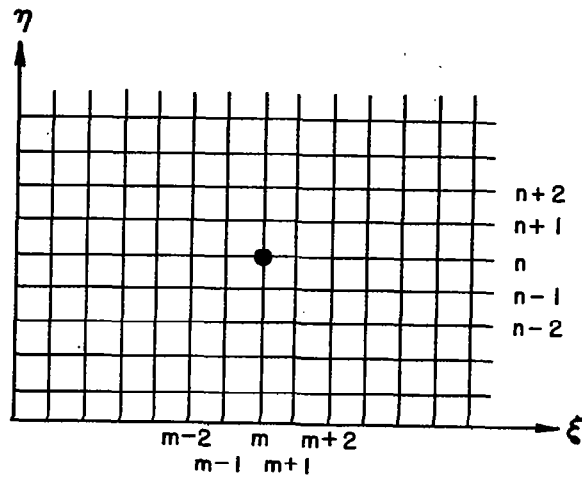
Figure 28. Grid system for finite difference solution.

$$\left.\frac{\partial^2 T}{\partial \eta^2}\right|_{n,m+1} = \frac{T_{n+1,m+1} - 2T_{n,m+1} + T_{n-1,m+1}}{(\Delta\eta)^2}$$

$$\left.\frac{\partial T}{\partial \eta}\right|_{n,m+1} = \frac{T_{n+1,m+1} - T_{n-1,m+1}}{2\Delta\eta}$$

$$\left.\frac{\partial T}{\partial \xi}\right|_{n,m+1} = \left[\frac{h_2}{h_1(h_1 + h_2)}\right]T_{n,m-1} - \left[\frac{h_1 + h_2}{h_1 h_2}\right]T_{n,m} + \left[\frac{h_1 + 2h_2}{h_2(h_1 + h_2)}\right]T_{n,m+1}$$

where $h_1 = \xi_m - \xi_{m-1}$, $h_2 = \xi_{m+1} - \xi_m$, and $\Delta\eta$ = equal stepsize in the n direction. Equation 41 is now rewritten as

---

* This method is based on that presented by Cebeci and Smith in McDonnell-Douglas Aircraft Co. Inc. Report No. DAC-67130, October 1968, "A Finite-Difference Solution to the Incompressible Turbulent Boundary Layer Equations by an Eddy-Viscosity Concept".

60

$$\left[\frac{1}{(\Delta\eta)^2} + \frac{\alpha_1}{2\Delta\eta}\right]T_{n+1,m+1} + \left[\frac{-2}{(\Delta\eta)^2} + \alpha_2\{\frac{h_1 + 2h_2}{h_2(h_1 + h_2)}\}\right]T_{n,m+1} + \left[\frac{1}{(\Delta\eta)^2} - \frac{\alpha_1}{2\Delta\eta}\right]T_{n-1,m+1}$$

$$+ \alpha_2\left[\{\frac{h_2}{h_1(h_1 + h_2)}\}T_{n,m-1} - \{\frac{h_1 + h_2}{h_1 h_2}\}T_{n,m}\right] = 0 \qquad (44)$$

or,

$$A_n T_{n+1,m+1} + B_n T_{n,m+1} + C_n T_{n-1,m+1} = D_n \; , \qquad (45)$$

where

$$A_n = \frac{1}{(\Delta\eta)^2} + \frac{\alpha_1}{2\Delta\eta}$$

$$B_n = \frac{-2}{(\Delta\eta)^2} + \alpha_2 \frac{h_1 + 2h_2}{h_2(h_1 + h_2)}$$

$$C_n = \frac{1}{(\Delta\eta)^2} - \frac{\alpha_1}{2\Delta\eta}$$

$$D_n = \alpha_2 \{\frac{-h_2}{h_1(h_1 + h_2)}\}T_{n,m-1} + \{\frac{h_1 + h_2}{h_1 h_2}\}T_{n,m} \quad . \qquad (46)$$

The total number, n_{max}, of n-stations must be odd. The bottom of the wake ($\eta \to -\infty$) is defined by n = 1 while the top ($\eta \to +\infty$) is defined by n = n_{max}. The wake center is defined by $n_{mid} = (n_{max} - 1)/2 + 1$. The boundary conditions can therefore be specified using the index n as

$$@ \; n = 1 \qquad T_{n,m+1} = 1$$

$$@ \; n = n_{mid} \qquad f(\xi,0) + 2\xi \left.\frac{\partial f}{\partial \xi}\right|_{(\xi,0)} = 0 \qquad (47)$$

$$@ \; n = n_{max} \qquad T_{n,m+1} = 1 \; .$$

Equation 45, when written in matrix form, becomes:

$$
\begin{bmatrix}
1 & 0 & 0 & 0 \\
C_2 & B_2 & A_2 & 0 \\
0 & C_3 & B_3 & A_3 \\
 & & & \ddots \\
 & & C_{n-2} & B_{n-2} & A_{n-2} & 0 \\
 & & 0 & C_{n-1} & B_{n-1} & A_{n-1} \\
 & & 0 & 0 & 0 & 1
\end{bmatrix}
\begin{bmatrix}
T_1 \\ T_2 \\ T_3 \\ \vdots \\ T_{n-2} \\ T_{n-1} \\ T_n
\end{bmatrix}
=
\begin{bmatrix}
1 \\ D_2 \\ D_3 \\ \vdots \\ D_{n-2} \\ D_{n-1} \\ 1
\end{bmatrix}
$$

The solution procedure for this set of equations can be greatly simplified because the matrix is tridiagonal. If the matrix is denoted by A, then

$$ A \, T = D . \tag{49} $$

Now let

$$ A = L \, X \tag{50} $$

where

$$
L =
\begin{bmatrix}
\omega_1 & 0 & 0 \\
\beta_2 & \omega_2 & 0 \\
0 & \beta_3 & \omega_3 \\
 & & & \ddots \\
 & & & \beta_{n-1} & \omega_{n-1} & 0 \\
 & & & 0 & \beta_n & \omega_n
\end{bmatrix}
, \quad
X =
\begin{bmatrix}
1 & -E_1 & 0 \\
0 & 1 & -E_2 \\
 & & & \ddots \\
 & & & 0 & 1 & -E_{n-1} \\
 & & & 0 & 0 & 1
\end{bmatrix}
$$

and

62

$$LX = \begin{bmatrix} \omega_1 & -\omega_1 E_1 & 0 & 0 & 0 \\ \beta_2 & (-E_1\beta_2 + \omega_2) & -E_2\omega_2 & 0 & 0 \\ 0 & \beta_3 & (-E_2\beta_3 + \omega_3) & -E_3\omega_3 & 0 \\ 0 & 0 & \beta_4 & (-E_3\beta_4 + \omega_4) & -\omega_4 E_4 \\ & & & & \ddots \end{bmatrix}$$

thus, $\beta_2 = C_2$ $\omega_1 = 1$ $-\omega_1 E_1 = 0$

$\beta_3 = C_3$ $-E_1\beta_2 + \omega_2 = B_2$ $-\omega_2 E_2 = A_2$

$\beta_4 = C_4$ $-E_2\beta_3 + \omega_3 = B_3$ $-\omega_3 E_3 = A_3$

$\vdots$ $\vdots$ $\vdots$

$\beta_n = C_n$ $-E_{n-1}\beta_n + \omega_n = B_n$ $-\omega_n E_n = A_n$

Applying the above equations, a step by step procedure is used to evaluate the β's, ω's, and E's given the A_n's, B_n's, and C_n's. From Equations 49 and 50,

$$L \, X \, T = D \, , \tag{51}$$

and if

$$X \, T = e \, , \tag{52}$$

then

$$L \, e = D \, , \tag{53}$$

or

$$
\begin{bmatrix}
\omega_1 & 0 & 0 & 0 & & & & \\
\beta_2 & \omega_2 & 0 & 0 & & & & \\
0 & \beta_3 & \omega_3 & 0 & & & & \\
0 & 0 & \beta_4 & \omega_4 & & & & \\
& & & & \ddots & & & \\
& & & & & \beta_{n-1} & \omega_{n-1} & 0 \\
& & & & & 0 & \beta_n & \omega_n
\end{bmatrix}
\begin{bmatrix}
e_1 \\ e_2 \\ e_3 \\ e_4 \\ \vdots \\ e_{n-1} \\ e_n
\end{bmatrix}
=
\begin{bmatrix}
D_1 \\ D_2 \\ D_3 \\ D_4 \\ \vdots \\ D_{n-1} \\ D_n
\end{bmatrix}
$$

If $e_1 = 1$ and $E_1 = 0$ then all the e's and E's are evaluated using the relations below

$$
e_n = \frac{D_n - C_n e_{n-1}}{B_n + C_n E_{n-1}} \qquad \text{and} \qquad E_n = \frac{-A_n}{B_n + C_n E_{n-1}} . \tag{54}
$$

The matrix Equation 52 may now be written as

$$
\begin{bmatrix}
1 & -E_1 & 0 & 0 & & & \\
0 & 1 & -E_2 & 0 & & & \\
0 & 0 & 1 & -E_3 & & & \\
& & & \ddots & & & \\
& & & & 0 & 1 & -E_{n-1} \\
& & & & 0 & 0 & 1
\end{bmatrix}
\begin{bmatrix}
T_1 \\ T_2 \\ T_3 \\ \vdots \\ T_{n-1} \\ T_n
\end{bmatrix}
=
\begin{bmatrix}
e_1 \\ e_2 \\ e_3 \\ \vdots \\ e_{n-1} \\ e_n
\end{bmatrix}
$$

Starting with T_n, the n values of T are obtained by using the recursive relation given below:

$$
T_n = e_n + E_n T_{n+1} . \tag{55}
$$

These T_n values represent the solution at the ξ station $m + 1$.

64

The general procedure given above may be summarized in the following manner:

(1) The solution is assumed to be known at the station ξ_m for all n.

(2) An approximate solution, T_{old} is assumed at the ξ_{m+1} station in order to evaluate the A_n's, B_n's, C_n's, D_n's, e_n's, and E_n's. (This approximate solution at station m+1 is usually taken to be the solution found for station m.)

(3) Using the computed values of e_n and E_n, the solution T_{new} is calculated using Equation 55.

(4) T_{old} and T_{new} are then compared to see if they are the same at every n station to within a certain accuracy; if not the T_{old} is set equal to T_{new} and steps (2) and (3) are repeated.

(5) This iteration procedure is continued until T_{old} and T_{new} are sufficiently close signaling a converged solution at the ξ station m+1. Usually, no more than two or three iterations are required.

(6) The procedure given in steps (1) through (5) is merely repeated for each subsequent downstream station.

As noted in (1) above, the finite difference technique requires that a solution be known at some ξ station in order to compute solutions downstream. While an actual velocity profile in the wing wake is not known in general, a profile shape can be found at the trailing edge of an airfoil on both the upper and lower surfaces whenever the flow over the airfoil is calculated. One method of finding the viscous solution over an airfoil is given in the 2-D Airfoil program of Reference 4. The flow is computed by solving the boundary layer flow over the airfoil with a momentum integral technique. Using the program output, the velocity profiles on both surfaces may be determined from their respective boundary layer thicknesses and form factors using the equations below:

$$\frac{u_u}{U_\infty} = (\frac{y}{\delta_u})^{(H_u-1)/2} \qquad \text{and} \qquad \frac{u_\ell}{U_\infty} = (\frac{y}{\delta_\ell})^{(H_\ell-1)/2} \qquad (56)$$

where
δ = boundary layer thickness at the trailing edge
H = turbulent form factor of the trailing edge
u & ℓ = subscripts denoting upper and lower surfaces.

Although Equations 56 do yield an initial velocity profile, there is still a problem due to the singular nature of the boundary layer equations at the airfoil trailing edge. From Equation 33, it is evident that η is unbounded at $\xi = 0$. Some procedure or technique must therefore be used to provide an initial profile downstream of the trailing edge. An investigation of the experimental

data given in Reference 26 and 27 indicated that at small distances downstream of the trailing edge, the velocity profile shape is still much the same as at the trailing edge. Based on this information, the assumption was made that the profile shape at a small distance downstream, say .01 chord lengths, is the same as the profile at the trailing edge. This technique was used to establish a profile at ξ = .01 in the WAKE program, and by assuming this profile satisfies the wake boundary layer equations, the initial requirements for the finite difference solution are satisfied. Although the program permits initial values other than .01 by requiring the value to be read into the program, this value was found to be satisfactory for all test cases presented in a later section of this report. Values of ξ less than .01 tended to make the maximum value of η too large, requiring an excessive number of steps in the η direction (Equation 33). For values larger than .01 the profile shape can no longer be approximated adequately by the trailing edge profile shape as seen from the experimental profiles.

Another problem which must be discussed arises from the fact that the boundary layer equation (Equation 35) contains no terms to account for pressure fluctuations in the y-direction. In the development of the boundary layer equations the pressure was assumed constant in the direction normal to the flow, eliminating the pressure gradient term. Far downstream this pressure variation is obviously small. Near the airfoil trailing edge, however, the deviations from freestream static pressure may be large. The fluctuations are virtually impossible to predict unless the complete Navier Stokes equations are solved which at the present time is an unrealistic task. The WAKE program was written with the pressure terms excluded with the hope that it would still match experimental data reasonably well. The results obtained indicated that these hopes were attained. Correlations with several test cases are given in the next section of this report.

The eddy viscosity model used in the WAKE program is that given by Equation 13 in the literature review. This model was derived by Prandtl for a fully-developed wake flow. In general, the velocity term in parentheses represents the difference between the maximum and minimum velocity in a profile while b represents the wake thickness or height at a velocity station halfway between the maximum and minimum velocity values. These parameters can be estimated given a velocity profile in a fully-developed wake, but if the initial profile is the trailing edge profile, then another set of parameters must be defined which will correlate with experimental measurement. It should be emphasized that while some experimental data exist for velocity profiles in the wakes of airfoils, these data must be described as very limited (Refs. 7, 26, 27, 28). Noting Figure 29, the velocity difference for the trailing edge profile would always be u_{max} since u_{min} is zero, while in the fully-developed profile it is never as large as u_{max}. Also, the wake width at half-depth for the trailing edge profile is always smaller than the same width for a fully-developed wake.
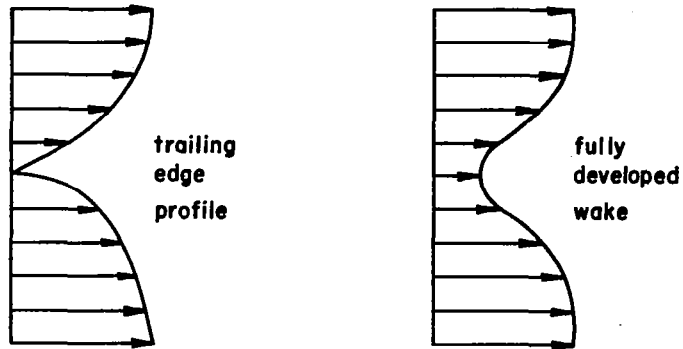
Figure 29. Sample velocity profiles at airfoil trailing edge and in a fully developed wake.

A value for the constant, c, in the eddy viscosity model must also be chosen which will bring about a match between experimental and theoretical data. In Equation 40 the eddy viscosity appears in the parameter c_1 as

$$c_1 = 100c_d tU_\infty/\varepsilon \qquad \text{where} \qquad \varepsilon = bc(u_{max} - u_{min}) .$$

This may also be written in the following form

$$c_1 = 100c_d t/\varepsilon \qquad \text{where} \qquad \varepsilon = bc(u_{max} - u_{min})/U_\infty . \qquad (57)$$

For wakes considered in this report, the maximum velocity in the profile will be the outer edge velocity, U_∞. Then $\varepsilon = bc(1 - \frac{u_{min}}{U_\infty})$. If c is defined as a positive constant, then the value of c_1 is obviously positive. By making several test runs of the WAKE program, it was found that at a given distance downstream of the initial profile the larger the value of c_1, the lower the value of the centerline velocity and the smaller the wake width. Thus, it was necessary to find new definitions of the terms b and $(1 - u_{min}/U_\infty)$ to be used

67

with the trailing edge profile shape to evaluate ε. New definitions were sought which would, in general, produce the proper variation of ε with wing angle of attack without making the functional relationships more complex. As seen in Figure 29, in order to achieve approximately the same wake widths using these two profiles, the width of the trailing edge profile must be measured at a y station with a larger velocity. Using this new wake width, a relationship was sought between the term $(1 - u_{min}/U)$ and the profile drag coefficient. Based on a comparison of many computer runs of the WAKE program and their correlations with experimental profiles, it was found that (1) if b is defined as the wake width at the y station where the velocity is 75 percent of the freestream value, and (2) if u_{min}/U_{∞} is represented by the expression $(1 - c_{d_{min}}/c_d)$, then good agreement with downstream wake profiles is obtained.

Having defined new relationships for b and $(1 - u_{min}/U_{\infty})$, the only remaining parameter needed to complete the definition of ε is the constant c. While the value of c for wakes behind circular cylinders using the conventional definitions of b and $(u_{max} - u_{min})$ is given as .047 in Reference 20, little has been published in the open literature regarding the value of c in airfoil wakes. For profiles generated using the WASH program with the new parameters defining the eddy viscosity, a constant value of c = .03 was found to work very well for all the airfoils tested. Although this value produces good correlation, the value of c is read into the WAKE program to allow the user the option of modifying the constant if he desires. The parameters b and $(1 - c_{d_{min}}/c_d)$ are also defined on cards FIN 51 and 52, respectively, in the program listing given in Appendix B. This permits the user to experiment with new ideas when more experimental data become available.

It is well to note here that a constant value of ε for all x locations is realistic only for relatively weak wakes, i.e., $C_d \to 0$. ε is really a measure of the eddy size and intensity in the wake. In high drag situations, large eddies are shed. These have very large internal shears which cause them to disintegrate progressively into smaller eddies with smaller shears as one moves downstream. For such a situation a constant eddy viscosity is obviously not realistic. It will be noted, however, that the procedure for computing the boundary layer on the wing does not admit significant regions of separated flow. Since the wing drag is always relatively small when the boundary layers are attached and since the airfoil boundary layers are computed with constant eddy viscosities, it seems reasonable to continue this practice in the wake computations. As a result, however, the determination of the momentum defect must be limited to those cases where these conditions of unseparated flow and low drag are always satisfied: generally for section lift coefficients of 0.8 or less.

In order to carry out the numerical integration of the WASH program, the user must specify the grid spacing in both the ξ and η direction. The program is designed to use a maximum of 2001 points in the η direction or 1000 points

on each side of the centerline. The maximum values of η for the initial upper and lower profiles are computed using the boundary layer thickness δ in Equation 33:

$$\left(\eta_{max}\right)_{\substack{upper \\ or \\ lower}} = \frac{\delta_{\substack{upper \\ or \\ lower}}}{100c_d tx_{initial}} \tag{58}$$

Dividing the larger of the two η values by 1000 yields the minimum stepsize in η. While the program is written for the general case (unequal stepsize) it is recommended that only even stepsize be used. If the specified even stepsize is too large, very small oscillations in u/U_∞ at the outer edge of the wake profile may result; hence, a stepsize which increases with η would only compound the oscillations. For every case presented in this report a stepsize of .00125 was found to be satisfactory. Using this stepsize and η_{max} from Equation 58, the number of points in the η direction may be computed from

$$NPTS = 2k_1 \eta_{max}/.00125 + 1$$

where NPTS is the total number of η stations for the entire wake and k_1 is a factor to insure that an η region is defined which is a little larger than the actual wake thickness at the initial station; k_1 should therefore have a value of 1.1 or 1.2. NPTS must be an odd integer. For the cases presented in this report it was usually specified as 1201, 1401, 1601, 1801, or 2001, depending on the maximum value of η. Since the value of NPTS is directly proportional to execution time it is suggested that less than 2001 points be used if possible; however, inexperienced users will probably want to choose one of the suggested values of NPTS given above depending on the value of η_{max}.

Along with an η stepsize, a stepsize must also be specified in the streamwise or ξ direction. For ξ an uneven stepsize which is very small initially and progressively larger downstream is recommended. The WAKE program is designed to use a stepsize which increases every step by the factor $(1 + DXSTEP)$. If $DXSTEP = 0$ then equal step downstream will be taken. Unequal steps are suggested because the initial solutions are very sensitive to stepsize while downstream they are relatively insensitive. The user must specify both the initial stepsize DX and the stepsize increment DXSTEP. For most of the cases presented here, an initial stepsize in ξ of .00005 was used with $DXSTEP = .05$; thus, at every step the stepsize increased by 5 percent from its previous value. Using this stepsize and increment, approximately 150 steps

are required to traverse a distance of two chord lengths downstream (ξ = 2.0). One disadvantage of the unequal stepsize is that if the solution is desired at ξ = 2.0 it is very difficult to choose DX and DXSTEP so that one of the steps falls on this ξ station; the solution nearest the desired station must therefore be used. Figure 30 presents a list of downstream station number (NXPRNT in the WAKE program) and ξ distance for the different stepsize increments .05, .075, and .10 all starting with an initial stepsize of .00005. This data should be helpful in determining the station number at which a solution is printed as well as the total number of steps required downstream (NXSTEP in the program) to achieve a desired ξ distance.

The WAKE program consists of a mainline and five subroutines. The mainline (1) reads and prints the input data set, (2) calls subroutine PROFIL to obtain the initial profile at ξ = .01, (3) calls subroutine GETF to obtain a value of f (Equation 41) at the first ξ station downstream given the derivative f' or T, (4) calls subroutines ABCR, COEFF, and SOLVE to obtain a new value for the profile T at the ξ station, (5) compares the new profile with the last profile calculated at the ξ station to see if convergence is attained, and (6) after convergence, prints the solution and repeats the same procedure for the next downstream station. A listing of the WAKE program with user instructions, a sample data set, and sample output are given in Appendix B. The sample data set should be particularly valuable to the unfamiliar user in giving examples of stepsizes and possible print options.

DISTANCE FROM TRAILING EDGE IN CHORDS

STATION NUMBER	DXSTEP=.05	DXSTEP=.075	DXSTEP=.01
1	0.010000	0.010000	0.010000
2	0.010050	0.010050	0.010050
3	0.010103	0.010104	0.010105
4	0.010158	0.010162	0.010166
5	0.010216	0.010224	0.010232
6	0.010276	0.010290	0.010305
7	0.010340	0.010362	0.010386
8	0.010407	0.010439	0.010474
9	0.010477	0.010522	0.010572
10	0.010551	0.010611	0.010679
11	0.010629	0.010707	0.010797
12	0.010710	0.010810	0.010927
13	0.010796	0.010921	0.011069
14	0.010886	0.011040	0.011226
15	0.010980	0.011168	0.011399
16	0.011079	0.011306	0.011589
17	0.011183	0.011454	0.011797
18	0.011292	0.011613	0.012027
19	0.011407	0.011784	0.012280
20	0.011527	0.011968	0.012558
21	0.011653	0.012165	0.012864
22	0.011786	0.012378	0.013200
23	0.011925	0.012606	0.013570
24	0.012072	0.012851	0.013977
25	0.012225	0.013115	0.014425
26	0.012386	0.013399	0.014917
27	0.012556	0.013704	0.015459
28	0.012733	0.014032	0.016055
29	0.012920	0.014384	0.016710
30	0.013116	0.014763	0.017432
31	0.013322	0.015170	0.018225
32	0.013538	0.015608	0.019097
33	0.013765	0.016078	0.020057
34	0.014003	0.016584	0.021113
35	0.014253	0.017128	0.022274
36	0.014516	0.017713	0.023551
37	0.014792	0.018341	0.024956
38	0.015081	0.019017	0.026502
39	0.015385	0.019743	0.028202
40	0.015705	0.020524	0.030072
41	0.016040	0.021363	0.032130
42	0.016392	0.022265	0.034393
43	0.016762	0.023235	0.036882
44	0.017150	0.024278	0.039620
45	0.017557	0.025398	0.042632
46	0.017985	0.026603	0.045945
47	0.018434	0.027898	0.049590
48	0.018906	0.029291	0.053599
49	0.019401	0.030788	0.058009
50	0.019921	0.032397	0.062859
51	0.020467	0.034126	0.068195
52	0.021041	0.035986	0.074065
53	0.021643	0.037985	0.080521
54	0.022275	0.040134	0.087624
55	0.022939	0.042444	0.095436
56	0.023636	0.044927	0.104030
57	0.024367	0.047597	0.113483
58	0.025136	0.050466	0.123881
59	0.025943	0.053551	0.135319
60	0.026790	0.056868	0.147901
61	0.027679	0.060433	0.161741
62	0.028613	0.064265	0.176965
63	0.029594	0.068385	0.193711
64	0.030623	0.072814	0.212133
65	0.031705	0.077575	0.232396
66	0.032840	0.082693	0.254685
67	0.034032	0.088195	0.279204
68	0.035283	0.094110	0.306174
69	0.036598	0.100468	0.335842
70	0.037978	0.107303	0.368476
71	0.039426	0.114651	0.404373
72	0.040948	0.122550	0.443861
73	0.042545	0.131041	0.487297
74	0.044222	0.140169	0.535077
75	0.045984	0.149982	0.587634
76	0.047833	0.160530	0.645448
77	0.049774	0.171870	0.709042
78	0.051813	0.184061	0.778997
79	0.053954	0.197165	0.855946
80	0.056201	0.211252	0.940591
81	0.058561	0.226398	1.033700
82	0.061040	0.242676	1.136120
83	0.063641	0.260177	1.248782
84	0.066374	0.278990	1.372710
85	0.069242	0.299214	1.509031
86	0.072254	0.320955	1.658985
87	0.075417	0.344327	1.823933
88	0.078738	0.369452	2.005376
89	0.082225	0.396460	2.204964
90	0.085886	0.425495	2.424510
91	0.089730	0.456707	2.666011
92	0.093767	0.490260	2.931662
93	0.098005	0.526330	3.223879
94	0.102455	0.565104	3.545317
95	0.107128	0.606787	3.898898
96	0.112035	0.651596	4.287838
97	0.117186	0.699766	4.715672
98	0.122596	0.751548	5.186289
99	0.128276	0.807215	5.703968
100	0.134239	0.867056	6.273415
101	0.140501	0.931385	6.899806
102	0.147076	1.000539	7.588837
103	0.153980	1.074879	8.346770
104	0.161229	1.154795	9.180498
105	0.168841	1.240705	10.097597
106	0.176833	1.333057	11.106407
107	0.185224	1.432337	12.216098
108	0.194035	1.539062	13.436757
109	0.203287	1.653792	14.779463
110	0.213002	1.777126	16.256482
111	0.223202	1.909711	17.881180
112	0.233912	2.052239	19.668348
113	0.245157	2.205457	21.634232
114	0.256965	2.370166	23.796706
115	0.269363	2.547228	26.175426
116	0.282382	2.737571	28.792019
117	0.296051	2.942188	31.670271
118	0.310403	3.162152	34.836348
119	0.325473	3.396614	38.319033
120	0.341297	3.652810	42.149986
121	0.357912	3.926071	46.364034
122	0.375358	4.219826	50.999488
123	0.393675	4.535613	56.098487
124	0.412909	4.875084	61.707385
125	0.433105	5.240015	67.877174
126	0.454310	5.632316	74.663941
127	0.476575	6.054040	82.129385
128	0.499954	6.507393	90.341374
129	0.524502	6.994748	99.374561
130	0.550277	7.518654	*********
131	0.577341	8.081853	*********
132	0.605758	8.687292	*********
133	0.635596	9.338138	*********
134	0.666926	10.037799	*********
135	0.699822	10.789934	*********
136	0.734363	11.598479	*********
137	0.770631	12.467665	*********
138	0.808713	13.402040	*********
139	0.848698	14.406493	*********
140	0.890683	15.486279	*********
141	0.934767	16.647050	*********
142	0.981056	17.894879	*********
143	1.029659	19.236295	*********
144	1.080691	20.678317	*********
145	1.134276	22.228491	*********
146	1.190540	23.898928	*********
147	1.249617	25.686348	*********
148	1.311648	27.612124	*********
149	1.376780	29.682333	*********
150	1.445169	31.907808	*********
151	1.516977	34.300193	*********
152	1.592376	36.872008	*********
153	1.671545	39.636709	*********
154	1.754672	42.608762	*********
155	1.841956	45.803719	*********
156	1.933604	49.238298	*********
157	2.029834	52.930470	*********
158	2.130876	56.899555	*********
159	2.236970	61.166322	*********
160	2.348368	65.753096	*********
161	2.465336	70.683878	*********
162	2.588153	75.984469	*********
163	2.717111	81.682604	*********
164	2.852516	87.808100	*********
165	2.994692	94.393007	*********
166	3.143977	*********	*********

Figure 30. Tabulation of downstream station number and ξ distance for stepsize increments of .05, .075, and .10.

DISCUSSION OF PROGRAM RESULTS

Correlations of the WAKE program results with available experimental velocity profiles are presented in Figures 31 through 37. The figures show the experimental data, results obtained by the theoretical method of Reference 7, and the WAKE program results for specified stations downstream of the trailing edge. Each airfoil was analyzed using an initial x/c value of .01 and an eddy viscosity constant of .03. The profiles presented are not intended to show the relative distance of the profile above or below the trailing edge, but only the profile shape about the wake centerline as it moves downstream. In Figures 31 through 34 the WAKE program results are shown for two Reynolds numbers. In order to achieve a theoretical drag coefficient approximately equal to the experimental drag measured in References 26 and 27, it was necessary to run the two-dimensional airfoil program of Reference 4 at a Reynolds number of approximately half (.21 million) the indicated test value of .42 million. Tunnel turbulence or model surface conditions during the wind tunnel test may have produced more drag on the airfoil than would normally be expected at the test Reynolds number. The experimental drag was measured using a momentum rake which indicates the momentum defect in the wake at a station downstream of the trailing edge. Since the velocity profiles depend on drag coefficient, the calculated profiles should agree better with experiment if a theoretical drag coefficient is used which agrees with the experimental value. It was therefore decided to compute and compare profiles using both the specified test Reynolds number and a "corrected" Reynolds number, i.e., one at which the theoretical drag matches the experimental drag.

Figures 31 and 32 show that the WAKE program results agree well with experiment for the symmetrical Joukowski airfoil at both angles of attack ($0°$ and $6°$). While results at both Reynolds numbers show good agreement, that for the lower Reynolds number case is better. Although no experimental data were available at x/c = 2.0, the results are shown at this station for this and all other airfoils to give the reader an idea of the profile shape in the vicinity of the horizontal tail.

Figures 33 and 34 present program results for a symmetrical Piercy airfoil at angles of attack of $0°$ and $6°$, respectively. The experimental points were taken from Reference 27. The WAKE program profiles give good agreement with experiment except near the minimum velocity region of the wake centerline. While the method of Reference 7 predicts the minimum velocity quite well, it over-predicts the wake thickness at other velocity stations in the profiles.

Experimental measurements of a modified 15 percent symmetrical airfoil at an angle of attack of $8°$ are presented in Reference 28, and these results are compared with the WAKE program prediction in Figure 35. Both the WAKE program and the method of Reference 7 predict the profile shape accurately as compared with experimental data except near the outer edge where the experimental data points appear questionable.

As a final test case the USA 45 airfoil was analyzed at angles of attack of - 5.3° and 1.6° and compared with experimental data presented in Reference 7. It should be pointed out that the profiles given in Reference 7 were not presented to make comparisons of this type, but rather only to give approximate dynamic pressure profile shapes in the general sense. The reader should bear this in mind when considering these two figures because the experimental profile shapes in Reference 7 have been greatly enlarged to make these comparisons. For the angle of attack - 5.3° the WAKE program did a better job of predicting the profile shape; however, for $\alpha = 1.6°$ the method of Reference 7 appears to match experiment better.

In general, agreement between the WAKE program profiles and experiment was good and, in most cases, better than the method of Reference 7. The minimum velocity at x/c stations near the trailing edge was generally larger than experiment while centerline velocities at stations greater than 1.0 were generally smaller than experimental values. The correlation of profile width using the WAKE program with experimental profile shape was excellent. The reasons the coefficients of the eddy viscosity were chosen to give a better fit to the experimental data further downstream of the wing rather than at the trailing edge were first that downstream is the region of major interest and second that a boundary-layer-type analysis obviously cannot describe the initial portion of a base flow wake adequately. Thus to favor a data match in a region where the analytical model is known to be inadequate is to lose the opportunity to attain a match in a region where it should be reasonably correct.

74
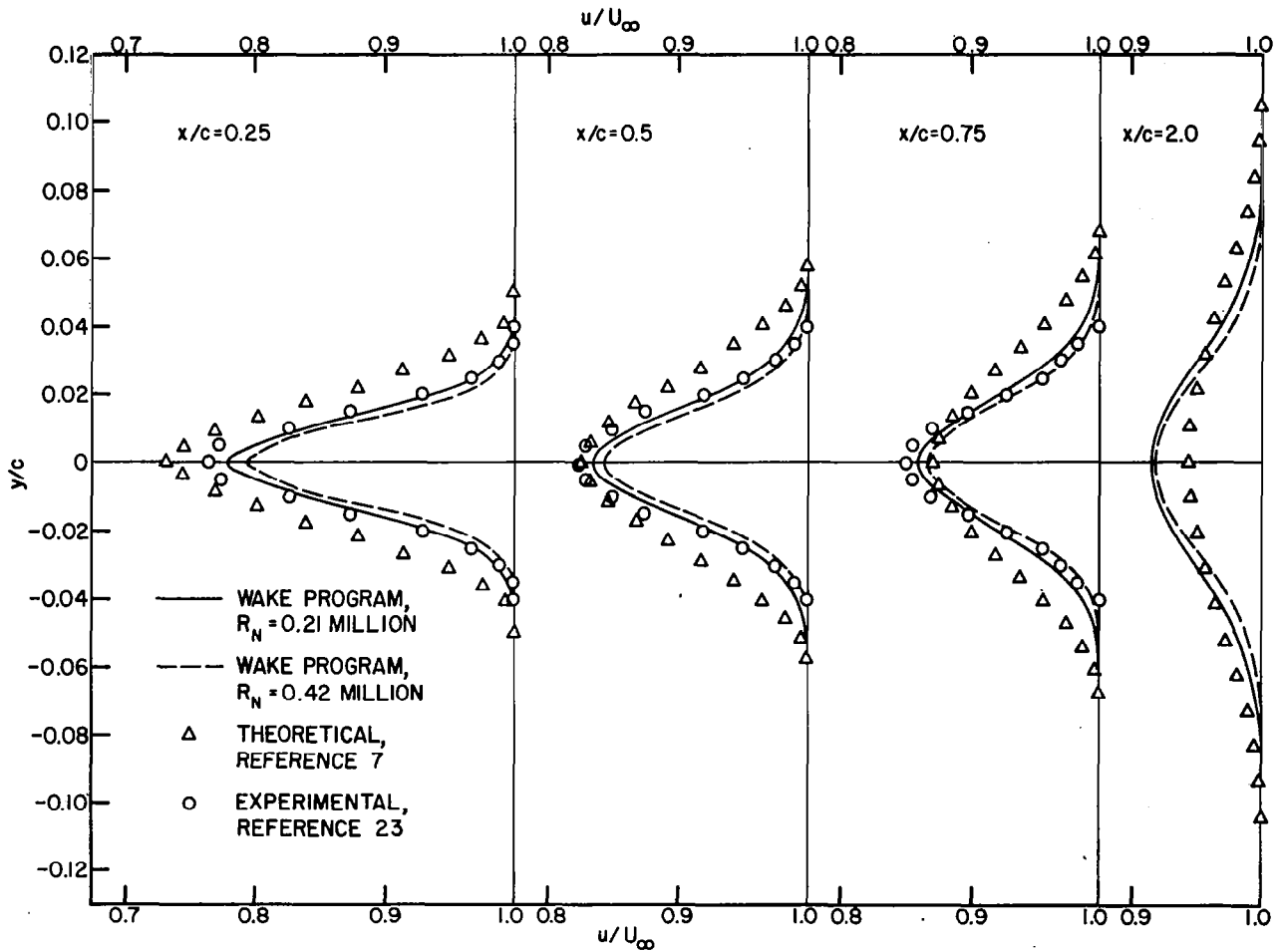
Figure 31.   Comparison of velocity profiles with experiment (Ref. 26) for the Joukowski
             airfoil at α = 0°.
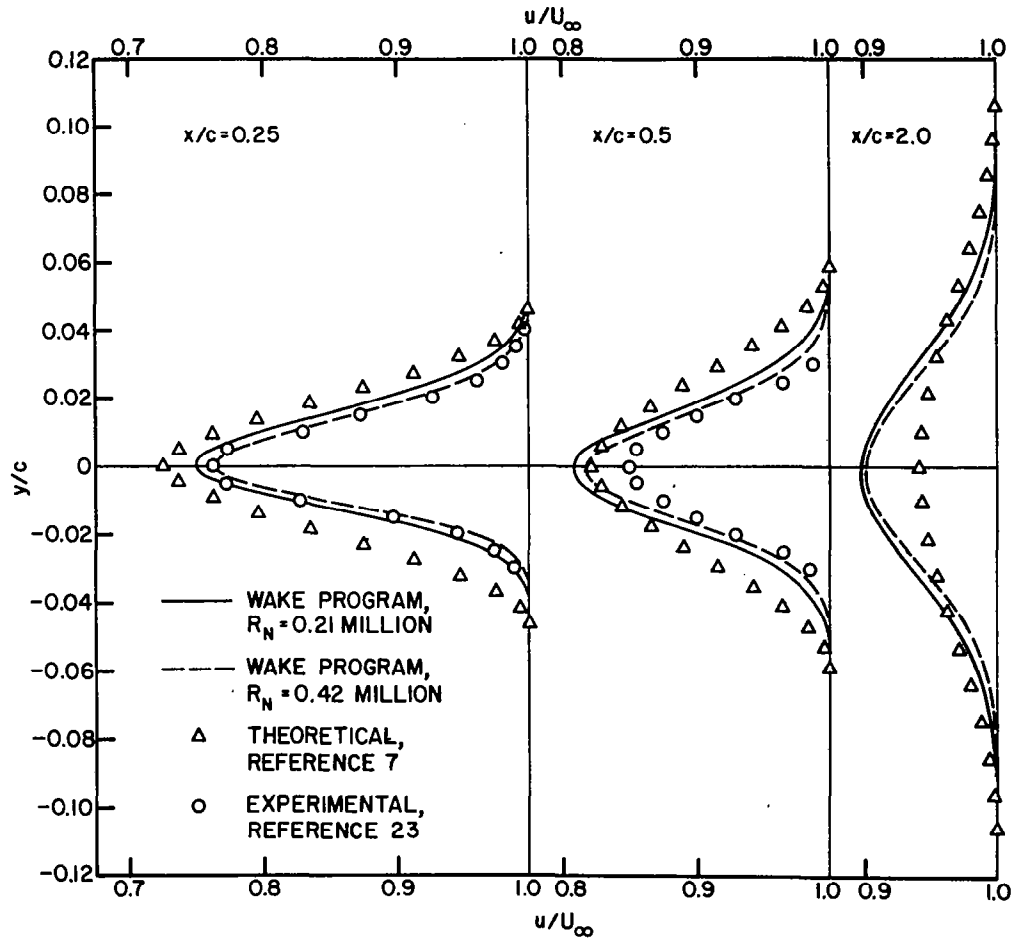
Figure 32. Comparison of velocity profiles with experiment (Ref. 26) for the Joukowski airfoil at $\alpha = 6°$.
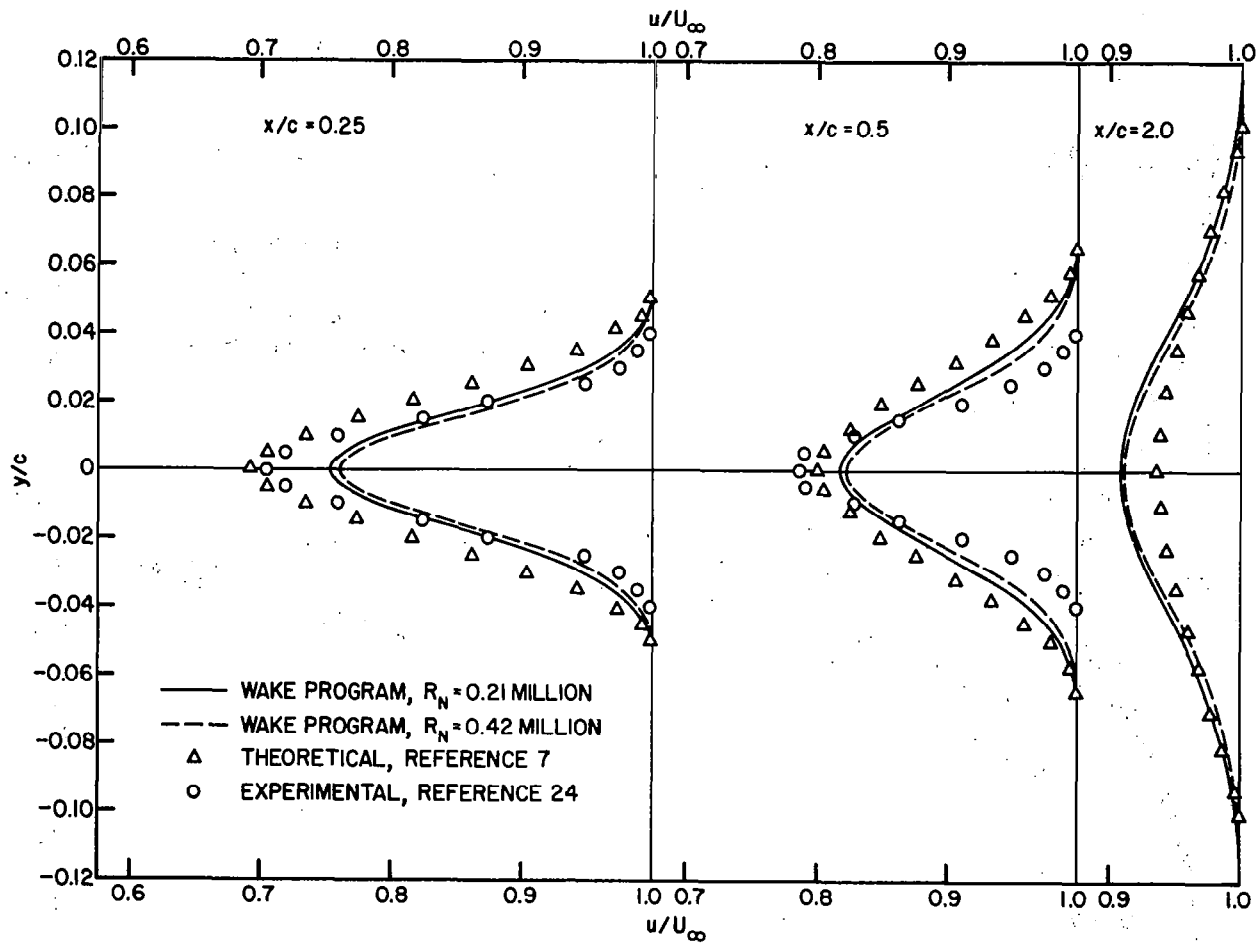
Figure 33. Comparison of velocity profiles with experiment (Ref. 27) for the Piercy airfoil at α = 0°.
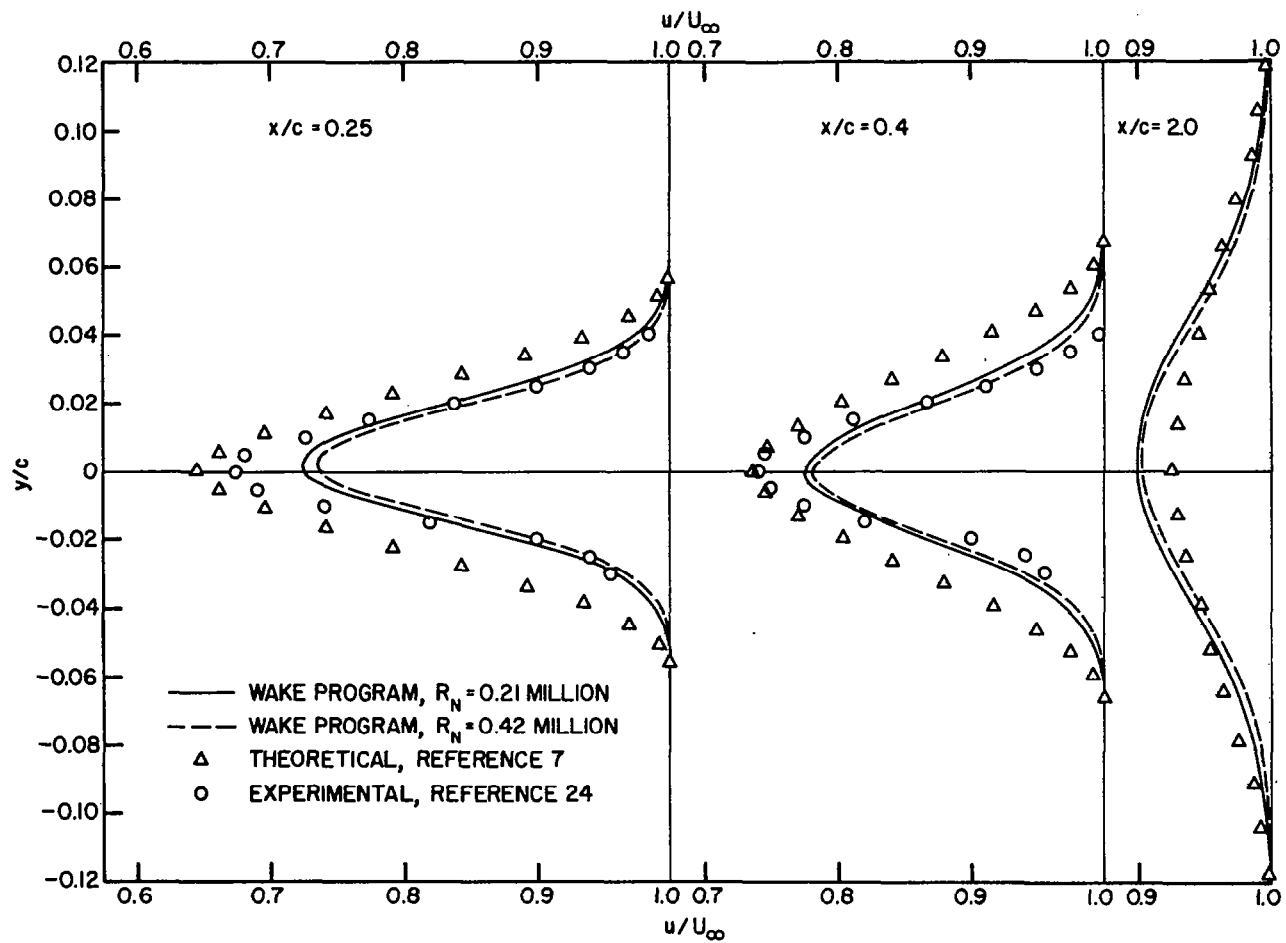
Figure 34. Comparison of velocity profiles with experiment (Ref. 27) for the Piercy airfoil at α = 6°.
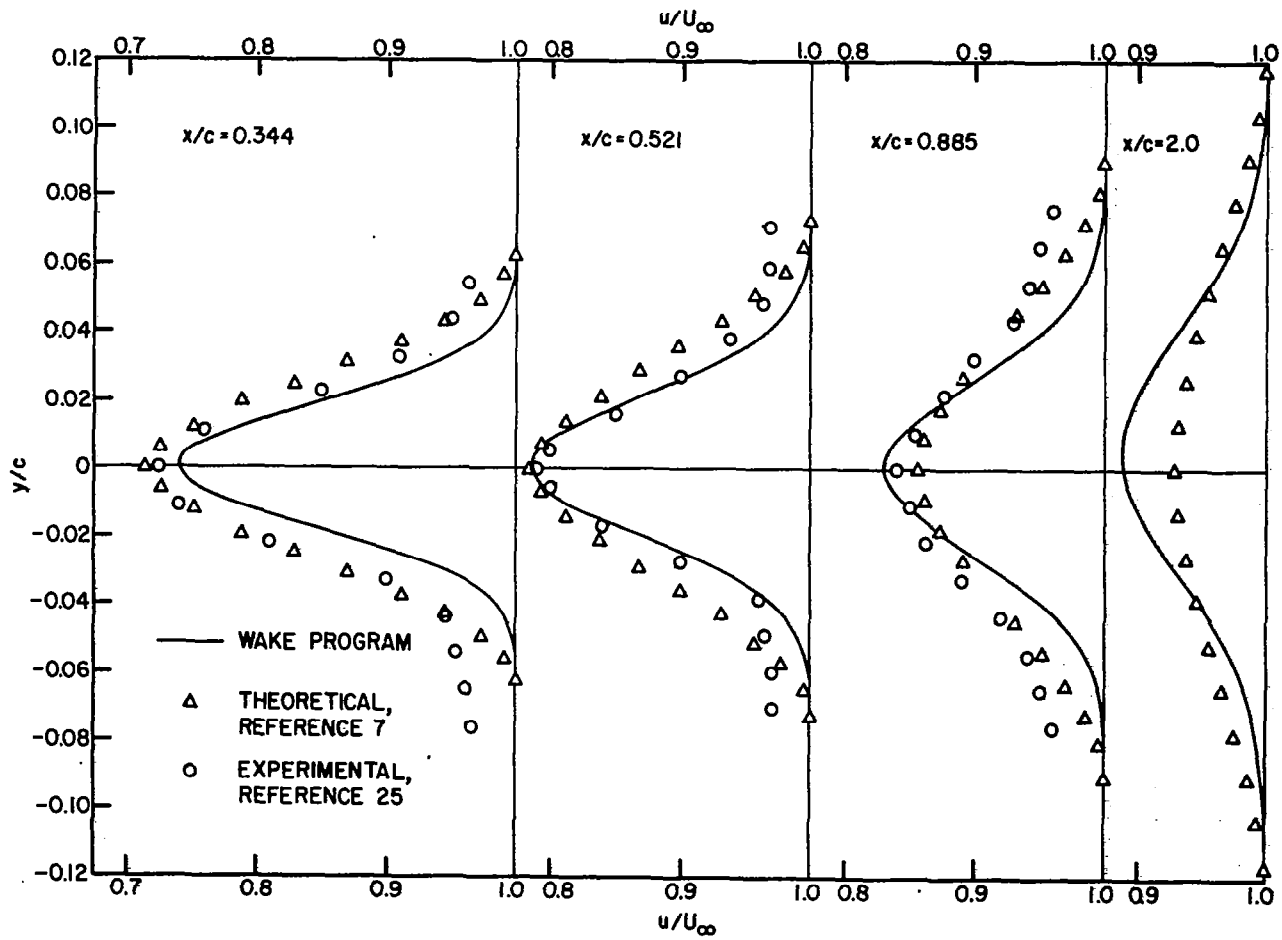
Figure 35. Comparison of velocity profiles with experiment (Ref. 28) for a modified 0015 airfoil at α = 8°.
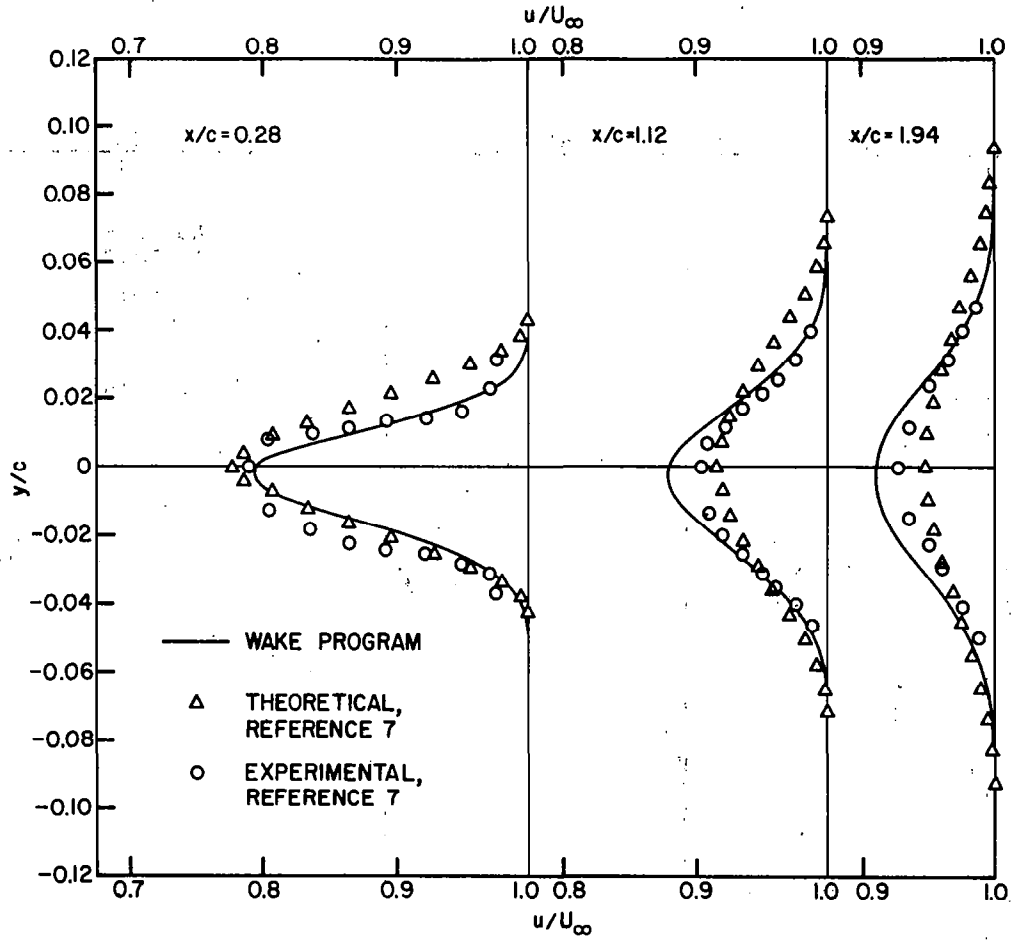
Figure 36.   Comparison of velocity profiles with experiment (Ref. 7)
for the USA 45 airfoil at $\alpha = -5.3°$.
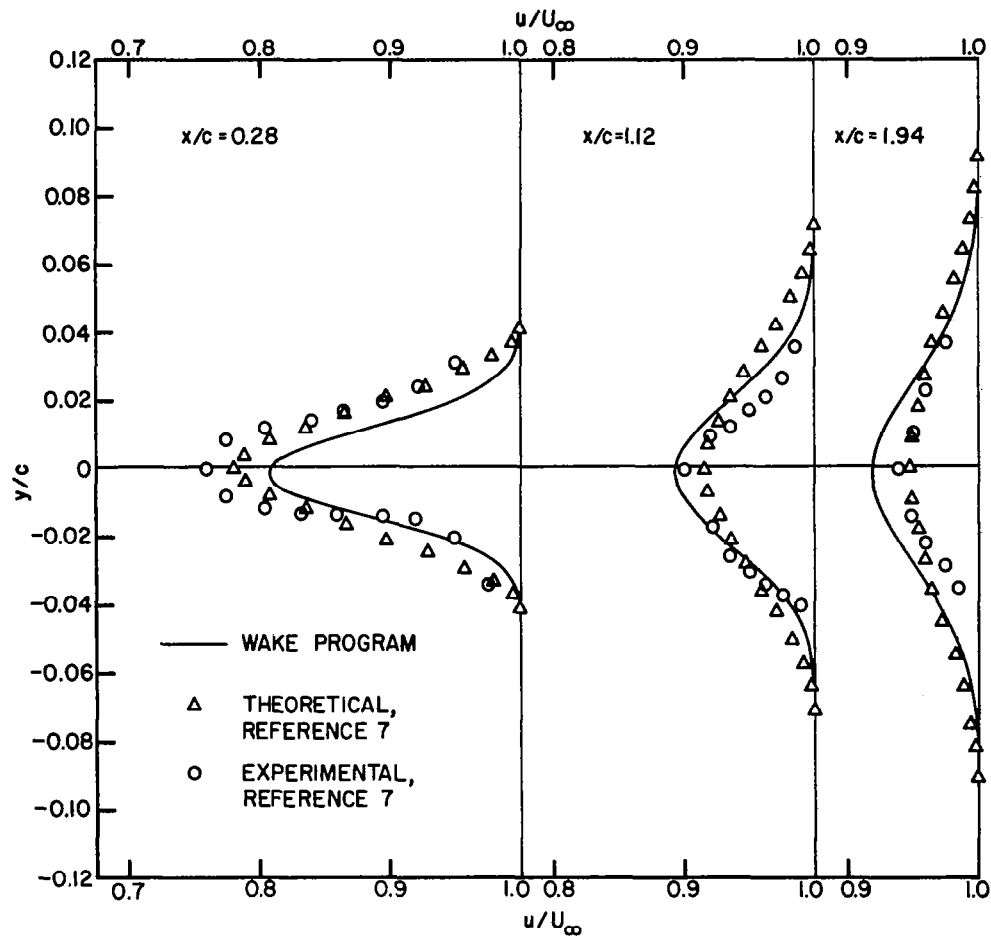
Figure 37. Comparison of velocity profiles with experiment (Ref. 7) for the USA 45 airfoil at $\alpha = 1.6°$.

APPLICATION TO THE CALCULATION OF HORIZONTAL TAIL ONSET FLOW

In the preceding, the programs for determining the wake sheet location and the velocity profile in the wake have been discussed independently; consideration will now be given to combining them so as to compute the onset flow field at an aircraft's horizontal tail. The trailing vortex streamline locations are calculated using WASH. Naturally velocity profile solutions need be computed only along those streamlines which pass near the horizontal tail. Given the section drag coefficient of the wing at the spanwise origin of each streamline used in the computation and the total streamline length to the x-station of interest, WAKE determines the velocity profile centered about the z-location of the wake sheet. The total distance traced by a streamline in going from the y-axis to some downstream x-station is given in the WASH program output in the section specifying the coordinates of the trailing vortex sheet. An example of how these are properly combined is presented in Figure 38 for the ATLIT wing at three stations downstream of the wing trailing edge in the wing plane of symmetry. The profile at the horizontal tail is therefore computed as the profile at the station $x/c = 2.0$ of Figure 38. Similar profiles may be calculated at other spanwise stations in order to show the spanwise variation of the profiles.

In the strictest sense profiles should be calculated along the 4 or 5 most inboard vortices to describe the spanwise variation of the onset flow at the horizontal tail. However, from a practical point of view unless the spanwise curvature of the wake is large there is, as may be seen in the wake sheet plots, little vertical variation in sheet location for y distance equal to normal tail semispan lengths. Also, a check of Figures 31 through 37 will indicate that at $x/c = 2.0$ the velocity profiles across the wake are very nearly the same for all airfoils tested, indicating that the effect of spanwise variations in section drag coefficient on the velocity profiles are small. As a result velocity profiles at different spanwise stations will usually have essentially the same velocity deficit. If the spanwise and downstream curvature is small for vortices which pass in the vicinity of the horizontal tail, it is therefore possible to execute only one case of each program and obtain the approximate wake position, flow angularity, and profile shape in the region of the horizontal tail (the most inboard vortex is used). This approximation can be improved if desired by applying the single WAKE program velocity profile to each of the desired spanwise vortex positions calculated in the WASH program. If a more rigorous analysis is desired, a boundary layer solution may be determined along each of the 4 or 5 most inboard streamlines noting the spanwise variation of section drag coefficient.
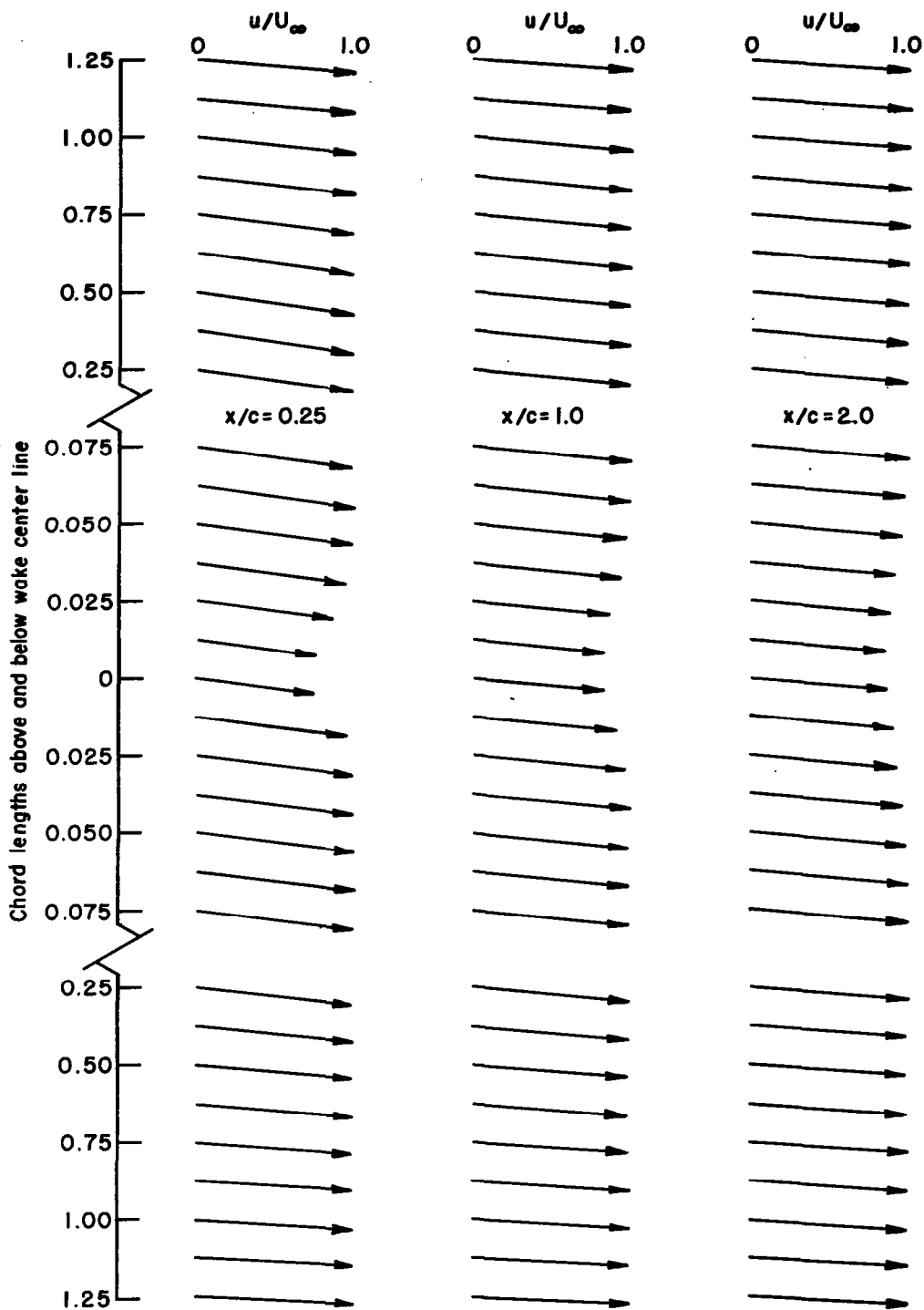
Figure 38. Velocity profiles with proper flow directions in the plane of symmetry behind the ATLIT wing.

With the profile shape in the tail region determined, estimation of the forces on the tail plane due to the flow angularity and velocity variations can be undertaken. By executing the WASH program for a range of aircraft lift coefficients the wake position as a function of C_L may be used to determine whether or not the tail ever passes through the wing wake.* If the tail always remains 10 to 20 percent of a wing chord length above or below the wake, the velocity deficit analysis may be neglected. Even if the tail is always out of the wake, the downwash computations are still important because the change in downwash at the tail with angle of attack must be known in order to predict tail trim angles and longitudinal stability. If the tail does pass through the wake, then the tail must be sized so that it produces the required control force even when the tail is located directly in the wake. The effect of spanwise variation in downwash may be accounted for by assuming it to be similar to a wing twist. While most light aircraft horizontal tails do not have twist, a twist variation can be assumed which will produce a spanwise angle of attack variation similar to that imposed by the downwash variation. This technique can be applied to the three-dimensional program given in Reference 4 when computing tail characteristics.

The determination of the proper flow velocity to use in calculating the aerodynamic characteristics of a section of the horizontal tail flying in a wake is complicated by the fact that the wake momentum defect is confined to a rather thin region which is on the order of the thickness of the airfoil for airfoils at low-to-moderate angles of attack. In this thin region the magnitude of the flow velocity may vary from 0.88 freestream to freestream. Since two-dimensional airfoil analysis has not yet progressed to the point of calculating aerodynamic coefficients in shear flow, it is necessary to find an average velocity squared over the thickness of the airfoil beginning at the point on the velocity profile intersected by a line parallel to the airfoil chord at $t/2$. This is best done graphically using plots of the $\frac{1}{2}\rho V^2$ distribution.

If the average $q = \frac{1}{2}\rho V^2$ varies significantly along the tailplane, its effects can be included in the three-dimensional aerodynamics calculation program (Ref. 4) in several ways: (1) artificially reduce the wing chord in proportion to q_{local}/q_∞, (2) reduce only the local Reynolds number by the factor V_{local}/V_∞ or some function thereof, and (3) multiply C_L and C_D by q_{local}/q_∞. If these procedures result in significant changes in planform or aerodynamic properties, they cannot be accommodated readily within the framework of the 3-D characteristics program. However, if the changes are small enough to be capable of linear representation, then one of these procedures will serve nicely. Which procedure will yield the best result cannot be stated with certainty since time did not permit them to be investigated in detail. The author is inclined to favor the first as representing the least compromise with physical reality within the context of the two-dimensional airfoil analysis. Since the wake region is quite turbulent, it seems reasonable to insist that when the tailplane enters it, the analysis should consider the airfoil boundary layer fully turbulent from nose to trailing edge.

* Although the analysis does not include the effects of the tail upwash on the wing downwash field, this distortion is not large. The wake position or magnitude is therefore not altered significantly.

CONCLUDING REMARKS

The present work provides two computer programs useful for predicting the flow magnitude and direction in the region where one would wish to locate an aircraft's horizontal tail (pitch trimming surface). The calculation of the contribution of this surface to the overall aircraft lift, drag, and moment is much enhanced if one has available more realistic values of the onset flow.

WASH ties together for the first time in a computer program a soundly-based inviscid method for determining the shape and location of the downwash wake sheet with a method previously used to determine the spanwise lift distribution for unswept moderate-to-high aspect ratio wings and wing bodies in incompressible flow. Excellent qualitative agreement is obtained with available experimental results. Quantitatively, the predicted flow directions at any point in the downwash field agree to within a degree or so of the measured values. Considering the experimental error present and the effects of boundary layers on the aft fuselage, this is about as good as one could expect. The results show there was little spanwise variation in wake position for normal horizontal tail semispans. Execution time for the program is 15-20 seconds on an IBM 370/165; it is thus a low cost means of mapping the downwash field during design analysis.

WAKE calculates the momentum defect downstream along the wake centerline. It uses as input section drag data developed analytically by the aforementioned spanwise lift distribution program. It provides velocities that are within 2 percent of the measured values at all stations for which data were available on two wings with different airfoil sections. Computation time for the flow along one streamline is 2 min 42 sec. The results indicate that the momentum defect due to wing drag is confined to a region no more than 0.43 m high for typical light aircraft in the cruise configuration. The region of noticeable defect (> 2 percent less than freestream) is only about 0.21 m high. There is little spanwise variation in wake velocity profile for typical light aircraft horizontal tail semispans. Thus, unless there is some compelling reason to locate the trim surface near the wake centerline, use of WAKE is not required.

The flight condition for which this type of information is of most interest is approach. In this configuration the wake is large and the momentum defect significant. While the inviscid downwash calculation as used here applies equally well, the viscous treatment suffers from the fact that the method used to determine the wing drag cannot accommodate separated flows. Further, flows with large separations can not be considered to possess constant eddy viscosities as was assumed here. It is apparent, therefore, that if horizontal onset flow is to be computed during approach the problems of the analytical determination of the correct aerodynamic characteristics of airfoils near stall and the characterization of turbulent flow eddy viscosity magnitude and decay rate in terms of the size of the initial separation must first be solved.

REFERENCES

1. Smetana, F. O.; Summey, D. C.; and Johnson, W. D.: "Riding and Handling Qualities of Light Aircraft - A Review and Analysis". NASA CR-1975, March 1972, 409 pages.

2. Smetana, F. O.; Summey, D. C.; and Johnson, W. D.: "Flight Testing for the Evaluation of Light Aircraft Stability Derivatives - A Review and Analysis". NASA CR-2016, May 1972, 110 pages.

3. Smetana, F. O.; Summey, D. C.; and Johnson, W. D.: "Point and Path Performance of Light Aircraft - A Review and Analysis". NASA CR-2272, June 1973, 131 pages.

4. Smetana, F. O.; Summey, D. C.; Smith, N. S.; and Carden, R. K.: "Light Aircraft Lift, Drag, and Moment Prediction - A Review and Analysis". NASA CR-2523, May 1975, 480 pages.

5. Dwinnell, James H.: Principles of Aerodynamics. McGraw-Hill Book Co. Inc., New York, 1949, 389 pages.

6. von Karman, Theodore: Aerodynamics. Cornell University Press, 1954, 203 pages.

7. Silverstein, A.; Katzoff, S.; and Bullivant, W. K.: "Downwash and Wake Behind Plain and Flapped Airfoils". NACA TR-651, 1939, 28 pages.

8. Kuethe, A. M.; and Schetzer, J. D.: Foundations of Aerodynamics. John Wiley & Sons Inc., New York, 1959, 445 pages.

9. Glauert, H.: The Elements of Aerofoil and Airscrew Theory. Cambridge University Press, New York, 1926.

10. Silverstein, A.; and Katzoff, S.: "Design Charts for Predicting Downwash Angles and Wake Characteristics behind Plain and Flapped Wings". NACA TR-648, 1939, 24 pages.

11. Hoggard, H. P., Jr.; and Hagerman, J. R.: "Downwash and Wake Behind Untapered Wings of Various Aspect Ratios and Angles of Sweep". NACA TN-1703, October 1948, 149 pages.

12. Tolhurst, William H., Jr.: "Downwash Characteristics and Vortex-Sheet Shape Behind a 63° Swept-Back Wing-Fuselage Combination at a Reynolds Number of 6.1×10^6". NACA TN-3175, May 1954, 45 pages.

13. Rogers, Arthur W.: "Application of Two-Dimensional Vortex Theory to the Prediction of Flow Fields Behind Wings of Wing-Body Combinations at Subsonic and Supersonic Speeds". NACA TN-3227, September 1954, 91 pages.

14. Butter, D. J.; and Hancock, G. J.: "A Numerical Method for Calculating the Trailing Vortex System behind a Swept Wing at Low Speed". Aeronautical Journal, Royal Aeronautical Society, Vol. 75, pp. 564-568, August 1971.

15. Labrujere, T. E.: "A Numerical Method for the Determination of the Vortex Sheet Location behind a Wing in Incompressible Flow". National Aerospace Laboratory (NLR), Amsterdam, The Netherlands, Report NLR TR 72091 U, July 1972, 29 pages.

16. Donaldson, C. D.; Dilanin, A. J.; and Korkegi, R. H.: "Vortex Wakes of Conventional Aircraft". Advisory Group for Aerospace Research and Development, Paris. Report No. AG 204, 1975, 85 pages.

17. Aerodynamic Analyses Requiring Advanced Computers. NASA SP-347, 1975, 1465 pages.

18. Streiter, J. R.; and Sachs, A.: "The Rolling-Up of the Trailing Vortex Sheet and Its Effect on the Downwash behind the Wing". Journal of the Aeronautical Sciences, Vol. 18, No. 1, 1951, pp. 21-32, 72.

19. Cebeci, T.; Smith, A. M. O.; and Wang, L. C.: "A Finite-Difference Method for Calculating Compressible Laminar and Turbulent Boundary Layers", Part 1, General Description. McDonnell-Douglas Corp. Report No. DAC-67131, March 1969, 97 pages.

20. Schlichting, Hermann: Boundary Layer Theory. McGraw-Hill Book Co., Inc., New York, 1960, 647 pages.

21. Liepmann, H. W.; and Laufer, J.: "Investigation of Free Turbulent Mixing". NACA TN-1257, August 1947, 59 pages.

22. Elassar, R. J.; and Pandolfini, P. P.: "An Examination of Eddy Viscosity Models for Turbulent Free Shear Flows". Transactions of the ASME, Paper No. 71-FE-17, or Journal of Basic Engineering, December 1971, pp. 624-630.

23. Wygnanski, I.; and Fiedler, H. E.: "Jets and Wakes in Tailored Pressure Gradient". The Physics of Fluids, Vol. 11, No. 12, December 1968, pp. 2513-2523.

24. Oh, Y. H.: "Calculation of Compressible Turbulent Free Shear Layers". AIAA Journal, Vol. 12, No. 3, March 1974, pp. 401-403.

25. Oh, Y. H.: "Analysis of Two-Dimensional Free Turbulent Mixing". Paper Presented at the AIAA Seventh Fluid and Plasma Dynamics Conference, Palo Alto, California, June 17-19, 1974, 12 pages.

26. Preston, J. H.; and Sweeting, N. E.: "The Experimental Determination
     of the Boundary Layer and Wake Characteristics of a Simple Joukowski
     Aerofoil, with Particular Reference to the Trailing Edge Region".
     A.R.C. R&M No. 1998, March 1943, 25 pages.

27. Preston, J. H.; Sweeting, N. E.; and Cox, D. K.: "The Experimental
     Determination of the Boundary Layer and Wake Characteristics of a
     Piercy 12/40 Aerofoil, with Particular Reference to the Trailing
     Edge Region". A.R.C. R&M 2013, February 1945, 12 pages.

28. Goradia, S. H.; and Lilley, D. E.: "Theoretical and Experimental Study
     of a New Method for Prediction of Profile Drag of Airfoil Sections".
     NASA CR-2539, June 1975, 166 pages.

29. Stevens, W. A.; Goradia, S. H.; and Braden, J. A.: "Mathematical Model
     for Two-Dimensional Multi-Component Airfoils in Viscous Flow". NASA
     CR-1843, July 1971, 181 pages.

30. Murphy, James S.: "Some Effects of Surface Curvature on Laminar
     Boundary-Layer Flow". Journal of the Aeronautical Sciences, May
     1953, pp. 338-344.

31. Williams, J. C., III; Cheng, E. H.; and Kim, K. H.: "Curvature Effects
     in the Laminar and Turbulent Freejet Boundary". AIAA Journal,
     Vol. 9, No. 4, April 1971, pp. 733-736.

32. Patel, V. C.: "The Effects of Curvature on the Turbulent Boundary
     Layer". A.R.C. R&M 3599, August 1968, 31 pages.

33. Ahlberg, J. H.; Nilson, E. N.; and Walsh, J. L.: The Theory of Splines
     and Their Applications. Academic Press, New York, 1967.

34. Gradshteyn, I. S.; and Ryzhik, I. M.: Table of Integrals, Series, and
     Products. Academic Press, New York, 1965.

APPENDICES

APPENDIX A – WASH PROGRAM

User Instructions

The program is written in FORTRAN IV and is designed to run in double precision on an IBM 370-165 computer. This program evaluates (1) the location of the wake centerline by tracing the path of 18 vortices shed at the wing trailing edge, and (2) the total flow angle, sidewash angle, and downwash angle behind an unswept wing in any plane perpendicular to the wake centerline at a specified distance aft of the wing trailing edge or in the plane of symmetry of the wing. Downwash information in a single plane behind the wing using 15 downstream steps requires an average execution time of 20 to 25 seconds. The program requires the specification of the following input data:

Card Number	Variable Name	Variable Description
1	TITLE	The 80 character array which is used as a header to identify output. Termination of execution is achieved by following the last set of wing data to be analyzed by a title card having only the word END in the first three spaces.
2	NSTEP	The number of downstream steps to be taken aft of the wing trailing edge. The total distance the vortex system is traced downstream is given by NSTEP*DX. The maximum value of NSTEP is 18.
2	JPUNCH	The control variable giving the user the option of obtaining a punched plot data set which may be used to plot the vortex system using the PLOT program in Reference 4. JPUNCH=1 gives punched output while the default JPUNCH=0 gives none.
3	ALPHA	The wing angle of attack in degrees.
3	B2	The wing semispan in feet.
3	TR	The wing taper ratio (tip chord/root chord).
3	CR	The wing root chord in feet.
3	DX	The step size in the streamwise direction specified as ratio of wing semispan.
4-5	Y	The 10 variable array specifying the Y-coordinates of the positive Y-axis (axis in the spanwise direction) at which the section lift coefficients are read. The order of specification is from positive wing tip to wing root as a ratio of wing semispan (from Y(1) at the tip to Y(10) at the root). All of the Y values must be non-zero.
6-7	CLS	The 10 variable array specifying the section lift coefficients corresponding to the Y-coordinates described above using the same ordering scheme.

Card Number	Variable Name	Variable Description
8	NXORY	The control variable used to specify the type of plane in which downwash calculations are made. NXORY=0 gives no downwash analysis in a plane. NXORY=1 gives downwash information in a Y-Z plane where X is the streamwise direction. The Y-Z plane is located at a value of X = STAT (see next variable). Downwash information is calculated for the 6 most inboard Y-stations at several Z locations. NXORY=2 gives downwash information in the X-Z plane at Y=0 for X values ranging from .25 to 1.75 semispans aft of the trailing edge. Z ranges from .5 semispans above and below a specified midpoint value of Z = STAT (see next variable). NXORY=3 gives downwash (or negative upwash) information in X-Z plane at Y=0 for negative values of X ranging from the wing leading edge to -.5 semispans ahead of the wing leading edge. Z ranges from .25 semispans above to .25 semispans below the leading edge value of Z.
8	STAT	Variable used with NXORY to specify in semispans the proper location of the plane of interest. If NXORY=1 then STAT specifies the X-station at which the Y-Z plane is to be located. This distance in semispans may be either positive or negative depending on whether downwash or upwash information is desired, but it must be measured from the wing trailing edge. If NXORY=2 then STAT specifies in semispans the midpoint of the Z-range for the downwash calculations in the X-Z plane. This Z-range is specified above (positive) or below (negative) the trailing edge in semispans. IF NXORY=3 the variable STAT is not used.
Last Card		Blank.

Cards 1 through 8 represent a complete data set for the WASH Program. Several data sets may be executed for a single program compile by placing subsequent data sets behind the first. More than one plane may be analyzed during a program execution by specifying new values for NXORY and STAT on other cards placed behind card eight and before the blank card.

The entire program execution is terminated when the END title card is encountered. The format specification for the above data is given in Figure A-1. A sample data set is given in Figure A-2, and the output of this data set is presented in Figure A-3.

```
1 2 3 4 5 6 7 8 9 10 11 12 13 14 15 16 17 18 19 20 21 22 23 24 25 26 27 28 29 30 31 32 33 34 35 36 37 38 39 40 41 42 43 44 45 46 47 48 49 50 51 52 53 54 55 56 57 58 59 60 61 62 63 64 65 66 67 68 69 70 71 72 73 74 75 76 77 78 79 80
```

TITLE
20A4

NSTEP	JPUNCH	
I10	I10	

ALPHA	B2	TR	CR	DX	
F10.5	F10.5	F10.5	F10.5	F10.5	

Y(1)	Y(2)	Y(3)	Y(4)	Y(5)	Y(6)	Y(7)	Y(8)
F10.5	F10.5	F10.5	F10.5	F10.5	F10.5	F10.5	F10.5

Y(9)	Y(10)	
F10.5	F10.5	

CLS(1)	CLS(2)	CLS(3)	CLS(4)	CLS(5)	CLS(6)	CLS(7)	CLS(8)
F10.5	F10.5	F10.5	F10.5	F10.5	F10.5	F10.5	F10.5

CLS(9)	CLS(10)	
F10.5	F10.5	

NXORY	STAT	
I10	F10.5	

```
1 2 3 4 5 6 7 8 9 10 11 12 13 14 15 16 17 18 19 20 21 22 23 24 25 26 27 28 29 30 31 32 33 34 35 36 37 38 39 40 41 42 43 44 45 46 47 48 49 50 51 52 53 54 55 56 57 58 59 60 61 62 63 64 65 66 67 68 69 70 71 72 73 74 75 76 77 78 79 80
```

Figure A-1. Format specification of input data for the WASH program.

```
                                                                    Last Card
END
1 2 3 4 5 6 7 8 9 10 11 12 13 14 15 16 17 18 19 20 21 22 23 24 25 26 27 28 29 30 31 32 33 34 35 36 37 38 39 40 41 42 43 44 45 46 47 48 49 50 51 52 53 54 55 56 57 58 59 60 61 62 63 64 65 66 67 68 69 70 71 72 73 74 75 76 77 78 79 80

        (BLANK  CARD)

        NXORY
          3

        NXORY  STAT
          2  -.2

        NXORY  STAT
          1   .6

            CLS(10)
1.3666      1.39108

CLS(1)    CLS(2)   . . .
.48487    .8103    1.0086    1.1299    1.2084    1.26147   1.3004    1.33085

            Y(10)
.2015797  .09315479

 Y(1)     Y(2)   . . .
.987946   .9520884  .8933827  .8133888  .7142811  .598922   .4709653  .3355246

ALPHA     B2      TR       CR      DX
10.       19.85   .5       5.167   .2

        NSTEP     JPUNCH
          18         1

                        TITLE
WHITCOMB AIRFOIL CL=1.2217  B/2=19.85  DATA FOR ATLIT         First Card
```

Program Listing

```
   90 FORMAT (1X,F7.3,5X,F15.8)                                    WSH 121
   95 CONTINUE                                                     WSH 122
C***  THE TRAILING EDGE IS AT X=0, Z=0, Y=-B/2 TO B/2             WSH 123
C***  CALCULATE DOWNSTREAM LOCATION OF EACH TRAILING EDGE VORTEX   WSH 124
C***  ASSUMING A MIRROR IMAGE FOR THE POSITIVE Y-AXIS. THE NEGATIVE AXIS  WSH 125
C***  VALUES ARE STORED BUT USING SYMMETRY THE POSITIVE VALUES ARE ALSO   WSH 126
C***  KNOWN                                                       WSH 127
C***  V(I,J,K)=-I#VORTEX INDEX(1-9) , J=COMPONENT INDEX(1-3)(XYZ),  WSH 128
C***  K=STATION INDEX(1-20)                                       WSH 129
C***  P(I,J,K)=-I#VORTEX INDEX(1-9) , J=COMPONENT INDEX(1-3)(XYZ),  WSH 130
C***  K=STATION INDEX(1-20)                                       WSH 131
C***  STATION 1 IS AT THE BOUND VORTEX                            WSH 132
C***  STATION 2 IS AT THE TRAILING EDGE (X=0, Y=Y(I), Z=0)        WSH 133
C***  STATION 3 IS AT FIRST DOWNSTREAM STEP, ETC.                 WSH 134
      DO 100 I=1,9                                                 WSH 135
      DO 100 J=1,2                                                 WSH 136
      S(I,J)=0.D0                                                  WSH 137
      V(I,1,J)=1.D0                                                WSH 138
      V(I,3,J)=0.D0                                                WSH 139
  100 V(I,2,J)=0.D00                                               WSH 140
      DO 105 I=1,9                                                 WSH 141
      P(I,1,1)=XB                                                  WSH 142
      P(I,2,1)=YGANS(I)                                            WSH 143
      P(I,3,1)=ZB                                                  WSH 144
      P(I,1,2)=0.D0                                                WSH 145
      P(I,2,2)=YGANS(I)                                            WSH 146
  105 P(I,3,2)=0.D0                                                WSH 147
C***  LOOP OVER ALL DOWNSTREAM STATIONS                           WSH 148
      DO 170 J=2,NSTEP                                             WSH 149
      DO 165 I=1,9                                                 WSH 150
      DELX=DX/2.D0                                                 WSH 151
      DELY=V(I,2,J)#DELX                                           WSH 152
      DELZ=V(I,3,J)#DELX                                           WSH 153
      IF (J.EQ.2)DELZ=-DTAN(ALP)#DELX                              WSH 154
      P0(1)=P(I,1,J)+DELX                                          WSH 155
      P0(2)=P(I,2,J)+DELY                                          WSH 156
      P0(3)=P(I,3,J)+DELZ                                          WSH 157
C***  CALCULATE BOUND VORTEX CONTRIBUTION                         WSH 158
      CALL WB(P0,UU,VV,WW)                                         WSH 159
      WT(1)=UU                                                     WSH 160
      WT(2)=VV                                                     WSH 161
      WT(3)=WW                                                     WSH 162
C***  LOOP OVER ALL 10 TRAILING VORTICES                          WSH 163
      DO 155 K=1,18                                                WSH 164
      KKM=19-K                                                     WSH 165
C***  VORTEX CANNOT INDUCE VELOCITY ON ITSELF                     WSH 166
      IF (I.EQ.K) GO TO 155                                        WSH 167
      DO 150 L=1,J                                                 WSH 168
      LL=L+1                                                       WSH 169
      IF (K.GT.9) GO TO 110                                        WSH 170
      P1(1)=P(K,1,L)                                               WSH 171
      P1(2)=P(K,2,L)                                               WSH 172
      P1(3)=P(K,3,L)                                               WSH 173
      GO TO 115                                                    WSH 174
  110 P1(1)=P(KKM,1,L)                                             WSH 175
      P1(2)=-P(KKM,2,L)                                            WSH 176
      P1(3)=P(KKM,3,L)                                             WSH 177
  115 IF (L.EQ.J) GO TO 125                                        WSH 178
      IF (K.GT.9) GO TO 120                                        WSH 179
      P2(1)=P(K,1,LL)                                              WSH 180

      P2(2)=P(K,2,LL)                                              WSH 181
      P2(3)=-P(K,3,LL)                                             WSH 182
      GO TO 135                                                    WSH 183
  120 P2(1)=P(KKM,1,LL)                                            WSH 184
      P2(2)=-P(KKM,2,LL)                                           WSH 185
      P2(3)=P(KKM,3,LL)                                            WSH 186
      GO TO 135                                                    WSH 187
  125 IF (K.GT.9) GO TO 130                                        WSH 188
C***  SET LAST POINT AT K = INFINITY                              WSH 189
      P2(1)=100000.D0                                              WSH 190
      P2(2)=P(K,2,L)                                               WSH 191
      P2(3)=P(K,3,L)                                               WSH 192
      GO TO 135                                                    WSH 193
  130 P2(1)=100000.D0                                              WSH 194
      P2(2)=-P(KKM,2,L)                                            WSH 195
      P2(3)=P(KKM,3,L)                                             WSH 196
  135 IF (K.GT.9) GO TO 140                                        WSH 197
      GM=GANS(K)                                                   WSH 198
      GO TO 145                                                    WSH 199
  140 GM=-GANS(KKM)                                                WSH 200
C***  CALCULATE TRAILING VORTEX CONTRIBUTIONS                     VSH 201
  145 CALL WTRAIL(P1,P2,P0,GM,UU,VV,WW,B2)                         VSH 202
      WT(1)=WT(1)+UU                                               WSH 203
      WT(2)=WT(2)+VV                                               WSH 204
      WT(3)=WT(3)+WW                                               WSH 205
  150 CONTINUE                                                     WSH 206
  155 CONTINUE                                                     WSH 207
      JJ=J+1                                                       WSH 208
      DO 160 I=1,3                                                 WSH 209
  160 V(I,I,JJ)=WT(I)                                              WSH 210
      DY=WT(2)#DX                                                  WSH 211
      DZ=WT(3)#DX                                                  WSH 212
      P(I,1,JJ)=P(I,1,J)+DX                                        WSH 213
      P(I,2,JJ)=P(I,2,J)+DY                                        WSH 214
      P(I,3,JJ)=P(I,3,J)+DZ                                        WSH 215
      S(I,2,JJJ)=S(I,2,JJJ)+DSQRT((P(I,1,JJJ)-P(I,1,JJJ-1))**2+(P(I,2,JJJ)  WSH 216
     1-P(I,2,JJJ-1))**2+(P(I,3,JJJ)-P(I,3,JJJ-1))**2)              WSH 217
  165 CONTINUE                                                     WSH 218
  170 CONTINUE                                                     WSH 219
C***  USING SYMMETRY PRINT THE COORDINATES OF EACH VORTEX SHED FOR THE  WSH 220
C***  POSITIVE Y-AXIS                                             WSH 221
      MOD=NSTEP+1                                                  WSH 222
      DO 205 M=2,MOD                                               WSH 223
      MM2=M-2                                                      WSH 224
      IF (MM2.GT.0) GO TO 180                                      WSH 225
      WRITE (IWRITE,175)                                           WSH 226
  175 FORMAT (1H1//1X, 93HCOORDINATES FOR DOWNSTREAM SHED VORTICES ALONG  WSH 227
     1 THE POSITIVE Y-AXIS (FROM WING ROOT TO WING TIP),//,1X,87HS DENOT  WSH 228
     1ES PATH DISTANCE DOWNSTREAM FROM TRAILING EDGE FOR EACH VORTEX AT  WSH 229
     1THE GIVEN STEP,///,1X,13HTRAILING EDGE)               WSH 230
      GO TO 190                                                    WSH 231
  180 WRITE (IWRITE,185) MM2                                       WSH 232
  185 FORMAT (//,4X,4HSTEP,I3)                                     WSH 233
  190 DO 250 L=1,4                                                 WSH 234
      DO 205 J=1,9                                                 WSH 235
      K=10-J                                                       WSH 236
      IF (L.EQ.2) GO TO 195                                        WSH 237
      IF (L.EQ.4) GO TO 200                                        WSH 238
      PRINT(J)=P(K,L,M)                                            WSH 239
      GO TO 205                                                    WSH 240
```

100

```
195 PPRINT(J)=-PIK(L,M)
    GO TO 205
200 PPRINT(J)=S(K,M)
205 CONTINUE
    GO TO (210,220,230,240),L
210 WRITE (IWRITE,215) (PPRINT(N),N=1,9)
215 FORMAT (7X,1HX,9X,9(F9.6,3X))
    GO TO 250
220 WRITE (IWRITE,225) (PPRINT(N),N=1,9)
225 FORMAT (7X,1HY,9X,9(F9.6,3X))
    GO TO 250
230 WRITE (IWRITE,235) (PPRINT(N),N=1,9)
235 FORMAT (7X,1HZ,9X,9(F9.6,3X))
    GO TO 250
240 WRITE (IWRITE,245) (PPRINT(N),N=1,9)
245 FORMAT (20A4)
250 CONTINUE
255 CONTINUE
    WRITE (IWRITE,260) (TITLE(I),I=1,20)
260 FORMAT (1H1,//1X, 47HLISTING OF PLOT DATA SET FOR SHED VORTEX SYSTE
   1N,//,1X,20A4,//)
    WRITE (IWRITE,295) (P(9,1,J),J=2,MOD)
    IF (JPUNCH.NE.1) GO TO 275
    WRITE (IPUNCH,265) (TITLE(IP),IP=1,20)
265 FORMAT (20A4)
C*** PUNCH CONTROL INTEGERS FOR PLOT DATA SET
    MODP=MOD-1
    WRITE (IPUNCH,270) MODP
270 FORMAT (6X,3H ,18X,6H ,I9,I13)
    WRITE (IPUNCH,300) (P(9,1,J),J=2,MOD)
C*** SET-UP DATA FOR PLOT DATA SET
275 DO 305 J=2,MOD
    WORK1(1)=0.D0
    WORK2(1)=P(9,3,J)
    DO 280 M=2,10
    MM=11-M
    WORK1(M)=-P(MM,2,J)
280 WORK2(M)=P(MM,3,J)
    MMM=9
285 WORK2(M)=-P(MM,2,J)
    WORK1(10)=0.D0
    WORK2(10)=P(9,3,J)
    WRITE (IWRITE,290)
290 FORMAT (10X)
    WRITE (IWRITE,295) (WORK1(LM),LM=1,19)
    WRITE (IWRITE,295) (WORK2(LM),LM=1,19)
295 FORMAT (1X,10F10.4)
    IF (JPUNCH.NE.1) GO TO 305
    WRITE (IPUNCH,300) (WORK1(LM),LM=1,19)
    WRITE (IPUNCH,300) (WORK2(LM),LM=1,19)
300 FORMAT (10F7.4)
305 CONTINUE
C*** READ CONTROL VARIABLE SPECIFYING DOWNWASH PLANE INFORMATION
C*** DESIRED. NXORY=1 YIELDS INFORMATION IN THE PLANE X-STAT.
C*** NXORY=2 YIELDS INFORMATION IN THE Y=0 PLANE BEHIND THE WING.
C*** NXORY=3 YIELDS INFORMATION IN THE Y=0 PLANE AHEAD OF THE WING.
310 READ (IREAD,315) NXORY,STAT
315 FORMAT (I10,F10.5)

    IF (NXORY.EQ.0) GO TO 5
C*** CALL PLANE TO CALCULATE DOWNWASH IN SPECIFIED PLANE
    CALL PLANE(STAT,NXORY)
    IF (NXORY.EQ.2) GO TO 365
    IF (NXORY.EQ.3) GO TO 425
    DO 320 NI=1,6
    MI=7-NI
320 PPRINT(MI)=-YPLIM(I)
    DO 380 L=1,3
    DO 330 JL=1,6
    KL=7-JL
    DO 330 KM=1,11
    IF (L.EQ.2) GO TO 325
    WPRINT(JL,KM)=DWASHK(KL,KM,L)
    GO TO 330
325 WPRINT(JL,KM)=-DWASHK(KL,KM,L)
330 CONTINUE
C*** PRINT TOTAL FLOW ANGULAR DEVIATION, SIDEWASH, AND DOWNWASH FOR
C*** SPECIFIED PLANE ALONG THE POSITIVE X OR V AXIS. ALTHOUGH THE
C*** ANGLES ARE CALCULATED FOR THE NEGATIVE Y-AXIS THEY ARE PRINTED FOR
C*** THE POSITIVE Y-AXIS USING SYMMETRY.
    GO TO (335,345,355),L
335 WRITE (IWRITE,340) (TITLE(MML),MML=1,20),STAT
340 FORMAT (1H1//10X,20A4,//,1X,81HTOTAL FLOW ANGULAR DEVIATION INFOR
   1MATION FOR POSITIVE Y-AXIS AT THE X STATION OF ,F7.4,11H SEMI-SPAN
   2S,//)
    GO TO 305
345 WRITE (IWRITE,350) STAT
350 FORMAT (//1X,61HSIDEWASH INFORMATION FOR POSITIVE Y-AXIS AT THE X
   1STATION OF ,F7.4,11H SEMI-SPANS,//)
    GO TO 365
355 WRITE (IWRITE,360) STAT
360 FORMAT (//1X,61HDOWNWASH INFORMATION FOR POSITIVE Y-AXIS AT THE X
   1STATION OF ,F7.4,11H SEMI-SPANS,//)
365 WRITE (IWRITE,370) (PPRINT(I),I=1,6)
370 FORMAT (6X,6(3HY =,F7.4,11X),/,6X,6(1HZ,6X,5HANGLE,9X))
    WRITE (IWRITE,375) ((ZPL(I,J),WPRINT(I,J),I=1,6),J=1,11)
375 FORMAT (11(6(3X,F7.4,2X,F6.2,3X)/))
380 CONTINUE
    GO TO 310
385 WRITE (IWRITE,390) (TITLE(MML),MML=1,20)
390 FORMAT (1H1,/1X,74HDOWNWASH INFORMATION FOR THE POSITIVE X-AXIS AT
   1 THE PLANE OF SYMMETRY. Y=0.//,1X,20A,///)
    I1=1
    I2=12
    DO 410 KK=1,2
    WRITE (IWRITE,395) (XPL(I),I=I1,I2)
395 FORMAT (5X,1HZ,5X,12(3HX =,F5.2,2X),//1X,12(1X,5HANGLE,4X))
400 FORMAT (2(12X,F6.3,3X,12(F6.2,4X)/))
405 FORMAT (//)
410 I2=12+I2
    WRITE (IWRITE,415) (XPL(I),I=25,31)
415 FORMAT (5X,1HZ,5X,7(3HX =,F5.2,2X)//,11X,7(1X,5HANGLE,4X))
    WRITE (IWRITE,420) (ZPL(J),(DWASHY(I,J),I=25,31),J=1,21)
420 FORMAT (21(2X,F6.3,3X,7(F6.2,4X)/))
    GO TO 310
425 WRITE (IWRITE,430) (TITLE(MML),MML=1,20)
```

101

```
430 FORMAT (1H1//1X,74HDOWNWASH INFORMATION FOR THE NEGATIVE X-AXIS AT    WSH 361
   1 THE PLANE OF SYMMETRY, Y=0.//1X,20AA,//)                             WSH 362
    WRITE (IWRITE,435) (KPL(I),I=1,11)                                    WSH 363
435 FORMAT (5X,1H2,45X,11(2HX=,F6.3,2X),/11X,11(1X,5HANGLE,4X))           WSH 364
    WRITE (IWRITE,440) (ZPLL(J),(DWASHY(I,J),I=1,11),J=1,11)              WSH 365
440 FORMAT (111(2X,F6.3,3X,11(F6.2,4X)/))                                 WSH 366
    GO TO 310                                                             WSH 367
445 CALL EXIT                                                             WSH 368
    END                                                                   WSH 369

    SUBROUTINE WB(P0,UU,VV,WN)                                            WB   1
C***  THIS SUBROUTINE CALCULATES VELOCITY COMPONENTS AT THE POINT P0      WB   2
C***  DUE TO THE BOUND WING VORTEX AT THE WING QUARTER CHORD              WB   3
C***  P0(I)=X,Y,Z LOCATIONS OF PCINT AT WHICH DOWNWASH IS COMPUTED        WB   4
C***  XB,ZB ARE XCZ LOCATIONS OF BOUND VORTEX X=0.Y=0.Z=0 IS AT T.E.      WB   5
    IMPLICIT REAL*8(A-H,O-Z)                                              WB   6
    COMMON ALP,CL,CD,BZ,TR,CR,XB,ZB,AA(4,20),YI(20),YGAMS(9),GAM(20),GA   WB   7
   1MS(9),WT(3),V(9,3,20),P(9,3,20),DWASHK(6,11,3),DWASHY(31,21),XPL(3    WB   8
   11),YPL(6),ZPL(6,11),ZPLL(21),DX,NSTEP                                 WB   9
    COMMON /WASH/A,B,DEL,XK                                               WB  10
    EXTERNAL WBB                                                          WB  11
    DIMENSION P0(3)                                                       WB  12
    PHI=3.1715926535E979                                                  WB  13
    AS=DSQRT((P0(1)-XB)*(P0(1)-XB)+(P0(3)-ZB)*(P0(3)-ZB))                 WB  14
    A=AS*AS-P0(2)*P0(2)                                                   WB  15
    B=-2.D0*P0(2)                                                         WB  16
    DEL=4.D0*A-B*B                                                        WB  17
    KK=AS/(4.D0*PHI*B2)                                                   WB  18
    WTT=0.D0                                                              WB  19
    DO 5 I=1,19                                                           WB  20
    YY2=Y(I+1)                                                            WB  21
    YY1=Y(I)                                                              WB  22
  5 WTT=WTT+WBB(I,YY2)-WBB(I,YY1)                                         WB  23
    WN=WTT*(P0(1)-XB)/AS                                                  WB  24
    UU=WTT*(P0(3)-ZB)/AS                                                  WB  25
    VV=0.D0                                                               WB  26
    RETURN                                                                WB  27
    END                                                                   WB  28

    FUNCTION WBB(I,X)                                                     WBB  1
C***  THIS FUNCTION CALCULATES THE VELOCITY COMPONENTS AT THE POINT P0    WBB  2
C***  FOR THE INDIVIDUAL SPLINE SEGMENTS OF THE BOUND VORTEX              WBB  3
    IMPLICIT REAL*8(A-H,O-Z)                                              WBB  4
    COMMON ALP,CL,CD,BZ,TR,CR,XB,ZB,AA(4,20),YI(20),YGAMS(9),GAM(20),GA   WBB  5
   1MS(9),WT(3),V(9,3,20),P(9,3,20),DWASHK(6,11,3),DWASHY(31,21),XPL(3    WBB  6
   11),YPL(6),ZPL(6,11),ZPLL(21),DX,NSTEP                                 WBB  7
    COMMON /WASH/A,B,DEL,XK                                               WBB  8
    R=DSQRT(A+B*X+X*X)                                                    WBB  9
    WBB=(XK/(DEL*R))*(AA(1,I)*(DEL*X*X+B*(10.D0*A-3.D0*B*B)*X+8.D0*A*A     WBB 10
   1-3.D0*A*B*B)+AA(2,I)*(B*B-DEL)*X+2.D0*A*B)+AA(3,I)*(-4.D0*A-2.D0*     WBB 11
   1B*X)+AA(4,I)*(B+2.D0*X))                                              WBB 12
    WBB=WBB+KK*(4.D0*A-2.D0*B*B)*AA(1,I)-1.5D0*B*AA(2,I))*DLOG(           WBB 13
   1.D0*R+2.D0*X+B)                                                       WBB 14
    RETURN                                                                WBB 15
    END                                                                   WBB 16

    SUBROUTINE WTRAIL(P1,P2,P0,GAM,U,V,W,B2)                              VTL  1
C***  THIS SUBROUTINE CALCULATES THE VLEOCITY COMPONENTS INDUCED AT THE   VTL  2
C***  POINT P0 DUE TO A STRAIGHT-LINE VORTEX SEGMENT FROM P1 TO P2        VTL  3
    IMPLICIT REAL*8(A-H,O-Z)                                              VTL  4
    DIMENSION P0(3),P1(3),P2(3)                                           VTL  5
    PHI=3.1715926535E979                                                  VTL  6
    X21=P2(1)-P1(1)                                                       VTL  7
    Y21=P2(2)-P1(2)                                                       VTL  8
    Z21=P2(3)-P1(3)                                                       VTL  9
    X01=P0(1)-P1(1)                                                       VTL 10
    Y01=P0(2)-P1(2)                                                       VTL 11
    Z01=P0(3)-P1(3)                                                       VTL 12
    X02=P0(1)-P2(1)                                                       VTL 13
    Y02=P0(2)-P2(2)                                                       VTL 14
    Z02=P0(3)-P2(3)                                                       VTL 15
    D21SQ=X21*X21+Y21*Y21+Z21*Z21                                         VTL 16
    D01SQ=X01*X01+Y01*Y01+Z01*Z01                                         VTL 17
    D02SQ=X02*X02+Y02*Y02+Z02*Z02                                         VTL 18
    D21=DSQRT(D21SQ)                                                      VTL 19
    D01=DSQRT(D01SQ)                                                      VTL 20
    D02=DSQRT(D02SQ)                                                      VTL 21
    COSTH1=(D21SQ+D01SQ-D02SQ)/(2.D0*D21*D01)                             VTL 22
    COSTH2=(D21SQ+D02SQ-D01SQ)/(2.D0*D21*D02)                             VTL 23
    IF (P2(1).LT.99999.D0) GO TO 5                                        VTL 24
    COSTH1=DSQRT((X01*X01)/(X01*X01+Y01*Y01+Z01*Z01))                     VTL 25
    IF (P0(1).LT.P1(1))COSTH1=-COSTH1                                     VTL 26
    COSTH2=1.D0                                                           VTL 27
  5 AP=Y21*Z01-Y01*Z21                                                    VTL 28
    BP=-X21*Z01+X01*Z21                                                   VTL 29
    CP=X21*Y01-X01*Y21                                                    VTL 30
    RAD=DSQRT(AP*AP+BP*BP+CP*CP)                                          VTL 31
    WTT=(GAM/4.D0/PHI)*(COSTH1+COSTH2)/(D01*B2*DSQRT(1.D0-COSTH1*COSTH    VTL 32
   1))                                                                    VTL 33
    U=WTT*AP/RAD                                                          VTL 34
    V=WTT*BP/RAD                                                          VTL 35
    W=WTT*CP/RAD                                                          VTL 36
    RETURN                                                                VTL 37
    END                                                                   VTL 38

    SUBROUTINE SPLINE(N,Y,X,AA)                                           SPL  1
C***  THIS SUBROUTINE PERFORMS A SPLINE FIT ON THE TABULATED              SPL  2
C***  DATA Y VS. X, THE SPLINE FIT PROVIDES A CURVE FIT OF THE            SPL  3
C***  TABULATED DATA, THAT HAS A CONTINUOUS FIRST DERIVATIVE. THE         SPL  4
C***  FORM OF THE CURVE FIT IS                                            SPL  5
C***      Y = AA(1,I)*X**3 + AA(2,I)*X**2                                 SPL  6
C***          + AA(3,I)*X + AA(4,I)                                       SPL  7
C***  FOR       X(I) <= X <= X(I+1).                                      SPL  8
C***      N   - NUMBER OF TABULATED DATA POINTS                           SPL  9
C***      Y   - TABULATED FUNCTION VALUES                                 SPL 10
C***      X   - TABULATED ARGUEMENT VALUES                                SPL 11
C***      AA  - ARRAY OF COEFFICIENTS OF THE CUBIC POLYNOMIAL             SPL 12
C***            SPLINE FIT. DIMENSIONS OF AA ARE 4 BY N-1.                SPL 13
C***  REFERENCE FOR THIS METHOD IS                                        SPL 14
C***      THE THEORY OF SPLINES AND THEIR APPLICATIONS                    SPL 15
C***      J.H. AHLBERG, ET AL, ACADEMIC PRESS, NEW YORK , 1967            SPL 16
    IMPLICIT REAL*8(A-H,O-Z)                                              SPL 17
```

```
      DIMENSION AA(6,20),H(20),D(20),U(20),X(20),Y(20)
      NN1=N-1
      DO 5 I=1,NN1
5     H(I)=X(I+1)-X(I)
C***  MODIFIED LEFT HAND END CONDITION THAT ALEVIATES THE NEED
C***  TO SPECIFY THE X-DERIVATIVE OF Y AT POINT 1
      Q(1)=-31.0D0/32.0D0
      H1=H(1)
      H2=H(2)
      H3=H(3)
      U(1)=-Y(1)*(32.0D0*H1+42.0D0*H2+21.0D0*H3)/(H1+H2)/(H1+H2+H3)-Y(2)*
     1(11.0D0*H1+42.0D0*H2+21.0D0*H3)/H2*Y(3)*H1*(11.0D0*H1+21.0
     100*(H2+H3))/(H1+H2)/H2/H3-Y(4)*H1*H1*(11.0D0*H1+21.0D0*H2)/(H2+H3)/(H1
     1+H2+H3)/H3
C***  GENERATE INTERNAL U(I) BY ALGORITHM GIVEN BY AHLBERG
      U(1)=3.0D0*U(1)/H1/16.0D0
      HM=H(1)
      YY=Y(2)
      YM=Y(1)
      DO 10 I=2,NM1
      HH=H(I)
      YPP=Y(I+1)
      D=3.0D0*((YP-YY)/HH-(YY-YM)/(HM+HM))
      C=0.50D0*HH/(HH+HM)
      A=0.500-C
      P=A*Q(I-1)+1.0D0
      Q(I)=-C/P
      U(I)=(D-A*U(I-1))/P
      HM=HH
      YM=YY
10    YY=YPP
C***  MODIFIED RIGHT HAND END CONDITION THAT ALEVIATES THE NEED
C***  TO SPECIFY THE X-DERIVATIVE OF Y AT POINT N
      A=31.0D0/32.0D0
      P=A*Q(N-1)+1.0D0
      H1=H(NM1)
      H2=H(NM1-1)
      H3=H(NM1-2)
      DHY(N)=(32.0D0*H1+42.0D0*H2+21.0D0*H3)/(H1+H2)/(H1+H2+H3)*Y(N)+
     1(11.0D0*H1+42.0D0*H2+21.0D0*H3)/(H2+H3)/H2*Y(NM1-1)*H1*(11.0D0*H1+2
     11.0D0*(H2+H3))/(H1+H2)/H2/H3-Y(NM1-2)*H1*(11.0D0*H1+21.0D0*H2)/(H2
     1+H3)/(H1+H2+H3)/H3
      D=3.0D0*DHY/H1/16.0D0
      U(N)=(D-A*U(N-1))/P
C***  SOLVE FOR THE SPLINE COEFFICIENTS CORRESPONDING TO AHLBERG'S
C***  M(0) TO M(N) AND STORE THEM IN THE U(I).
      DO 15 J=1,NM1
      I=N-J
15    U(I)=U(I)+Q(I)*U(I+1)
C***  FORM THE AA(J,1) COEFFICIENTS FOR THE CONVENTIONAL FORM OF
C***  A. CUBIC POLYNOMIAL FROM THE U(I)
      UU=U(1)
      XX=X(1)
      YY=Y(1)
      DO 20 I=1,NM1
      UP=U(I+1)
      XP=X(I+1)
      YP=Y(I+1)
      HH=H(I)
      AA(1,I)=(UP-UU)/HH/6.0D0
      AA(2,I)=0.5D0*(XP*UU-X*UP)/HH
      AA(3,I)=0.5D0*(UP*XX*X-UU*X*XP)/HH*(UU-UP)/HH/6.0D0*(YP-YY)/HH
      AA(4,I)=(UU*XP*XP*XP-UP*X*XX*XX)/HH/6.0D0*(UP*XX-UU*XP)*HH/6.0D0+
     1(YY*XP-YP*XX)/HH
      XX=XP
      UU=UP
20    YY=YP
      RETURN
      END

      SUBROUTINE PLANE(STAT,NXORY)
C***  THIS SUBROUTINE CALCULATES THE DOWNWASH AND SIDEWASH FOR THE
C***  SPECIFIED PLANE OF INTEREST. NXORY=1 CALCULATES DOWNWASH AND
C***  SIDEWASH ANGLES FOR NEGATIVE Y-AXIS AT ANY DOWNSTREAM X-STEP
C***  STATION (STAT). THIS STATION MUST BE ONE OF THE STEP LOCATIONS AFT
C***  OF THE TRAILING EDGE OR ANY X-STATION AHEAD OF THE WING LEADING
C***  EDGE. DOWNWASH AND SIDEWASH PROFILES ARE CALCULATED AT EACH OF THE
C***  MOST INBOARD Y-COORDINATES OF THE SHED VORTICES. THE
C***  Z-COORDINATES OF EACH OF THESE 6 Y-STATIONS RANGES FROM +.25 TO
C***  -.25 IN STEPS OF +05 SEMISPANS ABOVE AND BELOW THE WAKE CENTERLINE
C***  FOR THE SPECIFIED X-STAT PLANE. NXORY=2 CALCULATES DOWNWASH ANGLES
C***  ON THE POSITIVE X-AXIS FROM X=.25 TO X=1.75 SEMISPANS IN THE Y=0
C***  PLANE. Z RANGES FROM STAT=.5 TO STAT=-.5 IN STEPS OF .05 WHERE
C***  STAT IS SPECIFIED AS THE MIDPOINT OF THE Z-RANGE DESIRED.
C***  NXORY=3 CALCULATES THE UPWASH (NEGATIVE DOWNWASH) ANGLES ON THE
C***  NEGATIVE X-AXIS FROM X=X-LEADING EDGE TO X=.5 SEMISPANS AHEAD OF
C***  THE LEADING EDGE IN THE Y=0 PLANE. Z RANGES FROM .25 SEMISPANS
C***  ABOVE TO .25 SEMISPANS BELOW Z-LEADING EDGE.
      IMPLICIT REAL*8(A-H,O-Z)
      COMMON ALP,CL,CD,B2,TR,CR,XB,ZB,AA(4,20),YI(20),YGANS(9),GAN(20),GA
     1NS(9),WT(3),VI(9,3,20),PI(9,3,20),DWASH(6,11,3),DWASHV(31,21),XPL(3
     11),YPL(6),ZPL(6,11),ZPLL(21),DX,NSTEP
      DIMENSION P0(3),PI(3),P2(3)
      CRAD=57.295779510D0
      IF (NXORY.EQ.2) GO TO 70
      IF (NXORY.EQ.3) GO TO 105
C***  CALCULATE INFORMATION FOR PLANE AT X=CONSTANT FOR THE 6 MOST
C***  INBOARD SHED VORTICES (I=4,9)
      NX=(STAT-.0001D0)/DX+2
      IF (STAT.LT.0.0D0)NX=1
      DO 65 I=4,9
      M=10-I
      ZPL(M,6)=P(I,3,NX)
      DO 5 K=1,5
      ZPL(M,6+K)=ZPL(M,6+K-1)-.05D0
5     ZPL(M,6-K)=ZPL(M,6-K+1)+.05D0
      DO 60 J=1,11
      P0(I)=P(I,1,NX)
      IF (STAT.LT.0.0D0)P0(I)=STAT
      VPL(M)=P(I,2,NX)
      P0(2)=YPL(M)
      P0(3)=ZPL(M,J)
      CALL WB(P0,WASHU,WASHV,WASHW)
      DO 55 K=1,18
      KM1=19-K
      IF (I.EQ.K) GO TO 55
      DO 50 L=1,NSTEP
      LL=L+1
```

```
      IF (K.GT.9) GO TO 10                                            PLA  49
      P1(1)=P(K,1,L)                                                  PLA  50
      P1(2)=P(K,2,L)                                                  PLA  51
      P1(3)=P(K,3,L)                                                  PLA  52
      GO TO 15                                                        PLA  53
   10 P1(1)=P(KM1,1,L)                                                PLA  54
      P1(2)=-P(KM1,2,L)                                               PLA  55
      P1(3)=P(KM1,3,L)                                                PLA  56
   15 IF (L.EQ.NSTEP) GO TO 25                                        PLA  57
      IF (K.GT.9) GO TO 20                                            PLA  58
      P2(1)=P(K,1,LL)                                                 PLA  59
      P2(2)=P(K,2,LL)                                                 PLA  60
      P2(3)=P(K,3,LL)                                                 PLA  61
      GO TO 35                                                        PLA  62
   20 P2(1)=P(KM1,1,LL)                                               PLA  63
      P2(2)=-P(KM1,2,LL)                                              PLA  64
      P2(3)=P(KM1,3,LL)                                               PLA  65
      GO TO 35                                                        PLA  66
   25 IF (K.GT.9) GO TO 30                                            PLA  67
      P2(1)=100000.D0                                                 PLA  68
      P2(2)=P(K,2,L)                                                  PLA  69
      P2(3)=P(K,3,L)                                                  PLA  70
      GO TO 35                                                        PLA  71
   30 P2(1)=100000.D0                                                 PLA  72
      P2(2)=-P(KM1,2,L)                                               PLA  73
      P2(3)=P(KM1,3,L)                                                PLA  74
   35 IF (K.GT.9) GO TO 40                                            PLA  75
      GM=GAMS(K)                                                      PLA  76
      GO TO 45                                                        PLA  77
   40 GM=-GAMS(KM1)                                                   PLA  78
   45 CALL WTRAIL(P1,P2,P0,GM,UU,VV,WW,B2)                            PLA  79
      WASHU=WASHV+UU                                                  PLA  80
      WASHV=WASHV+VV                                                  PLA  81
      WASHW=WASHW+WW                                                  PLA  82
   50 CONTINUE                                                        PLA  83
   55 CONTINUE                                                        PLA  84
      RAD=DSQRT(WASHV*WASHV+WASHW*WASHW)                              PLA  85
C***  DWASHX(M,J,1)=TOTAL ANGULAR DEVIATION FROM FREESTREAM AT A POINT PLA  86
C***  IN THE PLANE X=CONSTANT                                        PLA  87
C***  DWASHX(M,J,2)=SIDEWASH ANGLE AT A POINT IN THE PLANE X=CONSTANT PLA  88
C***  DWASHX(M,J,3)=DOWNWASH ANGLE AT A POINT IN THE PLANE X=CONSTANT PLA  89
      DWASHX(M,J,1)=DATAN(RAD)*CRAD                                   PLA  90
      DWASHX(M,J,2)=DATAN(WASHV)*CRAD                                 PLA  91
      DWASHX(M,J,3)=-DATAN(WASHW)*CRAD                                PLA  92
   60 CONTINUE                                                        PLA  93
   65 CONTINUE                                                        PLA  94
      RETURN                                                          PLA  95
C***  CALCULATE INFORMATION FOR THE POSITIVE X-AXIS IN THE Y=0 PLANE  PLA  96
   70 XPL(1)=-.2500                                                   PLA  97
      DO 75 I=2,31                                                    PLA  98
   75 XPL(I)=XPL(I-1)+.0500                                           PLA  99
      ZPLL(1)=STAT*.500                                               PLA 100
      DO 80 I=2,21                                                    PLA 101
   80 ZPLL(I)=ZPLL(I-1)-.0500                                         PLA 102
      PO(2)=0.D0                                                      PLA 103
      DO 100 I=1,31                                                   PLA 104
      PO(1)=XPL(I)                                                    PLA 105
      DO 100 J=1,21                                                   PLA 106
      PO(3)=ZPLL(J)                                                   PLA 107
      CALL WB(PO,WASHU,WASHV,WASHW)                                   PLA 108
C***  OMIT SHED VORTEX AT STATION NEAREST WING ROOT                   PLA 109
      DO 95 K=1,8                                                     PLA 110
      DO 95 L=1,NSTEP                                                 PLA 111
      LL=L+1                                                          PLA 112
      P1(1)=P(K,1,L)                                                  PLA 113
      P1(2)=P(K,2,L)                                                  PLA 114
      P1(3)=P(K,3,L)                                                  PLA 115
      IF (L.EQ.NSTEP) GO TO 85                                        PLA 116
      P2(1)=P(K,1,LL)                                                 PLA 117
      P2(2)=P(K,2,LL)                                                 PLA 118
      P2(3)=P(K,3,LL)                                                 PLA 119
      GO TO 90                                                        PLA 120
   85 P2(1)=100000.D0                                                 PLA 121
      P2(2)=P(K,2,L)                                                  PLA 122
      P2(3)=P(K,3,L)                                                  PLA 123
   90 GM=GAMS(K)                                                      PLA 124
      WASHW=WASHW*2.D0+WW                                             PLA 125
      CALL WTRAIL(P1,P2,P0,GM,UU,VV,WW,B2)                            PLA 126
C***  DWASHY(I,J)=DOWNWASH ANGLE AT A POINT IN THE PLANE Y=0          PLA 127
  100 DWASHY(I,J)=-DATAN(WASHW)*CRAD                                  PLA 128
      RETURN                                                          PLA 129
C***  CALCULATE INFORMATION FOR THE NEGATIVE X-AXIS IN THE Y=0 PLANE  PLA 130
  105 ZPLL(1)=CR*DSIN(ALP)/B2*+.2500                                  PLA 131
      XPL(1)=-CR*DCOS(ALP)/B2                                         PLA 132
      DO 110 I=2,11                                                   PLA 133
      XPL(I)=XPL(I-1)-.0500                                           PLA 134
  110 ZPLL(I)=ZPLL(I-1)-.0500                                         PLA 135
      PO(2)=0.D0                                                      PLA 136
      DO 130 I=1,11                                                   PLA 137
      PO(1)=XPL(I)                                                    PLA 138
      DO 130 J=1,11                                                   PLA 139
      PO(3)=ZPLL(J)                                                   PLA 140
      CALL WB(PO,WASHU,WASHV,WASHW)                                   PLA 141
      DO 125 K=1,9                                                    PLA 142
      DO 125 L=1,NSTEP                                                PLA 143
      LL=L+1                                                          PLA 144
      P1(1)=P(K,1,L)                                                  PLA 145
      P1(2)=P(K,2,L)                                                  PLA 146
      P1(3)=P(K,3,L)                                                  PLA 147
      IF (L.EQ.NSTEP) GO TO 115                                       PLA 148
      P2(1)=P(K,1,LL)                                                 PLA 149
      P2(2)=P(K,2,LL)                                                 PLA 150
      P2(3)=P(K,3,LL)                                                 PLA 151
      GO TO 120                                                       PLA 152
  115 P2(1)=100000.D0                                                 PLA 153
      P2(2)=P(K,2,L)                                                  PLA 154
      P2(3)=P(K,3,L)                                                  PLA 155
  120 GM=GAMS(K)                                                      PLA 156
      CALL WTRAIL(P1,P2,P0,GM,UU,VV,WW,B2)                            PLA 157
      WASHW=WASHW*2.D0+WW                                             PLA 158
  125 CONTINUE                                                        PLA 159
C***  DWASHY(I,J)=DOWNWASH ANGLE AT A POINT IN THE PLANE Y=0          PLA 160
  130 DWASHY(I,J)=-DATAN(WASHW)*CRAD                                  PLA 161
      RETURN                                                          PLA 162
      END                                                             PLA 163
```

104

Sample Output

WHITCOMB AIRFOIL CL=1.2217   B/2=19.85   DATA FOR ATLIT

```
ALPHA  =  0.1000000 02   DEGREES
BE     =  0.1985000 02   FEET
TR     =  0.5000000 00
CR     =  0.5167000 01   FEET
DK     =  0.7800000 00   SEMISPANS
XR     = -0.1922610 00   SEMISPANS
ZR     =  0.3390080-01   SEMISPANS
NSTEP  =  18
JPUNCH =   1
```

INPUT SEMI-SPAN VALUES

I	Y(I)	CLS(I)	
1	0.9879460 00	0.4848700 00	TIP VALUE (Y-POSITIVE)
2	0.9520880 00	0.5103000 00	
3	0.8933830 00	0.1008600 01	
4	0.8133890 00	0.1129900 01	
5	0.7142810 00	0.1208600 01	
6	0.5989220 00	0.1261470 01	
7	0.4709650 00	0.1300460 01	
8	0.3355250 00	0.1330850 01	
9	0.2015800 00	0.1366600 01	
10	0.9315480-01	0.1391080 01	ROOT VALUE

REORDERED FULL-SPAN VALUES

I	Y(I)	CLS(I)	C(I)	GAM(I)	
1	-0.9879460 00	0.4848700 00	0.2614840 01	0.6338810 00	TIP VALUE (Y-NEGATIVE)
2	-0.9520880 00	0.5103000 00	0.2707280 01	0.1096850 01	
3	-0.8933830 00	0.1008600 01	0.2958950 01	0.1441770 01	
4	-0.8133890 00	0.1129900 01	0.3045610 01	0.1731920 01	
5	-0.7142810 00	0.1208600 01	0.3321650 01	0.2006940 01	
6	-0.5989220 00	0.1261470 01	0.3614690 01	0.7283060 01	
7	-0.4709650 00	0.1300460 01	0.3950260 01	0.2500440 01	
8	-0.3355250 00	0.1330850 01	0.4300170 01	0.2961440 01	
9	-0.2015800 00	0.1366600 01	0.4646220 01	0.3174760 01	
10	-0.9315480-01	0.1391080 01	0.4926330 01	0.3426460 01	
11	0.9315480-01	0.1391080 01	0.4926330 01	0.3174760 01	
12	0.2015800 00	0.1366600 01	0.4646220 01	0.2961440 01	
13	0.3355250 00	0.1330850 01	0.4300170 01	0.2500440 01	
14	0.4709650 00	0.1300460 01	0.3950260 01	0.2588840 01	
15	0.5989220 00	0.1261470 01	0.3619690 01	0.2283060 01	
16	0.7142810 00	0.1208600 01	0.3321650 01	0.2006940 01	
17	0.8133890 00	0.1129900 01	0.3065610 01	0.1731920 01	
18	0.8933830 00	0.1008600 01	0.2958950 01	0.1441770 01	
19	0.9520880 00	0.5103000 00	0.2707280 01	0.1096850 01	
20	0.9879460 00	0.4848700 00	0.2614840 01	0.6338810 00	TIP VALUE (Y-POSITIVE)

LOCATIONS & STRENGTHS OF THE 9 SHED VORTICES ON THE NEGATIVE Y-AXIS
(A MIRROR IMAGE IS ASSUMED FOR POSITIVE AXIS)

I	YGAMS(I)	GAMS(I)	
1	-0.9700170 00	-0.4629740 00	TIP VALUE (Y-NEGATIVE)
2	-0.9227360 00	-0.3449120 00	
3	-0.8533860 00	-0.2901500 00	
4	-0.7638350 00	-0.2750270 00	
5	-0.6566020 00	-0.2751140 00	
6	-0.5349440 00	-0.2853940 00	
7	-0.4032450 00	-0.2929620 00	
8	-0.2685520 00	-0.3133190 00	
9	-0.1471670 00	-0.2517010 00	ROOT VALUE

SPLINE FIT OF BOUND VORTEX STRENGTHS VERSUS Y

Y	GAMMA
-1.000	0.41704749
-0.950	1.11620746
-0.900	1.41511899
-0.850	1.60694242
-0.800	1.77384479
-0.750	1.91536989
-0.700	2.04247056
-0.650	2.16364133
-0.600	2.28057997
-0.550	2.39421149
-0.500	2.50511641
-0.450	2.61350071
-0.400	2.72137160
-0.350	2.82947890
-0.300	2.94063201
-0.250	3.05629117
-0.200	3.17875850
-0.150	3.30515759
-0.100	3.41427559
-0.050	3.48345737
-0.000	3.50652189
0.050	3.48345737
0.100	3.41427555
0.150	3.30515759
0.200	3.17875850
0.250	3.05629117
0.300	2.94063201
0.350	2.82947890
0.400	2.77137160
0.450	2.61350071
0.500	2.50511641
0.550	2.39421149
0.600	2.28057997
0.650	2.16364133
0.700	2.04247056
0.750	1.91536989
0.800	1.77384479
0.850	1.60694242
0.900	1.41511899
0.950	1.11620246
1.000	0.41704749

Figure A-3.   Sample output of WASH program.

COORDINATES FOR DOWNSTREAM SHED VORTICES ALONG THE POSITIVE Y-AXIS (FROM WING ROOT TO WING TIP)

S DENOTES PATH DISTANCE DOWNSTREAM FROM TRAILING EDGE FOR EACH VORTEX AT THE GIVEN STEP

TRAILING EDGE

X	0.0	0.0	0.0	0.0	0.0	0.0	0.0	0.0	0.0
Y	0.147347	0.268552	0.403245	0.534944	0.656602	0.763935	0.853186	0.922736	0.970017
Z	0.0	0.0	0.0	0.0	0.0	0.0	0.0	0.0	0.0
S	0.0	0.0	0.0	0.0	0.0	0.0	0.0	0.0	0.0

STEP 1

X	0.200000	0.200000	0.200000	0.200000	0.200000	0.200000	0.200000	0.200000	0.200000
Y	0.147945	0.269177	0.404195	0.536043	0.658319	0.765992	0.856959	0.929348	0.974307
Z	-0.022234	-1.023112	-0.019645	-0.017308	-0.015431	-0.013981	-0.012585	-0.309521	0.312445
S	0.202126	0.201356	0.200969	0.200751	0.200599	0.200499	0.200426	0.201291	0.200433

STEP 2

X	0.400000	0.400000	0.400000	0.400000	0.400000	0.400000	0.400000	0.400000	0.400000
Y	0.148616	0.269947	0.404709	0.536602	0.655742	0.767101	0.859515	0.936940	0.967587
Z	-0.052173	-0.040698	-0.034114	-0.029554	-0.026694	-0.024176	-0.322171	-0.311142	0.325191
S	0.403402	0.402128	0.401499	0.401140	0.400917	0.400772	0.400374	0.401314	0.400951

STEP 3

X	0.600000	0.600000	0.600000	0.600000	0.600000	0.600000	0.600000	0.600000	0.600000
Y	0.149547	0.270422	0.405113	0.537103	0.659492	0.768566	0.851312	0.944679	0.955749
Z	-0.073179	-0.056227	-0.046414	-0.040490	-0.016129	-0.013330	-0.329597	-0.311147	0.335433
S	0.604543	0.602715	0.601867	0.601429	0.601141	0.600963	0.600440	0.600056	0.601561

STEP 4

X	0.800000	0.800000	0.800000	0.800000	0.800000	0.800000	0.800000	0.800000	0.800000
Y	0.150731	0.270591	0.405503	0.537648	0.660184	0.770155	0.854551	0.362140	0.941474
Z	-0.093235	-0.070399	-0.057618	-0.050066	-0.044579	-0.040559	-0.335346	-0.337392	0.343492
S	0.805500	0.803217	0.802181	0.801656	0.801322	0.801115	0.800397	0.801436	0.802145

STEP 5

X	1.000000	1.000000	1.000000	1.000000	1.000000	1.000000	1.000000	1.000000	1.000000
Y	0.152177	0.271375	0.405905	0.538268	0.661466	0.772355	0.875222	0.371391	0.927673
Z	-0.111515	-0.083996	-0.068169	-0.059014	-0.052391	-0.047342	-0.313527	0.337105	0.041735
S	1.006385	1.003672	1.002460	1.001559	1.001477	1.001245	1.731151	1.002190	1.002622

STEP 6

X	1.200000	1.200000	1.200000	1.200000	1.200000	1.200000	1.200000	1.200000	1.200000
Y	0.153593	0.271891	0.406126	0.538974	0.662759	0.775535	0.851521	0.975252	0.915999
Z	-0.129744	-0.095924	-0.078292	-0.067541	-0.059753	-0.053513	-0.042199	0.328519	0.039746
S	1.207221	1.204097	1.202716	1.202042	1.201617	1.201361	1.201346	1.202972	1.202973

STEP 7

X	1.400000	1.400000	1.400000	1.400000	1.400000	1.400000	1.400000	1.400000	1.400000
Y	0.155847	0.272400	0.406769	0.539768	0.664262	0.779407	0.893115	0.372659	0.905390
Z	-0.147544	-0.109645	-0.088114	-0.075763	-0.066769	-0.059924	-0.043146	0.042387	0.035641
S	1.408022	1.404502	1.402959	1.402212	1.401746	1.401475	1.401509	1.403753	1.403275

STEP 8

X	1.600000	1.600000	1.600000	1.600000	1.600000	1.600000	1.600000	1.600000	1.600000
Y	0.158043	0.272956	0.407232	0.540648	0.665976	0.791597	0.735551	0.365129	0.898281
Z	-0.164901	-0.122131	-0.097709	-0.083746	-0.073494	-0.066525	-0.041798	0.357812	0.013026
S	1.609701	1.604892	1.603185	1.602174	1.601966	1.601589	1.601362	1.604504	1.603625

STEP 9

X	1.800000	1.800000	1.800000	1.800000	1.800000	1.800000	1.800000	1.800000	1.800000
Y	0.160528	0.273527	0.407714	0.541613	0.667896	0.799407	0.319156	0.954604	0.891291
Z	-0.182508	-0.134426	-0.107122	-0.091530	-0.079966	-0.069107	-0.037164	0.371171	0.028925
S	1.809519	1.805271	1.803410	1.802527	1.801940	1.801707	1.802414	1.805223	1.803559

STEP 10

X	2.000000	2.000000	2.000000	2.000000	2.000000	2.000000	2.000000	2.000000	2.000000
Y	0.163236	0.274112	0.408216	0.542663	0.670026	0.793321	0.333721	0.941952	0.885498
Z	-0.199913	-0.146563	-0.116383	-0.099141	-0.073870	-0.029167	0.281816	0.024219	
S	2.010263	2.005640	2.003625	2.002675	2.002088	2.001939	2.002356	2.005913	2.003725

STEP 11

X	2.200000	2.200000	2.200000	2.200000	2.200000	2.200000	2.200000	2.200000	2.200000
Y	0.166145	0.274713	0.408736	0.543799	0.672364	0.841273	0.327619	0.891267	
Z	-0.215441	-0.155563	-0.125513	-0.106597	-0.092216	-0.077959	-0.017967	0.099902	3.019940
S	2.210966	2.206000	2.203834	2.202817	2.202192	2.201971	2.203559	2.206579	2.203840

STEP 12

X	2.400000	2.400000	2.400000	2.400000	2.400000	2.400000	2.400000	2.400000	2.400000
Y	0.169375	0.275325	0.409271	0.545017	0.674994	0.897259	2.948724	0.913428	2.878304
Z	-0.231688	-0.170441	-0.134527	-0.113912	-0.099030	-0.090530	-0.001930	0.009907	0.013907
S	2.411650	2.406353	2.404038	2.402954	2.402293	2.402132	2.404191	2.407224	2.403873

STEP 13

X	2.600000	2.600000	2.600000	2.600000	2.600000	2.600000	2.600000	2.500000	2.600000
Y	0.172749	0.275945	0.409827	0.546515	0.677536	0.815161	0.952720	0.905751	2.978423
Z	-0.247659	-0.182206	-0.143433	-0.121097	-0.123644	-0.094974	0.011714	0.097725	0.009412
S	2.612316	2.606700	2.604237	2.603097	2.602390	2.632115	2.534135	2.507995	2.603971

STEP 14

X	2.800000	2.800000	2.800000	2.800000	2.800000	2.800000	2.800000	2.973000	2.800000
Y	0.174437	3.275567	0.410395	0.547689	0.680549	2.873499	0.953199	2.951315	2.873564
Z	-0.263355	-0.193966	-0.152230	-0.128144	-0.109362	-0.087909	0.027757	1.197710	0.006066
S	2.812964	2.807041	2.804432	2.803216	2.802485	2.837525	2.935179	2.534477	2.804003

STEP 15

X	3.000000	3.000000	3.000000	3.000000	3.000000	3.000000	3.000000	3.000000	3.000000
Y	0.193113	3.277197	3.000000	3.000000	3.000000	0.833385	0.950156	2.955511	1.994755
Z	-0.278775	-0.205426	-0.160948	-0.135066	-0.114253	-2.900061	0.063596	0.095233	0.004191
S	3.013595	3.007375	3.004622	3.003341	3.002577	3.336134	3.233579	3.233579	3.004025

STEP 16

X	3.200000	3.200000	3.200000	3.200000	3.200000	3.200000	3.233330	3.200000	3.200000
Y	3.184417	0.277900	0.411571	0.550043	0.684906	0.843560	0.944437	0.951332	0.885140
Z	-0.293916	-0.216490	-0.169565	-0.141990	-0.110253	-0.091594	0.344194	0.093400	0.003954
S	3.214200	3.207705	3.204809	3.203443	3.202655	3.733324	3.235771	3.233670	3.204251

STEP 17

X	3.400000	3.400000	3.400000	3.400000	3.400000	3.400000	3.433330	3.433000	3.400000
Y	3.199746	3.278398	0.412179	0.552266	0.690335	0.954275	0.935578	0.937575	0.888924
Z	-3.308777	-0.224292	-0.178090	-0.148527	-0.124010	-0.092217	3.172262	3.093479	0.005418
S	3.414908	3.409029	3.404991	3.403540	3.402751	3.433315	3.407631	3.413241	3.404093

STEP 18

X	3.600000	3.600000	3.600000	3.600000	3.600000	3.600000	3.633330	3.600000	3.633330
Y	0.193302	3.278977	3.412592	0.553951	0.693969	0.905330	0.924412	0.925300	2.992482
Z	-0.323154	-0.239546	-0.186529	-0.155070	-0.128531	-0.091557	3.384153	0.074767	0.008557
S	3.615390	3.608347	3.605170	3.603694	3.602835	3.633671	3.508131	3.512785	3.604148

Figure A-3. Continued.

LISTING OF PLOT DATA SET FOR SHED VORTEX SYSTEM

WHITCOMB AIRFOIL CL=1.2217 B/2=19.85 DATA FOR ATLIT

```
0.0       0.2000    0.4000    0.6000    0.8000    1.0000    1.2000    1.4000    1.6000    1.8000
2.0000    2.2000    2.4000    2.6000    2.8000    3.0000    3.2000    3.4000    3.6000

0.0       0.1474    0.2686    0.4032    0.5349    0.6566    0.7638    0.8534    0.9227    0.9700
0.9227    0.8534    0.7638    0.6566    0.5349    0.4032    0.2686    0.1474    0.0
0.0       0.0       0.0       0.0       0.0       0.0       0.0       0.0       0.0       3.0
0.0       0.0       0.0       0.0       0.0       0.0       0.0       0.0       0.0

0.0       0.1479    0.2694    0.4042    0.5360    0.6580    0.7659    0.8569    0.9293    0.9743
0.9293    0.8569    0.7659    0.6580    0.5360    0.4042    0.2694    0.1479    0.0
-0.0292   -0.0292   -0.0233   -0.0197   -0.0173   -0.0154   -0.0140   -0.0126   -0.0085   0.0124
-0.0085   -0.0126   -0.0140   -0.0154   -0.0173   -0.0197   -0.0233   -0.0292   -0.0292

0.0       0.1486    0.2699    0.4047    0.5366    0.6587    0.7671    0.8596    0.9369    0.9578
0.9369    0.8596    0.7671    0.6587    0.5366    0.4047    0.2699    0.1456    0.0
-0.0524   -0.0524   -0.0409   -0.0341   -0.0299   -0.0267   -0.0244   -0.0222   -0.0141   0.0252
-0.0141   -0.0222   -0.0244   -0.0267   -0.0299   -0.0341   -0.0409   -0.0524   -0.0524

0.0       0.1495    0.2704    0.4051    0.5371    0.6595    0.7686    0.8634    0.9487    0.9557
0.9487    0.8634    0.7686    0.6595    0.5371    0.4051    0.2704    0.1495    0.0
-0.0732   -0.0732   -0.0562   -0.0464   -0.0405   -0.0361   -0.0330   -0.0296   -0.0142   0.0354
-0.0142   -0.0296   -0.0330   -0.0361   -0.0405   -0.0464   -0.0562   -0.0732   -0.0732

0.0       0.1507    0.2709    0.4055    0.5376    0.6604    0.7705    0.8686    0.9621    0.9415
0.9621    0.8686    0.7705    0.6604    0.5376    0.4055    0.2709    0.1507    0.0
-0.0927   -0.0927   -0.0704   -0.0576   -0.0501   -0.0446   -0.0406   -0.0353   -0.0071   0.3439
-0.0071   -0.0353   -0.0405   -0.0446   -0.0501   -0.0576   -0.0704   -0.0927   -0.0927

0.0       0.1522    0.2714    0.4059    0.5383    0.6615    0.7729    0.8752    0.9720    0.9277
0.9720    0.8752    0.7723    0.6615    0.5383    0.4059    0.2714    0.1522    0.0
-0.1115   -0.1115   -0.0839   -0.0682   -0.0590   -0.0524   -0.0473   -0.0395   0.0071    0.0417
0.0071    -0.0395   -0.0473   -0.0524   -0.0590   -0.0682   -0.0839   -0.1115   -0.1115

0.0       0.1539    0.2719    0.4063    0.5390    0.6628    0.7758    0.8836    0.9753    0.9160
0.9753    0.8836    0.7758    0.6628    0.5390    0.4063    0.2719    0.1539    0.0
-0.1297   -0.1297   -0.0963   -0.0783   -0.0675   -0.0598   -0.0535   -0.0422   0.0246    0.0398
0.0246    -0.0422   -0.0535   -0.0598   -0.0675   -0.0783   -0.0963   -0.1297   -0.1297

0.0       0.1558    0.2724    0.4068    0.5398    0.6643    0.7790    0.8938    0.9725    0.9064
0.9725    0.8938    0.7794    0.6643    0.5398    0.4068    0.2724    0.1558    0.0
-0.1475   -0.1475   -0.1096   -0.0881   -0.0758   -0.0668   -0.0592   -0.0431   0.0421    0.0365
0.0421    -0.0431   -0.0592   -0.0668   -0.0758   -0.0881   -0.1096   -0.1475

0.0       0.1581    0.2730    0.4072    0.5406    0.6660    0.7836    0.9057    0.9551    0.8983
0.9651    0.9057    0.7836    0.6660    0.5406    0.4072    0.2730    0.1581    0.0
-0.1650   -0.1650   -0.1221   -0.0977   -0.0837   -0.0735   -0.0645   -0.0418   0.0578    0.0330
0.0578    -0.0418   -0.0645   -0.0735   -0.0837   -0.0977   -0.1221   -0.1650   -0.1650

0.0       0.1605    0.2735    0.4077    0.5416    0.6679    0.7884    0.9184    0.9546    0.8913
0.9546    0.9184    0.7884    0.6679    0.5416    0.4077    0.2735    0.1605    0.0
-0.1921   -0.1821   -0.1344   -0.1071   -0.0915   -0.0800   -0.0694   -0.0374   0.0711    0.0289
0.0711    -0.0374   -0.0694   -0.0800   -0.0915   -0.1071   -0.1344   -0.1821   -0.1821

0.0       0.1632    0.2741    0.4082    0.5427    0.6700    0.7939    0.9307    0.9419    0.8855
0.9419    0.9307    0.7939    0.6700    0.5427    0.4082    0.2741    0.1632    0.0
-0.1989   -0.1989   -0.1466   -0.1164   -0.0991   -0.0862   -0.0739   -0.0293   0.0918    0.0242
0.0818    -0.0293   -0.0739   -0.0862   -0.0991   -0.1164   -0.1466   -0.1989

0.0       0.1662    0.2747    0.4087    0.5438    0.6724    0.8002    0.9412    0.9276    0.8813
0.9276    0.9412    0.8002    0.6724    0.5438    0.4087    0.2747    0.1662    0.0
-0.2154   -0.2154   -0.1586   -0.1255   -0.1066   -0.0922   -0.0780   -0.0179   0.0393    0.0193
0.0898    -0.0179   -0.0780   -0.0922   -0.1066   -0.1255   -0.1586   -0.2154   -0.2154

0.0       0.1694    0.2753    0.4093    0.5450    0.6749    0.8073    0.9487    0.9124    0.8789
0.9124    0.9487    0.8073    0.6749    0.5450    0.4093    0.2753    0.1694    0.0
-0.2317   -0.2317   -0.1704   -0.1345   -0.1139   -0.0980   -0.0817   -0.0036   0.0951    0.0139
0.0951    -0.0036   -0.0817   -0.1704   -0.0980   -0.1139   -0.1345   -0.2317

0.0       0.1728    0.2759    0.4098    0.5463    0.6776    0.8152    0.9527    0.8968    0.8784
0.8968    0.9527    0.8152    0.6776    0.5463    0.4098    0.2759    0.1728    0.0
-0.2477   -0.2477   -0.1822   -0.1434   -0.1211   -0.1036   -0.0850   0.0117    0.0977    0.0496
0.0977    0.0117    -0.0850   -0.1036   -0.1211   -0.1434   -0.1822   -0.2477   -0.2477

0.0       0.1764    0.2766    0.4104    0.5477    0.6805    0.8239    0.9532    0.8810    0.8796
0.8810    0.9532    0.8239    0.6805    0.5477    0.4104    0.2760    0.1764    0.0
-0.2634   -0.2634   -0.1939   -0.1522   -0.1281   -0.1091   -0.0878   0.0278    0.0377    0.0081
0.0977    0.0278    -0.0878   -0.1091   -0.1281   -0.1522   -0.1939   -0.2634   -0.2634

0.0       0.1803    0.2772    0.4110    0.5491    0.6836    0.8334    0.9504    0.8556    0.8923
0.8656    0.9504    0.8334    0.6836    0.5491    0.4110    0.2772    0.1803    0.0
-0.2788   -0.2788   -0.2054   -0.1609   -0.1351   -0.1143   -0.0901   0.0036    0.0352    0.0042
0.0952    0.0436    -0.0901   -0.1143   -0.1351   -0.1609   -0.2054   -0.2788   -0.2798

0.0       0.1844    0.2778    0.4116    0.5507    0.6869    0.8438    0.9444    0.8510    0.8952
0.8510    0.9444    0.8438    0.6869    0.5507    0.4116    0.2778    0.1844    0.0
-0.2039   -0.2039   -0.2169   -0.1698   -0.1419   -0.1193   -0.0916   0.0586    0.0904    0.0049
0.0904    0.0586    -0.0916   -0.1193   -0.1419   -0.1698   -0.2169   -0.2939   -0.2939

0.0       0.1887    0.2784    0.4172    0.5523    0.6903    0.8543    0.9357    0.8376    0.8888
0.5376    0.9357    0.8543    0.6903    0.5523    0.4122    0.2784    0.1887    0.0
-0.3088   -0.3088   -0.2283   -0.1781   -0.1485   -0.1240   -0.0922   0.0723    0.0835    0.0554
0.0835    0.0723    -0.0922   -0.1240   -0.1485   -0.1781   -0.2283   -0.3088   -0.3088

0.0       0.1931    0.2790    0.4128    0.5540    0.6940    0.8654    0.9244    0.8257    0.8925
0.8257    0.9244    0.8654    0.6940    0.5540    0.4128    0.2790    0.1933    0.0
-0.3234   -0.3234   -0.2395   -0.1865   -0.1551   -0.1285   -0.0919   0.0842    0.0748    0.0386
0.0748    0.0842    -0.3913   -0.1285   -0.1551   -0.1865   -0.2395   -0.3234   -0.3234
```

Figure A-3. Continued.

WHITCOMB AIRFOIL CL=1.2217   B/2=19.85   DATA FOR ATLIT

TOTAL FLOW ANGULAR DEVIATION INFORMATION FOR POSITIVE Y-AXIS AT THE X STATION OF   0.6000 SEMI-SPANS

Y = 0.1495		Y = 0.2704		Y = 0.4051		Y = 0.5371		Y = 0.6595		Y = 0.7686	
Z	ANGLE	Z	ANGLE	Z	ANGLE	Z	ANGLE	Z	ANGLE	Z	ANGLE
0.1768	2.78	0.1938	2.89	0.2036	3.08	0.2095	3.38	0.2139	3.75	0.2170	4.22
0.1268	3.00	0.1435	3.04	0.1536	3.22	0.1595	3.55	0.1639	4.02	0.1673	4.57
0.0768	3.14	0.0938	3.12	0.1036	3.30	0.1095	3.67	0.1139	4.24	0.1170	4.96
0.0268	3.09	0.0438	3.08	0.0536	3.28	0.0595	3.59	0.0639	4.40	0.0670	5.30
-0.0232	2.70	-0.0062	2.82	0.0036	3.09	0.0095	3.56	0.0139	4.40	0.0170	5.73
-0.0732	2.29	-0.0562	2.53	-0.0464	2.87	-0.0405	3.35	-0.0361	4.21	-0.0330	5.77
-0.1232	2.62	-0.1062	2.67	-0.0964	2.81	-0.0905	3.32	-0.0861	4.39	-0.0830	5.42
-0.1732	2.83	-0.1562	2.85	-0.1464	3.03	-0.1405	3.39	-0.1361	4.03	-0.1330	4.93
-0.2232	2.75	-0.2062	2.85	-0.1964	3.03	-0.1905	3.38	-0.1861	3.80	-0.1830	4.47
-0.2732	2.57	-0.2562	2.73	-0.2464	2.93	-0.2405	3.24	-0.2361	3.67	-0.2333	4.06
-0.3232	2.36	-0.3062	2.56	-0.2964	2.78	-0.2905	3.07	-0.2861	3.42	-0.2830	3.69

SIDEWASH INFORMATION FOR POSITIVE Y-AXIS AT THE X STATION OF   0.6000 SEMI-SPANS

Y = 0.1495		Y = 0.2704		Y = 0.4051		Y = 0.5371		Y = 0.6595		Y = 0.7686	
Z	ANGLE	Z	ANGLE	Z	ANGLE	Z	ANGLE	Z	ANGLE	Z	ANGLE
0.1768	-2.32	0.1938	-2.04	0.2036	-1.76	0.2095	-1.45	0.2139	-1.01	0.2170	-0.56
0.1268	-2.45	0.1435	-2.10	0.1536	-1.81	0.1595	-1.52	0.1639	-1.09	0.1670	-0.61
0.0768	-2.44	0.0938	-2.06	0.1036	-1.78	0.1095	-1.52	0.1139	-1.12	0.1170	-0.64
0.0268	-2.15	0.0438	-1.82	0.0536	-1.56	0.0595	-1.36	0.0639	-1.04	0.0670	-0.56
-0.0232	-1.28	-0.0062	-1.14	0.0036	-0.96	0.0095	-0.88	0.0139	-0.69	0.0170	-0.26
-0.0732	0.39	-0.0562	0.13	-0.0464	0.05	-0.0405	0.01	-0.0351	0.02	-0.0330	0.25
-0.1232	1.80	-0.1062	1.37	-0.0964	1.08	-0.0905	0.91	-0.0861	0.78	-0.0630	0.42
-0.1732	2.43	-0.1562	1.98	-0.1464	1.64	-0.1405	1.42	-0.1361	1.16	-0.1330	0.72
-0.2232	2.46	-0.2062	2.14	-0.1964	1.84	-0.1905	1.59	-0.1861	1.23	-0.1933	0.69
-0.2732	2.32	-0.2562	2.11	-0.2464	1.85	-0.2405	1.58	-0.2361	1.16	-0.2330	0.61
-0.3232	2.13	-0.3062	1.99	-0.2964	1.77	-0.2905	1.49	-0.2861	1.06	-0.2830	0.54

DOWNWASH INFORMATION FOR POSITIVE Y-AXIS AT THE X STATION OF   0.6000 SEMI-SPANS

Y = 0.1495		Y = 0.2704		Y = 0.4051		Y = 0.5371		Y = 0.6595		Y = 0.7686	
Z	ANGLE	Z	ANGLE	Z	ANGLE	Z	ANGLE	Z	ANGLE	Z	ANGLE
0.1768	1.53	0.1935	2.05	0.2036	2.53	0.2095	3.06	0.2139	3.64	0.2170	4.18
0.1268	1.73	0.1435	2.20	0.1536	2.67	0.1595	3.21	0.1639	3.87	0.1670	4.53
0.0768	1.97	0.0935	2.35	0.1036	2.79	0.1095	3.34	0.1139	4.09	0.0670	4.92
0.0268	2.22	0.0438	2.49	0.0536	2.84	0.0595	3.43	0.0639	4.28	0.0670	5.35
-0.0232	2.38	-0.0062	2.58	0.0036	2.93	0.0095	3.45	0.0139	4.34	0.0170	5.73
-0.0732	2.26	-0.0562	2.53	-0.0464	2.87	-0.0405	3.35	-0.0361	4.21	-0.0330	5.76
-0.1232	1.82	-0.1062	2.29	-0.0964	2.70	-0.0905	3.19	-0.0861	4.21	-0.0830	5.38
-0.1732	1.45	-0.1562	2.06	-0.1464	2.54	-0.1405	3.08	-0.1361	3.86	-0.1330	4.88
-0.2232	1.23	-0.2062	1.88	-0.1964	2.41	-0.1905	2.95	-0.1861	3.69	-0.1830	4.47
-0.2732	1.10	-0.2562	1.73	-0.2464	2.28	-0.2405	2.83	-0.2361	3.48	-0.2332	4.01
-0.3232	1.02	-0.3062	1.61	-0.2964	2.15	-0.2905	2.69	-0.2861	3.25	-0.2830	3.65

DOWNWASH INFORMATION FOR THE POSITIVE X-AXIS AT THE PLANE OF SYMMETRY, Y=0

WHITCOMB AIRFOIL CL=1.2217   B/2=19.85   DATA FOR ATLIT

Z	X = 0.25	X = 0.30	X = 0.35	X = 0.40	X = 0.45	X = 0.50	X = 0.55	X = 0.60	X = 0.65	X = 0.70	X = 0.75	X = 0.80
	ANGLE	ANGLE	ANGLE	ANGLE	ANGLE	ANGLE	ANGLE	ANGLE	ANGLE	ANGLE	ANGLE	ANGLE
0.300	4.05	3.93	3.82	3.72	3.62	3.53	3.45	3.38	3.31	3.25	3.20	3.15
0.250	4.48	4.31	4.17	4.04	3.92	3.81	3.72	3.64	3.56	3.49	3.43	3.38
0.200	4.91	4.70	4.51	4.36	4.22	4.10	3.99	3.90	3.81	3.74	3.67	3.61
0.150	5.32	5.06	4.84	4.66	4.51	4.37	4.26	4.16	4.07	3.99	3.92	3.86
0.100	5.67	5.37	5.11	4.90	4.77	4.63	4.51	4.41	4.31	4.23	4.16	4.09
0.050	5.90	5.60	5.35	5.15	4.98	4.84	4.72	4.61	4.52	4.44	4.37	4.30
-0.000	5.99	5.69	5.46	5.27	5.10	4.97	4.85	4.75	4.67	4.59	4.52	4.46
-0.050	5.92	5.63	5.42	5.25	5.11	4.98	4.88	4.79	4.71	4.64	4.58	4.53
-0.100	5.64	5.42	5.25	5.10	4.98	4.87	4.78	4.71	4.64	4.59	4.53	4.48
-0.150	5.25	5.10	4.96	4.84	4.74	4.66	4.58	4.52	4.46	4.41	4.37	4.33
-0.200	4.42	4.71	4.61	4.52	4.44	4.37	4.31	4.26	4.21	4.17	4.14	4.11
-0.250	4.36	4.10	4.23	4.17	4.11	4.06	4.01	3.97	3.93	3.89	3.86	3.84
-0.300	3.92	3.90	3.86	3.82	3.78	3.74	3.70	3.67	3.63	3.60	3.58	3.56
-0.350	3.52	3.51	3.50	3.48	3.45	3.43	3.40	3.37	3.35	3.33	3.31	3.29
-0.400	3.15	3.17	3.17	3.16	3.15	3.14	3.12	3.10	3.09	3.06	3.05	3.03
-0.450	2.82	2.85	2.87	2.87	2.87	2.87	2.86	2.84	2.83	2.82	2.81	2.79
-0.500	2.53	2.57	2.59	2.61	2.62	2.62	2.61	2.61	2.60	2.59	2.58	2.57
-0.550	2.27	2.31	2.34	2.37	2.38	2.39	2.39	2.39	2.39	2.39	2.38	2.37
-0.600	2.04	2.09	2.13	2.15	2.17	2.19	2.19	2.19	2.19	2.19	2.19	2.19
-0.650	1.84	1.89	1.93	1.96	1.98	2.00	2.01	2.01	2.02	2.32	2.02	2.02
-0.750	1.67	1.72	1.76	1.79	1.81	1.83	1.84	1.85	1.96	1.86	1.86	1.96

Z	X = 0.85	X = 0.90	X = 0.95	X = 1.00	X = 1.05	X = 1.10	X = 1.15	X = 1.20	X = 1.25	X = 1.30	X = 1.35	X = 1.40
	ANGLE	ANGLE	ANGLE	ANGLE	ANGLE	ANGLE	ANGLE	ANGLE	ANGLE	ANGLE	ANGLE	ANGLE
0.300	3.10	3.06	3.02	2.99	2.95	2.92	2.89	2.87	2.84	2.82	2.80	2.77
0.250	3.33	3.28	3.24	3.20	3.16	3.13	3.10	3.07	3.04	3.02	2.99	2.97
0.200	3.56	3.51	3.46	3.42	3.38	3.35	3.32	3.28	3.26	3.23	3.20	3.18
0.150	3.80	3.75	3.70	3.65	3.61	3.58	3.54	3.51	3.48	3.45	3.42	3.40
0.100	4.03	3.98	3.93	3.93	3.84	3.80	3.77	3.73	3.70	3.67	3.65	3.62
0.050	4.25	4.19	4.14	4.10	4.06	4.02	3.98	3.95	3.92	3.89	3.86	3.83
-0.000	4.41	4.36	4.31	4.27	4.23	4.19	4.16	4.13	4.10	4.07	4.04	4.02
-0.050	4.48	4.44	4.40	4.36	4.33	4.30	4.27	4.24	4.21	4.19	4.17	4.15
-0.100	4.44	4.41	4.39	4.35	4.32	4.30	4.27	4.25	4.23	4.22	4.20	4.18
-0.150	4.30	4.27	4.25	4.22	4.20	4.19	4.17	4.16	4.15	4.13	4.12	4.11
-0.200	4.08	4.06	4.04	4.02	4.00	3.99	3.98	3.97	3.96	3.95	3.95	3.94
-0.250	3.82	3.80	3.78	3.77	3.75	3.74	3.74	3.73	3.72	3.72	3.72	3.71
-0.300	3.54	3.53	3.51	3.50	3.49	3.48	3.47	3.47	3.46	3.46	3.46	3.45
-0.350	3.27	3.26	3.25	3.23	3.23	3.22	3.21	3.20	3.20	3.20	3.19	3.19
-0.400	3.02	3.00	2.99	2.98	2.98	2.97	2.96	2.96	2.95	2.95	2.95	2.94
-0.450	2.78	2.77	2.76	2.75	2.74	2.74	2.73	2.73	2.72	2.72	2.71	2.71
-0.500	2.56	2.56	2.55	2.54	2.53	2.53	2.52	2.51	2.51	2.51	2.50	2.50
-0.550	2.36	2.36	2.35	2.34	2.34	2.33	2.33	2.32	2.32	2.31	2.31	2.31
-0.600	2.18	2.18	2.17	2.17	2.16	2.16	2.15	2.15	2.14	2.14	2.14	2.13
-0.650	2.01	2.01	2.01	2.00	2.00	1.99	1.99	1.97	1.98	1.95	1.98	1.97
-0.700	1.86	1.86	1.86	1.85	1.85	1.85	1.84	1.84	1.94	1.93	1.83	1.83

Figure A-3.   Continued.

Z	X = 1.45 ANGLE	X = 1.50 ANGLE	X = 1.55 ANGLE	X = 1.60 ANGLE	X = 1.65 ANGLE	X = 1.70 ANGLE	X = 1.75 ANGLE
0.300	2.75	2.74	2.72	2.70	2.69	2.67	2.66
0.250	2.95	2.93	2.91	2.89	2.88	2.86	2.84
0.200	3.16	3.13	3.11	3.09	3.09	3.06	3.04
0.150	3.37	3.35	3.33	3.31	3.29	3.27	3.25
0.100	3.59	3.57	3.55	3.52	3.50	3.48	3.46
0.050	3.81	3.78	3.76	3.74	3.72	3.70	3.68
-0.000	4.00	3.97	3.95	3.93	3.91	3.89	3.87
-0.050	4.15	4.11	4.09	4.07	4.05	4.03	4.02
-0.100	4.17	4.15	4.14	4.13	4.11	4.10	4.09
-0.150	4.10	4.09	4.08	4.08	4.07	4.06	4.05
-0.200	3.94	3.93	3.93	3.93	3.93	3.92	3.92
-0.250	3.71	3.71	3.71	3.71	3.71	3.71	3.71
-0.300	3.45	3.45	3.45	3.46	3.46	3.46	3.46
-0.350	3.19	3.19	3.19	3.19	3.20	3.20	3.20
-0.400	2.94	2.94	2.94	2.94	2.94	2.95	2.95
-0.450	2.71	2.71	2.71	2.71	2.71	2.71	2.71
-0.500	2.50	2.50	2.50	2.50	2.50	2.50	2.50
-0.550	2.31	2.30	2.30	2.30	2.30	2.30	2.30
-0.600	2.13	2.13	2.13	2.12	2.12	2.12	2.12
-0.650	1.97	1.97	1.97	1.97	1.96	1.96	1.96
-0.770	1.83	1.82	1.82	1.82	1.82	1.82	1.82

DOWNWASH INFORMATION FOR THE NEGATIVE X-AXIS AT THE PLANE OF SYMMETRY, Y=0

WHITCOMB AIRFOIL CL=1.2217 B/2=19.85 DATA FOR ATLIT

Z	X=-0.256 ANGLE	X=-0.306 ANGLE	X=-0.356 ANGLE	X=-0.406 ANGLE	X=-0.456 ANGLE	X=-0.506 ANGLE	X=-0.556 ANGLE	X=-0.606 ANGLE	X=-0.656 ANGLE	X=-0.706 ANGLE	X=-0.756 ANGLE
0.295	0.20	-0.62	-1.15	-1.42	-1.51	-1.50	-1.43	-1.34	-1.24	-1.14	-1.05
0.245	-0.31	-1.38	-1.91	-2.07	-2.03	-1.91	-1.74	-1.56	-1.42	-1.28	-1.16
0.195	-1.40	-2.70	-3.04	-2.92	-2.65	-2.34	-2.06	-1.81	-1.60	-1.41	-1.26
0.145	-3.97	-5.00	-4.60	-3.92	-3.29	-2.76	-2.35	-2.01	-1.76	-1.52	-1.36
0.095	-10.41	-8.45	-6.33	-4.84	-3.82	-3.09	-2.56	-2.16	-1.84	-1.53	-1.39
0.045	-20.55	-11.25	-7.38	-5.33	-4.08	-3.24	-2.65	-2.22	-1.59	-1.62	-1.41
-0.005	-15.24	-10.00	-6.93	-5.12	-3.98	-3.18	-2.61	-2.19	-1.88	-1.61	-1.40
-0.055	-6.07	-6.38	-5.15	-4.33	-3.52	-2.91	-2.44	-2.07	-1.78	-1.53	-1.38
-0.105	-2.15	-3.50	-3.63	-3.31	-2.90	-2.51	-2.17	-1.89	-1.65	-1.45	-1.29
-0.155	-0.55	-1.78	-2.29	-2.37	-2.25	-2.06	-1.84	-1.66	-1.48	-1.33	-1.19
-0.205	0.17	-0.80	-1.36	-1.62	-1.68	-1.63	-1.54	-1.42	-1.30	-1.19	-1.08

Figure A-3. Continued.

APPENDIX B – WAKE PROGRAM

User Instructions

The program is written in FORTRAN IV and is designed to run in double precision on an IBM 370-165 computer. Using a finite difference technique this program evaluates the velocity profile downstream of a wing trailing edge given the upper and lower surface profile shapes at the wing trailing edge. All the input information can be obtained from the two-dimensional airfoil program in Reference 4. Using 1601 points in the η or normal direction with an initial stepsize of .00005 in $\xi(x/c)$ and an increment in stepsize of .05, an average execution time of 2 minutes and 42 seconds was required to integrate the boundary layer equations downstream two wing chord lengths. The program requires the specification of the following input data:

Card Number	Variable Name	Variable Description
1	TITLE	The 80 character array which is used as a header to identify output. Termination of execution is achieved by following the last set of profile data to be analyzed by a title card having only the word END in the first three spaces.
2	DETA	Stepsize in the η-direction. A value of .00125 was found satisfactory for most cases, and using this value with a constant stepsize, the total number of η-points, NPTS, can be estimated using the equations given in the text.
2	DX	Stepsize in the X-direction. Best results were obtained for cases analyzed in this report using a very small stepsize, .00005 (specified in chords), and unequal spacing using the variable DXSTEP on card 3.
3	X(1)	The station in chords at which the initial velocity profile solution is assumed. A value of .01 was found satisfactory for most wake solutions.
3	CEDDY	A constant used to evaluate the eddy viscosity model required to solve for the velocity profile. A value of .03 correlated best with experimental data.
3	T	The thickness at the spanwise station of interest in chords.
3	CD	The drag coefficient at the spanwise station of interest.
3	CDMIN	The minimum drag coefficient of the wing section at the spanwise station of interest.

Card Number	Variable Name	Variable Description
3	DXSTEP	Stepsize increment in the X-direction. The stepsize in the X-direction is increased by the factor $DX_{\text{step } n+1} = (DX_{\text{step } n})(1 + DXSTEP)$. A table is given in Figure 30 which will help in determining the X-value at any station using unequal step increments of .05, .075, and .10.
4	NXPRNT	The NXPRT station numbers at which the user desires to have the velocity profile printed. The maximum number of stations which may be printed is 20 unless the solution is printed at every station (NXPRT=0 and all values of NXPRNT are specified as 0). The station number corresponds to a specific value of X downstream; if equal stepsize in the X-direction is used then the NXPRNT values at the desired X-station are easily calculated. However, for unequal stepsize which is the more useful case Figure 30 will help in determining the step number nearest the X-station at which the velocity profile is desired. The NXPRT values of NXPRNT are read using a 20I4 format. If only two stations were of interest then only columns 1-4 and 5-8 would contain integers representing the station numbers. The stations must be specified in the order of increasing station number.
5	DELTAU	The boundary layer thickness in chords at the trailing edge on the upper surface at the station of interest.
5	DELTAL	The boundary layer thickness in chords at the trailing edge on the lower surface at the station of interest.
5	HU	Form factor on the upper surface at the station of interest = boundary layer displacement thickness divided by the momentum thickness at the trailing edge.
5	HL	Form factor on the lower surface at the station of interest = boundary layer displacement thickness divided by the momentum thickness at the trailing edge.

Cards 1 through 5 represent a complete data set for the WAKE Program. Several data sets may be executed for a single program compile by placing subsequent data sets behind the first. The entire program execution is terminated when the END title card is encountered. The format specification for the above data is given in Figure B-1. A sample data set is given in Figure B-2, and the output of this data set is presented in Figure B-3.

112

NPTS | NETAPT | NXSTEP | NXPRT | AK | EPS | DETA | DX
I10 | I10 | I1 | I10 | F10.5 | F10.5 | F10.5 | F10.5

X(1) | CEDDY | T | CD | CDMIN | DXSTEP
F10.5 | F10.5 | F10.5 | F10.5 | F10.5 | F10.5

TITLE
20A4

NXPRNT(I),I=1,NXPRT ——→
I4 | I4 | · · · | etc.

DELTAU | DELTAL | HU | HL
F10.5 | F10.5 | F10.5 | F10.5

Figure B-1. Format specification of input data for the WAKE program.

END
1 2 3 4 5 6 7 8 9 10 11 12 13 14 15 16 17 18 19 20 21 22 23 24 25 26 27 28 29 30 31 32 33 34 35 36 37 38 39 40 41 42 43 44 45 46 47 48 49 50 51 52 53 54 55 56 57 58 59 60 61 62 63 64 65 66 67 68 69 70 71 72 73 74 75 76 77 78 79 80

Last Card

DELTAU   DELTAL   HU   HL
.024287D0   .024287D0 1.4139D0   1.4139D0

NXPRNT(I), I=1 TO 4
113 128 136 157

X(1)   CEDDY   T   CD   CDMIN   DXSTEP
.01D0   .03D0   .118D0   .010378D0 .010378D0 .05D0

NPTS   NETAPT   NXSTEP   NXPRT AK   EPS   DETA   DX
1601   20   156   4   1.D0   .00001D0   .00125D0   .00005D0

TITLE
JOUKOWSKI AIRFOIL/A=0/RN=.21/FREE TRANSITION/M=.05/CEDDY=.03/

First Card

COMPUTING CENTER
AT RALEIGH

HPT 10605

Figure B-2.   Example data set for the WAKE program.

114

Program Listing

```
C***  USING A FINITE DIFFERENCE METHOD THIS PROGRAM CALCULATES THE 2-D   FIN   1
C***  VELOCITY PROFILE IN THE WAKE OF AN AIRFOIL GIVEN THE BOUNDARY      FIN   2
C***  LAYER INFORMATION ON THE UPPER AND LOWER SURFACES OF THE AIRFOIL   FIN   3
C***  AT THE TRAILING EDGE.                                              FIN   4
      IMPLICIT REAL*8(A-H,O-Z)                                           FIN   5
      COMMON A,B,C,R,X(300),F(2001,3),W(2001,3),WOLD(2001),CAPE(2001),SM FIN   6
     1ALE(2001),ETA(2001),WALBC,OEBC,AK,DX11,DX12,DX13,BB,C1,ITER,NXS,N, FIN   7
     1NPTS,NEND                                                          FIN   8
      DIMENSION TITLE(20),NXPRNT(20)                                     FIN   9
      DATA END/4HEND /                                                   FIN  10
      IREAD=1                                                            FIN  11
      IPUNCH=2                                                           FIN  12
      IWRITE=3                                                           FIN  13
C***  READ TITLE CARD                                                    FIN  14
    5 READ (IREAD,10) (TITLE(I),I=1,20)                                  FIN  15
   10 FORMAT (20A4)                                                      FIN  16
      IF (TITLE(1).EQ.END) GO TO 170                                     FIN  17
C***    INPUT BASIC CONSTANTS                                            FIN  18
C***  NPTS=NUMBER OF ETA POINTS DESIRED                                  FIN  19
C***  NETAPT=NUMBER OF STEPS BETWEEN ETA POINTS PRINTED                  FIN  20
C***  NXSTEP=NUMBER OF STEPS IN X DIRECTION                              FIN  21
C***  NXPRT=NUMBER OF STATIONS AT WHICH SOLUTION IS TO BE PRINTED        FIN  22
C***       (NXPRT=0 PRINTS EVERY SOLUTION AT EVERY STATION)              FIN  23
C***       (THERE IS A MAXIMUM OF 20 STATIONS)                           FIN  24
C***       (THE FIRST STATION IS ALWAYS PRINTED)                         FIN  25
C***       (THE STATIONS MUST BE SPECIFIED IN ORDER OF INCREASING        FIN  26
C***        STATION NUMBER)                                              FIN  27
C***  T=THICKNESS TO CHORD RATIO OF WING                                 FIN  28
C***  B12=WAKE WIDTH FACTOR                                              FIN  29
C***  UMUDEL=VELOCITY DEFICIT FACTOR                                     FIN  30
C***  CK=CONSTANT USED IN EDDY VISCOSITY MODEL                           FIN  31
C***  AK=PROPORTIONALITY CONSTANT FOR UNEVEN STEP SIZE IN ETA DIRECTION  FIN  32
C***  EPS=ACCURACY FOR SOLUTION CONVERGENCE                              FIN  33
C***  DETA=INITIAL STEPSIZE IN ETA DIRECTION                             FIN  34
C***  DX=STEPSIZE IN X DIRECTION (INPUT AS RATIO TO CHORD LENGTH)        FIN  35
      READ (IREAD,15) NPTS,NETAPT,NXSTEP,NXPRT,AK,EPS,DETA,DX            FIN  36
   15 FORMAT (4I10,4F10.5)                                               FIN  37
      READ (IREAD,20) X(1),CEDDY,T,CD,CDMIN,DXSTEP                       FIN  38
   20 FORMAT (8F10.5)                                                    FIN  39
      NXPRT1=NXPRT                                                       FIN  40
      IF (NXPRT.EQ.0)NXPRT1=1                                            FIN  41
      READ (IREAD,25) (NXPRNT(I),I=1,NXPRT1)                             FIN  42
   25 FORMAT (20I4)                                                      FIN  43
      READ (IREAD,20) DELTAU,DELTAL,HU,HL                               FIN  44
      NEND=NPTS-1                                                        FIN  45
      INXPRT=1                                                           FIN  46
C***  SET OUTER EDGE BOUNDARY CONDITION AT 1.0                           FIN  47
      OEBC=1.0D0                                                         FIN  48
      PU=2.0D0/(HU-1.0D0)                                                FIN  49
      PL=2.0D0/(HL-1.0D0)                                                FIN  50
      B12=.5D0*(.75D0**PU*DELTAU+.75D0**PL*DELTAL)                       FIN  51
      UMUDEL=(CD-CDMIN)/CD                                               FIN  52
      C1=T*CD*100.0D0/(B12*CEDDY*(1.D0-UMUDEL))                          FIN  53
      NXS=1                                                              FIN  54
      NMID=(NPTS-1)/2+1                                                  FIN  55
      WRITE (IWRITE,30) (TITLE(I),I=1,20),NPTS,NMID,NETAPT,NXSTEP,NXPRT, FIN  56
     1(NXPRNT(I),I=1,NXPRT1)                                             FIN  57
   30 FORMAT (1H1,//5X,20A4,//5X,9HNPTS   = ,I4,/5X,9HNMID   = ,I4,/5X,9 FIN  58
     1HNETAPT = ,I4,/5X,9HNXPRT  = ,I4,/5X,9HNXPRNT = FIN  59
     1 ,20I4//)                                                          FIN  60

      WRITE (IWRITE,35) AK,EPS,DETA,DX,X(1),CEDDY,B12,T,UMUDEL,CD,DXSTEP FIN  61
     1,C1                                                                FIN  62
   35 FORMAT (5X,9HAK    = ,D15.8,/5X,9HEPS    = ,D15.8,/5X,9HDETA   = FIN  63
     1,D15.8,/5X,9HDX    = ,D15.8,/5X,9HX(1)   = ,D15.8,/5X,9HCEDDY  = FIN  64
     1,D15.8,/5X,9HB12   = ,D15.8,/5X,9HT      = ,D15.8,/5X,9HUMUDEL = FIN  65
     1,D15.8,/5X,9HCD    = ,D15.8,/5X,9HDXSTEP = ,D15.8,/5X,9HC1     = FIN  66
     1,D15.8//)                                                          FIN  67
      WRITE (IWRITE,40) DELTAU,DELTAL,HU,HL                              FIN  68
   40 FORMAT (5X,9HDELTAU = ,D15.8,/5X,9HDELTAL = ,D15.8,/5X,9HHU     = FIN  69
     1,D15.8,/5X,9HHL    = ,D15.8//)                                     FIN  70
C***     CALCULATE ETA(I)                                                FIN  71
      ETA(NMID)=0.D0                                                     FIN  72
      ETA(NMID-1)=-DETA                                                  FIN  73
      ETA(NMID+1)=DETA                                                   FIN  74
      J=NMID-1                                                           FIN  75
      JJ=NMID+2                                                          FIN  76
      DO 45 I=JJ,NPTS                                                    FIN  77
      J=J-1                                                              FIN  78
      ETA(I)=ETA(I-1)+AK*(ETA(I-1)-ETA(I-2))                             FIN  79
   45 ETA(J)=-ETA(I)                                                     FIN  80
      DO 50 I=1,NPTS                                                     FIN  81
      F(I,2)=0.0D0                                                       FIN  82
      F(I,3)=0.0D0                                                       FIN  83
      W(I,2)=0.0D0                                                       FIN  84
   50 W(I,3)=0.0D0                                                       FIN  85
      DO 55 I=2,300                                                      FIN  86
      IF (I.EQ.2) GO TO 55                                               FIN  87
      DX=DX*(1.D0*DXSTEP)                                                FIN  88
   55 X(I)=X(I-1)+DX                                                     FIN  89
C***    INITIAL PROFILE GUESS                                            FIN  90
      CU=(HU-1.D0)/2.D0                                                  FIN  91
      CL=(HL-1.D0)/2.D0                                                  FIN  92
      DELTAU=DELTAU/DSQRT(T*X(NXS)*100.D0*CD)                            FIN  93
      DELTAL=DELTAL/DSQRT(T*X(NXS)*100.D0*CD)                            FIN  94
      CALL PROFIL(DELTAU,DELTAL,CU,CL,DETA,NMID)                         FIN  95
      DO 60 I=1,NPTS                                                     FIN  96
   60 WOLD(I)=W(I,1)                                                     FIN  97
   65 IF (NXS-2) 75,75,70                                                FIN  98
   70 DX11=((1.0D0/(X(NXS)-X(NXS-1))+(1.0D0/(X(NXS)-X(NXS-2))))          FIN  99
      DX12=(X(NXS)-X(NXS-2))/((X(NXS)-X(NXS-1))*(X(NXS-1)-X(NXS-2)))     FIN 100
      DX13=(X(NXS)-X(NXS-1))/((X(NXS)-X(NXS-2))*(X(NXS-1)-X(NXS-2)))     FIN 101
   75 CONTINUE                                                           FIN 102
      F(NMID,1)=0.D0                                                     FIN 103
C***    START SOLUTION AT FIRST STATION                                  FIN 104
      ITER=1                                                             FIN 105
   80 N=1                                                                FIN 106
      CALL GETF(NMID)                                                    FIN 107
      IF (NXS.EQ.1) GO TO 110                                            FIN 108
   85 N=N+1                                                              FIN 109
C***    CALCULATE MATRIX COEFFICIENTS                                    FIN 110
      CALL ABCR                                                          FIN 111
      CALL COEFF                                                         FIN 112
      IF (N-NEND) 85,90,90                                               FIN 113
C***    CALCULATE NEW W ARRAY PROFILES                                   FIN 114
   90 CALL SOLVE                                                         FIN 115
C***    TEST FOR CONVERGENCE OF SCCESSIVE PROFILES                       FIN 116
      DO 95 I=2,NEND                                                     FIN 117
      IF (DABS(1.0D0-(WOLD(I)/W(I,1)))-EPS) 95,95,100                    FIN 118
   95 CONTINUE                                                           FIN 119
C***    CONVERGENCE ATTAINED                                             FIN 120
```

```
        GO TO 110                                                      FIN 121
C***    CONVERGENCE NOT ATTAINED-ITERATION SOLUTION                    FIN 122
  100 CONTINUE                                                         FIN 123
        IF (ITER.GT.99) GO TO 160                                      FIN 124
        ITER=ITER+1                                                    FIN 125
        DO 105 I=1,NPTS                                                FIN 126
        WOLD(I)=W(I,1)                                                 FIN 127
  105 CONTINUE                                                         FIN 128
        GO TO 80                                                       FIN 129
C***    PRINT CONVERGED SOLUTION                                       FIN 130
  110 IF (NXPRT.EQ.0) GO TO 115                                        FIN 131
        IF (NXS.EQ.1) GO TO 115                                        FIN 132
        IF (NXS.EQ.NXPRNT(INXPRT)) GO TO 115                           FIN 133
        GO TO 150                                                      FIN 134
  115 WRITE (IWRITE,135) ITER                                          FIN 135
        WRITE (IWRITE,120) NXS,X(NXS)                                  FIN 136
  120 FORMAT (/10X,23HRESULTS FOR X/C STATION,I4,5X,4HX = ,D15.8)      FIN 137
        WRITE (IWRITE,125) (TITLE(I),I=1,20)                           FIN 138
  125 FORMAT (/,1X,20A4,/)                                             FIN 139
        WRITE (IWRITE,140)                                             FIN 140
        CYETA=DSQRT(T*X(NXS)*100.D0*CO)                                FIN 141
        L=NPTS+NETAPT                                                  FIN 142
        DO 130 I=1,NPTS,NETAPT                                         FIN 143
        L=L-NETAPT                                                     FIN 144
        YETA=ETA(L)*CYETA                                              FIN 145
        WSQ=W(L,1)*W(L,1)                                              FIN 146
        WRITE (IWRITE,145) ETA(L),W(L,1),F(L,1),YETA,WSQ               FIN 147
  130 CONTINUE                                                         FIN 148
        IF (NXS.NE.1) INXPRT=INXPRT+1                                  FIN 149
        IF (NXPRT.NE.0.AND.INXPRT.GT.NXPRT) GO TO 5                    FIN 150
  135 FORMAT (1H1,/,10X,26HCONVERGENCE ATTAINED AFTER,I4,11H ITERATIONS)  FIN 151
     1                                                                 FIN 152
  140 FORMAT (/6X,3HETA,12X,6HMU/UDEL,13X,1HF,14X,3HY/C,9X,11H(U/UDEL)**2  FIN 153
     1)                                                                FIN 154
  145 FORMAT (5D16.8)                                                  FIN 155
C***    SET UP FOR NEXT X STATION                                      FIN 156
  150 DO 155 I=1,NPTS                                                  FIN 157
        W(I,3)=W(I,2)                                                  FIN 158
        F(I,3)=F(I,2)                                                  FIN 159
        W(I,2)=W(I,1)                                                  FIN 160
        F(I,2)=F(I,1)                                                  FIN 161
        WOLD(I)=W(I,1)                                                 FIN 162
  155 CONTINUE                                                         FIN 163
        NXS=NXS+1                                                      FIN 164
        IF (NXS-2.GE.NXSTEP) GO TO 5                                   FIN 165
        GO TO 65                                                       FIN 166
  160 WRITE (IWRITE,165) NXS                                           FIN 167
  165 FORMAT (/,5X,30HITER EXCEEDS 75 AT STEP NXS = ,I4)               FIN 168
        GO TO 5                                                        FIN 169
  170 CALL EXIT                                                        FIN 170
        END                                                            FIN 171


        SUBROUTINE GETF(NNID)                                          GET  1
C***    THIS SUBROUTINE INTEGRATES THE DERIVATIVE OF F TO OBTAIN F     GET  2
        IMPLICIT REAL*8(A-H,O-Z)                                       GET  3
        COMMON A,B,C,R,X(300),F(2001,3),W(2001,3),WOLD(2001),CAPE(2001),SM  GET  4
     1ALE(2001),ETA(2001),WALBC,OEBC,AK,DX11,DX12,DX13,BB,C1,ITER,NXS,N,  GET  5
     1NPTS,NEND                                                        GET  6
        FINL=0.D0                                                      GET  7
        FINU=0.D0                                                      GET  8
        JJ=NMID+1                                                      GET  9
        J=NMID                                                         GET 10
        JJJ=J-2                                                        GET 11
        NPTSM1=NPTS-1                                                  GET 12
        DO 5 I=JJ,NPTSM1                                               GET 13
        FINU=FINU+(WOLD(I)+WOLD(I-1))*(ETA(I)-ETA(I-1))/2.D0           GET 14
    5 F(I,1)=FINU                                                      GET 15
        DO 10 I=1,JJJ                                                  GET 16
        J=J-1                                                          GET 17
        FINL=FINL+(WOLD(J)+WOLD(J+1))*(ETA(J)-ETA(J+1))/2.D0           GET 18
   10 F(J,1)=FINL                                                      GET 19
        F(NPTS,1)=F(NEND,1)+(W(NPTS,1)+W(NEND,1))*(ETA(NPTS)-ETA(NPTS-1))/  GET 20
     12.D0                                                             GET 21
        F(1,1)=F(2,1)+(W(1,1)+W(2,1))*(ETA(1)-ETA(2))/2.D0             GET 22
        RETURN                                                         GET 23
        END                                                            GET 24


        SUBROUTINE ABCR                                                ABC  1
C***    THIS SUBROUTINE COMPUTES A,B,C, AND R MATRIX COEFFICIENTS      ABC  2
        IMPLICIT REAL*8(A-H,O-Z)                                       ABC  3
        COMMON A,B,C,R,X(300),F(2001,3),W(2001,3),WOLD(2001),CAPE(2001),SM  ABC  4
     1ALE(2001),ETA(2001),WALBC,OEBC,AK,DX11,DX12,DX13,BB,C1,ITER,NXS,N,  ABC  5
     1NPTS,NEND                                                        ABC  6
        DIMENSION ALPHA(2)                                             ABC  7
        D1=(ETA(N+1)-ETA(N))+AK*AK*(ETA(N)-ETA(N-1))                   ABC  8
        D2=(ETA(N+1)-ETA(N))**2+AK*AK*(ETA(N)-ETA(N-1))**2             ABC  9
C***    COMPUTE ALPHAS FOR MOMENTUM EQUATION                           ABC 10
        IF (NXS-2) 5,10,15                                             ABC 11
    5 ALPHA(1)=C1*F(N,1)/2.D0                                          ABC 12
        ALPHA(2)=0.D0                                                  ABC 13
        A=(2.D0/D2+ALPHA(1)/D1)                                        ABC 14
        B=-2.D0*(1.D0+AK)/D2-(1.D0-AK*AK)*ALPHA(1)/D1                  ABC 15
        C=2.D0*AK/D2-ALPHA(1)*AK*AK/D1                                 ABC 16
        R=0.D0                                                         ABC 17
        GO TO 20                                                       ABC 18
   10 ALPHA(1)=(F(N,1)/2.D0+X(NXS)*(F(N,1)-F(N,2))/(X(NXS)-X(NXS-1)))*C1  ABC 19
        ALPHA(2)=-X(NXS)*WOLD(N)*C1                                    ABC 20
        A=(2.D0/D2+ALPHA(1)/D1)                                        ABC 21
        B=-2.D0*(1.D0+AK)/D2-(1.D0-AK*AK)*ALPHA(1)/D1+ALPHA(2)/(X(NXS)-  ABC 22
     1X(NXS-1))                                                        ABC 23
        C=2.D0*AK/D2-ALPHA(1)*AK*AK/D1                                 ABC 24
        R=ALPHA(2)*W(N,2)/(X(NXS)-X(NXS-1))                            ABC 25
        GO TO 20                                                       ABC 26
   15 ALPHA(1)=(F(N,1)/2.D0+X(NXS)*(DX11*F(N,1)-DX12*F(N,2)+DX13*F(N,3))  ABC 27
     1)*C1                                                             ABC 28
        ALPHA(2)=-X(NXS)*WOLD(N)*C1                                    ABC 29
        A=(2.D0/D2+ALPHA(1)/D1)                                        ABC 30
        B=(-2.D0*(1.D0+AK)/D2-(1.D0-AK*AK)*ALPHA(1)/D1+ALPHA(2)*DX11)  ABC 31
        C=2.D0*AK/D2-ALPHA(1)*AK*AK/D1                                 ABC 32
        R=ALPHA(2)*DX12*W(N,2)-ALPHA(2)*DX13*W(N,3)                    ABC 33
   20 RETURN                                                           ABC 34
        END                                                            ABC 35


        SUBROUTINE COEFF                                               COF  1
```

```
C***   COEFF COMPUTES RECURSION COEFFICIENTS FOR TRIDIAGIONAL        COF   2
C***   MATRIX SYSTEMS                                                COF   3
       IMPLICIT REAL*8(A-H,O-Z)                                      COF   4
       COMMON A,B,C,R,X(300),F(2001,3),W(2001,3),WOLD(2001),CAPE(2001),SM COF  5
      1ALE(2001),ETA(2001),WALBC,OEBC,AK,DX11,DX12,DX13,BB,C1,ITER,NXS,N, COF 6
      1NPTS,NEND                                                     COF   7
       IF (N-2)  5,5,10                                              COF   8
     5 CAPE(N)=-A/B                                                  COF   9
       SMALE(N)=(R-C*OEBC)/B                                         COF  10
       GO TO 15                                                      COF  11
    10 CAPE(N)=-A/(B+C*CAPE(N-1))                                    COF  12
       SMALE(N)=(R-C*SMALE(N-1))/(B+C*CAPE(N-1))                     COF  13
    15 RETURN                                                        COF  14
       END                                                          COF  15


       SUBROUTINE SOLVE                                              SOL   1
C***   THIS SUBROUTINE SOLVES A TRIDIAGIONAL MATRIX SYSTEM BY        SOL   2
C***   BACK-SUBSTITUTION                                             SOL   3
       IMPLICIT REAL*8(A-H,O-Z)                                      SOL   4
       COMMON A,B,C,R,X(300),F(2001,3),W(2001,3),WOLD(2001),CAPE(2001),SM SOL  5
      1ALE(2001),ETA(2001),WALBC,OEBC,AK,DX11,DX12,DX13,BB,C1,ITER,NXS,N, SOL 6
      1NPTS,NEND                                                     SOL   7
       N=N+1                                                         SOL   8
       W(N,1)=OEBC                                                   SOL   9
     5 N=N-1                                                         SOL  10
       W(N,1)=CAPE(N)*W(N+1,1)+SMALE(N)                              SOL  11
       IF (N-2)  10,10,5                                             SOL  12
    10 W(1,1)=OEBC                                                   SOL  13
       RETURN                                                        SOL  14
       END                                                          SOL  15


       SUBROUTINE PROFIL(DELTAU,DELTAL,CU,CL,DETA,NMID)              PRO   1
C***   THIS SUBROUTINE EVALUATES THE INITIAL VELOCITY PROFILE FOR THE PRO  2
C***   FINITE DIFFERENCE SOLUTION GIVEN THE BOUNDARY LAYER THICKNESS AND PRO 3
C***   FORM FACTOR FOR BOTH UPPER AND LOWER SURFACES                 PRO   4
       IMPLICIT REAL*8(A-H,O-Z)                                      PRO   5
       COMMON A,B,C,R,X(300),F(2001,3),W(2001,3),WOLD(2001),CAPE(2001),SM PRO  6
      1ALE(2001),ETA(2001),WALBC,OEBC,AK,DX11,DX12,DX13,BB,C1,ITER,NXS,N, PRO 7
      1NPTS,NEND                                                     PRO   8
       NSTART=NMID                                                   PRO   9
       DELETA=-DETA                                                  PRO  10
       DO 10 I=NSTART,NPTS                                           PRO  11
       DELETA=DELETA+DETA                                            PRO  12
       IF (DELETA.GT.DELTAU) GO TO 5                                 PRO  13
       W(I,1)=(DELETA/DELTAU)**CU                                    PRO  14
       GO TO 10                                                      PRO  15
     5 W(I,1)=1.DO                                                   PRO  16
    10 CONTINUE                                                      PRO  17
       DELETA=0.D0                                                   PRO  18
       NNEND=NSTART-1                                                PRO  19
       NCNT=NSTART                                                   PRO  20
       DO 20 I=1,NNEND                                               PRO  21
       NCNT=NCNT-1                                                   PRO  22
       DELETA=DELETA+DETA                                            PRO  23
       IF (DELETA.GT.DELTAL) GO TO 15                                PRO  24
       W(NCNT,1)=(DELETA/DELTAL)**CL                                 PRO  25

       GO TO 20                                                      PRO  26
    15 W(NCNT,1)=1.DO                                                PRO  27
    20 CONTINUE                                                      PRO  28
       RETURN                                                        PRO  29
       END                                                          PRO  30
```

Sample Output

JOUKOWSKI AIRFOIL/A=0/RN=.21/FREE TRANSITION/W=.05/CEODY=.03/

NPTS	= 1601	R12	=	0.60486614D-02
NMID	= 801	T	=	0.118000000D 00
NETAPT	= 20	UMUDEL	=	0.0
NXSTEP	= 156	CO	=	0.103780000D-01
NXPRT	= 4	OXSTEP	=	0.5C000000D-01
NXPRNT	= 113 128 136 157	C1	=	0.67486227D 03
AK	= 0.100000000D 01			
EPS	= 0.100000000D-04			
DETA	= 0.125000000D-02	DELTAU	=	0.24267000D-01
DX	= 0.500000000D-04	DELTAL	=	0.24267000D-01
X(1)	= 0.100000000D-01	HU	=	0.141390000D 01
CEODY	= 0.300000000D-01	HL	=	0.141390000D 01

CONVERGENCE ATTAINED AFTER   1 ITERATIONS

RESULTS FOR X/C STATION   1   X = 0.100000000D-01

JOUKOWSKI AIRFOIL/A=0/RN=.21/FREE TRANSITION/W=.05/CEODY=.03/

ETA	U/UDEL	F	Y/C	(U/UDEL)**2
0.100000000D 01	0.100000000D 01	0.88088180D 00	0.34994342D-01	0.100000000D 01
0.975000000D 00	0.100000000D 01	0.85588180D 00	0.34119484D-01	0.100000000D 01
0.950000000D 00	0.100000000D 01	0.83088180D 00	0.33244625D-01	0.100000000D 01
0.925000000D 00	0.100000000D 01	0.80588180D 00	0.32369767D-01	0.100000000D 01
0.900000000D 00	0.100000000D 01	0.78088180D 00	0.31494908D-01	0.100000000D 01
0.875000000D 00	0.100000000D 01	0.75588180D 00	0.30620050D-01	0.100000000D 01
0.853000000D 00	0.100000000D 01	0.73088180D 00	0.29745191D-01	0.100000000D 01
0.825000000D 00	0.100000000D 01	0.70588180D 00	0.28870332D-01	0.100000000D 01
0.800000000D 00	0.100000000D 01	0.68088180D 00	0.27995474D-01	0.100000000D 01
0.775000000D 00	0.100000000D 01	0.65588180D 00	0.27120615D-01	0.100000000D 01
0.750000000D 00	0.100000000D 01	0.63088180D 00	0.26245757D-01	0.100000000D 01
0.725000000D 00	0.100000000D 01	0.60588180D 00	0.25370898D-01	0.100000000D 01
0.700000000D 00	0.100000000D 01	0.58088190D 00	0.24496040D-01	0.100000000D 01
0.675000000D 00	0.994263840D 00	0.55593621D 00	0.23621181D-01	0.988560580D 00
0.650000000D 00	0.986528530D 00	0.53117563D 00	0.22746323D-01	0.973235540D 00
0.625000000D 00	0.978553550D 00	0.50661178D 00	0.21871464D-01	0.957567060D 00
0.600000000D 00	0.970321450D 00	0.48225029D 00	0.20996605D-01	0.941523710D 00
0.575000000D 00	0.961812660D 00	0.45809802D 00	0.20121747D-01	0.925083600D 00
0.550000000D 00	0.953005240D 00	0.43416215D 00	0.19246886D-01	0.908218980D 00
0.525000000D 00	0.943874390D 00	0.41045046D 00	0.18372030D-01	0.890898840D 00
0.500000000D 00	0.934391910D 00	0.38697136D 00	0.17497171D-01	0.873084250D 00
0.475000000D 00	0.924525670D 00	0.36373406D 00	0.16622313D-01	0.854747710D 00
0.450000000D 00	0.914238610D 00	0.34074859D 00	0.15747454D-01	0.835832240D 00
0.425000000D 00	0.903487850D 00	0.31802600D 00	0.14672596D-01	0.816290300D 00
0.400000000D 00	0.892223270D 00	0.29557840D 00	0.13997737D-01	0.796062360D 00
0.375000000D 00	0.880385740D 00	0.27341961D 00	0.13122878D-01	0.775079050D 00
0.350000000D 00	0.867904840D 00	0.25156456D 00	0.12248020D-01	0.753258810D 00
0.325000000D 00	0.854695640D 00	0.23003044D 00	0.11373161D-01	0.730504650D 00
0.300000000D 00	0.840654370D 00	0.20883671D 00	0.10498303D-01	0.706699750D 00
0.275000000D 00	0.825652180D 00	0.18800573D 00	0.96234442D-02	0.681701520D 00
0.250000000D 00	0.809526210D 00	0.16756347D 00	0.87485560D-02	0.655332680D 00
0.225000000D 00	0.792066060D 00	0.14754053D 00	0.78737270D-02	0.627368640D 00
0.200000000D 00	0.772992690D 00	0.12797360D 00	0.69986685D-02	0.597517700D 00
0.175000000D 00	0.751924010D 00	0.10890750D 00	0.61240099D-02	0.565389720D 00
0.150000000D 00	0.728315100D 00	0.90398519D-01	0.52491514D-02	0.530442890D 00
0.125000000D 00	0.701346700D 00	0.72519648D-01	0.43742928D-02	0.491887190D 00
0.100000000D 00	0.669069527D 00	0.55369994D-01	0.34994142D-02	0.448491750D 00
0.750000000D-01	0.628948090D 00	0.39093127D-01	0.26245757D-02	0.395814596D 00
0.5000000CD-01	0.580201800D 00	0.23919414D-01	0.17497171D-02	0.336634110D 00
0.250000000D-01	0.502667620D 00	0.10295716D-01	0.87485560D-03	0.252674740D 00
0.0	0.0	0.0	0.0	0.0
-0.250000000D-01	0.502667620D 00	-0.10295716D-01	-0.87485560D-03	0.252674740D 00
-0.500000000D-01	0.580201800D 00	-0.23919414D-01	-0.17497171D-02	0.336634110D 00
-0.750000000D-01	0.630988080D 00	-0.39093127D-01	-0.26245757D-02	0.398145960D 00
-0.100000000D 00	0.669069527D 00	-0.55369994D-01	-0.34994342D-02	0.448491750D 00
-0.125000000D 00	0.701346700D 00	-0.72519648D-01	-0.43742928D-02	0.491887190D 00
-0.150000000D 00	0.728315100D 00	-0.90398519D-01	-0.52491514D-02	0.530442890D 00
-0.175000000D 00	0.751924010D 00	-0.10890750D 00	-0.61240099D-02	0.565389770D 00
-0.200000000D 00	0.772992690D 00	-0.12797360D 00	-0.69986685D-02	0.597517700D 00
-0.225000000D 00	0.792066060D 00	-0.14754053D 00	-0.78737270D-02	0.627368640D 00
-0.250000000D 00	0.809526210D 00	-0.16756347D 00	-0.87485560D-02	0.655332680D 00
-0.275000000D 00	0.825652180D 00	-0.18800573D 00	-0.96234442D-02	0.681701520D 00
-0.300000000D 00	0.840654370D 00	-0.20883671D 00	-0.10498303D-01	0.706699760D 00
-0.325000000D 00	0.854695640D 00	-0.23003044D 00	-0.11373161D-01	0.730504650D 00
-0.350000000D 00	0.867904840D 00	-0.25156456D 00	-0.12248020D-01	0.753258810D 00
-0.375000000D 00	0.880385740D 00	-0.27341961D 00	-0.13122878D-01	0.775079050D 00
-0.400000000D 00	0.892223270D 00	-0.29557848D 00	-0.13997737D-01	0.796062360D 00
-0.425000000D 00	0.903487850D 00	-0.31802600D 00	-0.14672596D-01	0.816290300D 00
-0.450000000D 00	0.914238610D 00	-0.34074859D 00	-0.15747454D-01	0.835832240D 00
-0.475000000D 00	0.924525670D 00	-0.36373406D 00	-0.16622313D-01	0.854747710D 00
-0.500000000D 00	0.934391910D 00	-0.38697136D 00	-0.17497171D-01	0.873084250D 00
-0.525000000D 00	0.943874350D 00	-0.41045046D 00	-0.18372030D-01	0.890898840D 00
-0.550000000D 00	0.953005240D 00	-0.43416215D 00	-0.19246886D-01	0.908218980D 00
-0.575000000D 00	0.961812660D 00	-0.45809802D 00	-0.20121747D-01	0.925083600D 00
-0.600000000D 00	0.970321450D 00	-0.48225029D 00	-0.20996605D-01	0.941523710D 00
-0.625000000D 00	0.978553550D 00	-0.50661178D 00	-0.21871464D-01	0.957567060D 00
-0.650000000D 00	0.986523530D 00	-0.53117563D 00	-0.22746323D-01	0.973235540D 00
-0.675000000D 00	0.994263840D 00	-0.55593621D 00	-0.23621181D-01	0.988560580D 00
-0.700000000D 00	0.100000000D 01	-0.58088180D 00	-0.24496040D-01	0.100000000D 01
-0.725000000D 00	0.100000000D 01	-0.60588180D 00	-0.25370898D-01	0.100000000D 01
-0.750000000D 00	0.100000000D 01	-0.63088180D 00	-0.26245757D-01	0.100000000D 01
-0.775000000D 00	0.100000000D 01	-0.65588180D 00	-0.27120615D-01	0.100000000D 01
-0.800000000D 00	0.100000000D 01	-0.68088180D 00	-0.27995474D-01	0.100000000D 01
-0.825000000D 00	0.100000000D 01	-0.70588180D 00	-0.28870332D-01	0.100000000D 01
-0.850000000D 00	0.100000000D 01	-0.73088180D 00	-0.29745191D-01	0.100000000D 01
-0.875000000D 00	0.100000000D 01	-0.75588180D 00	-0.30620500D-01	0.100000000D 01
-0.900000000D 00	0.100000000D 01	-0.78088180D 00	-0.31494908D-01	0.100000000D 01
-0.925000000D 00	0.100000000D 01	-0.80588180D 00	-0.32369767D-01	0.100000000D 01
-0.950000000D 00	0.100000000D 01	-0.83088180D 00	-0.33244625D-01	0.100000000D 01
-0.975000000D 00	0.100000000D 01	-0.85588180D 00	-0.34119484D-01	0.100000000D 01
-0.100000000D 01	0.100000000D 01	-0.88088180D 00	-0.34994342D-01	0.100000000D 01

Figure B-3.   Sample output of the WAKE program.

CONVERGENCE ATTAINED AFTER   4 ITERATIONS

RESULTS FOR X/C STATION 113   X = 0.24515737D 00

JOUKOWSKI AIRFOIL/A=0/RN=.21/FREE TRANSITION/M=.05/CEDDY=.03/

ETA	U/UDEL	F	Y/C	(U/UDEL)**2
0.100000000 01	0.100000000 01	0.980004600 00	0.173268780 00	0.100000000 01
0.975000000 00	0.100000000 01	0.955004600 00	0.168937060 00	0.100000000 01
0.950000000 00	0.100000000 01	0.930004600 00	0.164605340 00	0.100000000 01
0.925000000 00	0.100000000 01	0.905004600 00	0.160273620 00	0.100000000 01
0.900000000 00	0.100000000 01	0.880004600 00	0.155941900 00	0.100000000 01
0.875000000 00	0.100000000 01	0.855004600 00	0.151610180 00	0.100000000 01
0.850000000 00	0.100000000 01	0.830004600 00	0.147278460 00	0.100000000 01
0.825000000 00	0.100000000 01	0.805004600 00	0.142946740 00	0.100000000 01
0.800000000 00	0.100000000 01	0.780004600 00	0.138615020 00	0.100000000 01
0.775000000 00	0.100000000 01	0.755004600 00	0.134283300 00	0.100000000 01
0.750000000 00	0.100000000 01	0.730004600 00	0.129951580 00	0.100000000 01
0.725000000 00	0.100000000 01	0.705004600 00	0.125619860 00	0.100000000 01
0.700000000 00	0.100000000 01	0.680004600 00	0.121288140 00	0.100000000 01
0.675000000 00	0.100000000 01	0.655004600 00	0.116956420 00	0.100000000 01
0.650000000 00	0.100000000 01	0.630004600 00	0.112624710 00	0.100000000 01
0.625000000 00	0.100000000 01	0.605004600 00	0.108292990 00	0.100000000 01
0.600000000 00	0.100000000 01	0.580004600 00	0.103961270 00	0.100000000 01
0.575000000 00	0.100000000 01	0.555004600 00	0.996295470-01	0.100000000 01
0.550000000 00	0.100000000 01	0.530004600 00	0.952978270-01	0.100000000 01
0.525000000 00	0.100000000 01	0.505004600 00	0.909661080-01	0.100000000 01
0.500000000 00	0.100000000 01	0.480004600 00	0.866343880-01	0.100000000 01
0.475000000 00	0.100000000 01	0.455004600 00	0.823026690-01	0.100000000 01
0.450000000 00	0.100000000 01	0.430004600 00	0.779709500-01	0.100000000 01
0.425000000 00	0.100000000 01	0.405004600 00	0.736392300-01	0.100000000 01
0.400000000 00	0.100000000 01	0.380004600 00	0.693075110-01	0.999999990 00
0.375000000 00	0.999999960 00	0.355004600 00	0.649757910-01	0.999999930 00
0.350000000 00	0.999999630 00	0.330004610 00	0.606440720-01	0.999999250 00
0.325000000 00	0.999996970 00	0.305004640 00	0.563123530-01	0.999993950 00
0.300000000 00	0.999980160 00	0.280004870 00	0.519806330-01	0.999960320 00
0.275000000 00	0.999894480 00	0.255006170 00	0.476489140-01	0.999788980 00
0.250000000 00	0.999541050 00	0.230012280 00	0.433171940-01	0.999082320 00
0.225000000 00	0.998352190 00	0.205035900 00	0.389854750-01	0.996707100 00
0.200000000 00	0.995059550 00	0.180111980 00	0.346537550-01	0.990143510 00
0.175000000 00	0.987462000 00	0.155318680 00	0.303220360-01	0.975082190 00
0.150000000 00	0.972668450 00	0.130799060 00	0.259903170-01	0.946083910 00
0.125000000 00	0.948072950 00	0.106767720 00	0.216585970-01	0.898842320 00
0.100000000 00	0.912991800 00	0.834841380-01	0.173268780-01	0.833554030 00
0.750000000-01	0.870425920 00	0.611820620-01	0.129951580-01	0.757641290 00
0.500000000-01	0.827883860 00	0.399636620-01	0.866343880-02	0.685391690 00
0.250000000-01	0.795895170 00	0.196995790-01	0.433171940-02	0.633449130 00
0.0	0.783951300 00	0.0	0.0	0.614579630 00
-0.250000000-01	0.795895170 00	-0.196995790-01	-0.433171940-02	0.633449130 00
-0.500000000-01	0.827883860 00	-0.399636620-01	-0.866343880-02	0.685391690 00
-0.750000000-01	0.870425920 00	-0.611820620-01	-0.129951580-01	0.757641290 00
-0.100000000 00	0.912991800 00	-0.834841380-01	-0.173268780-01	0.833554030 00
-0.125000000 00	0.948072950 00	-0.106767720-01	-0.216585970-01	0.898842320 00
-0.150000000 00	0.972668450 00	-0.130799060 00	-0.259903170-01	0.946083910 00
-0.175000000 00	0.987462500 00	-0.155318680 00	-0.303220360-01	0.975082190 00
-0.200000000 00	0.995059550 00	-0.180111980 00	-0.346537550-01	0.990143510 00
-0.225000000 00	0.998352190 00	-0.205035900 00	-0.389854750-01	0.996707100 00
-0.250000000 00	0.999541050 00	-0.230012280 00	-0.433171940-01	0.999082320 00
-0.275000000 00	0.999894480 00	-0.255006170 00	-0.476489140-01	0.999788980 00
-0.300000000 00	0.999980160 00	-0.280004870 00	-0.519806330-01	0.999960320 00
-0.325000000 00	0.999996970 00	-0.305004640 00	-0.563123530-01	0.999993950 00
-0.350000000 00	0.999999630 00	-0.330004610 00	-0.606440720-01	0.999999250 00
-0.375000000 00	0.999999960 00	-0.355004600 00	-0.649757910-01	0.999999930 00
-0.400000000 00	0.100000000 01	-0.380004600 00	-0.693075110-01	0.999999990 00
-0.425000000 00	0.100000000 01	-0.405004600 00	-0.736392300-01	0.100000000 01
-0.450000000 00	0.100000000 01	-0.430004600 00	-0.779709500-01	0.100000000 01
-0.475000000 00	0.100000000 01	-0.455004600 00	-0.823026690-01	0.100000000 01
-0.500000000 00	0.100000000 01	-0.480004600 00	-0.866343880-01	0.100000000 01
-0.525000000 00	0.100000000 01	-0.505004600 00	-0.909661080-01	0.100000000 01
-0.550000000 00	0.100000000 01	-0.530004600 00	-0.952978270-01	0.100000000 01
-0.575000000 00	0.100000000 01	-0.555004600 00	-0.996295470-01	0.100000000 01
-0.600000000 00	0.100000000 01	-0.580004600 00	-0.103961270 00	0.100000000 01
-0.625000000 00	0.100000000 01	-0.605004600 00	-0.108292990 00	0.100000000 01
-0.650000000 00	0.100000000 01	-0.630004600 00	-0.112624710 00	0.100000000 01
-0.675000000 00	0.100000000 01	-0.655004600 00	-0.116956420 00	0.100000000 01
-0.700000000 00	0.100000000 01	-0.680004600 00	-0.121288140 00	0.100000000 01
-0.725000000 00	0.100000000 01	-0.705004600 00	-0.125619860 00	0.100000000 01
-0.750000000 00	0.100000000 01	-0.730004600 00	-0.129951580 00	0.100000000 01
-0.775000000 00	0.100000000 01	-0.755004600 00	-0.134283300 00	0.100000000 01
-0.800000000 00	0.100000000 01	-0.780004600 00	-0.138615020 00	0.100000000 01
-0.825000000 00	0.100000000 01	-0.805004600 00	-0.142946740 00	0.100000000 01
-0.850000000 00	0.100000000 01	-0.830004600 00	-0.147278460 00	0.100000000 01
-0.875000000 00	0.100000000 01	-0.855004600 00	-0.151610180 00	0.100000000 01
-0.900000000 00	0.100000000 01	-0.880004600 00	-0.155941900 00	0.100000000 01
-0.925000000 00	0.100000000 01	-0.905004600 00	-0.160273620 00	0.100000000 01
-0.950000000 00	0.100000000 01	-0.930004600 00	-0.164605340 00	0.100000000 01
-0.975000000 00	0.100000000 01	-0.955004600 00	-0.168937060 00	0.100000000 01
-0.100000000 01	0.100000000 01	-0.980004600 00	-0.173268750 00	0.100000000 01

Figure B-3.   Continued.

CCNVERGENCE ATTAINED AFTER   4 ITERATIONS

RESULTS FOR X/C STATION 128   X = 0.49995420D 00

JOUKCWSKI AIRFOIL/A=0/RN=.21/FREE TRANSITION/N=.05/CEDDY=.03/

ETA	U/UDEL	F	Y/C	(U/UDEL)**2
0.100000000D 01	0.100000000D 01	0.986592130D 00	0.247436040D 00	0.100000000D 01
0.975000000D 00	0.100000000D 01	0.961592130D 00	0.241250130D 00	0.100000000D 01
0.950000000D 00	0.100000000D 01	0.936592130D 00	0.235064230D 00	0.100000000D 01
0.925000000D 00	0.100000000D 01	0.911592130D 00	0.228876330D 00	0.100000000D 01
0.900000000D 00	0.100000000D 01	0.886592130D 00	0.222692430D 00	0.100000000D 01
0.875000000D 00	0.100000000D 01	0.861592130D 00	0.216506530D 00	0.100000000D 01
0.850000000D 00	0.100000000D 01	0.836592130D 00	0.210320630D 00	0.100000000D 01
0.825000000D 00	0.100000000D 01	0.811592130D 00	0.204134730D 00	0.100000000D 01
0.800000000D 00	0.100000000D 01	0.786592130D 00	0.197948830D 00	0.100000000D 01
0.775000000D 00	0.100000000D 01	0.761592130D 00	0.191762930D 00	0.100000000D 01
0.750000000D 00	0.100000000D 01	0.736592130D 00	0.185577030D 00	0.100000000D 01
0.725000000D 00	0.100000000D 01	0.711592130D 00	0.179391130D 00	0.100000000D 01
0.700000000D 00	0.100000000D 01	0.686592130D 00	0.173205220D 00	0.100000000D 01
0.675000000D 00	0.100000000D 01	0.661592130D 00	0.167019320D 00	0.100000000D 01
0.650000000D 00	0.100000000D 01	0.636592130D 00	0.160833420D 00	0.100000000D 01
0.625000000D 00	0.100000000D 01	0.611592130D 00	0.154647520D 00	0.100000000D 01
0.600000000D 00	0.100000000D 01	0.586592130D 00	0.148461620D 00	0.100000000D 01
0.575000000D 00	0.100000000D 01	0.561592130D 00	0.142275720D 00	0.100000000D 01
0.550000000D 00	0.100000000D 01	0.536592130D 00	0.136089820D 00	0.100000000D 01
0.525000000D 00	0.100000000D 01	0.511592130D 00	0.129903920D 00	0.100000000D 01
0.500000000D 00	0.100000000D 01	0.486592130D 00	0.123718020D 00	0.100000000D 01
0.475000000D 00	0.100000000D 01	0.461592130D 00	0.117532120D 00	0.100000000D 01
0.450000000D 00	0.100000000D 01	0.436592130D 00	0.111346220D 00	0.100000000D 01
0.425000000D 00	0.100000000D 01	0.411592130D 00	0.105160320D 00	0.100000000D 01
0.400000000D 00	0.100000000D 01	0.386592130D 00	0.989744140D-01	0.100000000D 01
0.375000000D 00	0.100000000D 01	0.361592130D 00	0.927885130D-01	0.100000000D 01
0.350000000D 00	0.999999980D 00	0.336592130D 00	0.866026120D-01	0.999999960D 00
0.325000000D 00	0.999999980D 00	0.311592130D 00	0.804167120D-01	0.999999600D 00
0.300000000D 00	0.999998290D 00	0.286592150D 00	0.742304110D-01	0.999996590D 00
0.275000000D 00	0.999988130D 00	0.261592290D 00	0.680449100D-01	0.999976250D 00
0.250000000D 00	0.999931220D 00	0.236593100D 00	0.618590090D-01	0.999864480D 00
0.225000000D 00	0.999681260D 00	0.211597220D 00	0.556731080D-01	0.999362620D 00
0.200000000D 00	0.998756660D 00	0.186614460D 00	0.494872070D-01	0.997514860D 00
0.175000000D 00	0.995951530D 00	0.161674750D 00	0.433013060D-01	0.991919440D 00
0.150000000D 00	0.988921980D 00	0.136851840D 00	0.371154050D-01	0.977966680D 00
0.125000000D 00	0.974360090D 00	0.112291640D 00	0.309295040D-01	0.949377580D 00
0.100000000D 00	0.949511110D 00	0.882206730D-01	0.247436040D-01	0.901571140D 00
0.750000000D-01	0.914986670D 00	0.649985710D-01	0.185577030D-01	0.837200610D 00
0.500000000D-01	0.877081590D 00	0.425010700D-01	0.123718020D-01	0.769272120D 00
0.250000000D-01	0.846877810D 00	0.209802540D-01	0.618590090D-02	0.717202020D 00
0.0	0.835268683D 00	0.0	0.0	0.697704090D 00
-0.250000000D-01	0.846877810D 00	-0.209802540D-01	-0.618590090D-02	0.717202020D 00
-0.500000000D-01	0.877081590D 00	-0.425010700D-01	-0.123718020D-01	0.769272120D 00
-0.750000000D-01	0.914986670D 00	-0.649985710D-01	-0.185577030D-01	0.837200610D 00
-0.100000000D 00	0.949511110D 00	-0.882206730D-01	-0.247436040D-01	0.901571360D 00
-0.125000000D 00	0.974360090D 00	-0.112291640D 00	-0.309295040D-01	0.949377590D 00
-0.150000000D 00	0.988921980D 00	-0.136851840D 00	-0.371154050D-01	0.977966680D 00
-0.175000000D 00	0.995951530D 00	-0.161674750D 00	-0.433013060D-01	0.991919440D 00
-0.200000000D 00	0.998756660D 00	-0.186614460D 00	-0.494872070D-01	0.997514860D 00
-0.225000000D 00	0.999681260D 00	-0.211597220D 00	-0.556731080D-01	0.999362620D 00
-0.250000000D 00	0.999932240D 00	-0.236593100D 00	-0.618590090D-01	0.999864480D 00
-0.275000000D 00	0.999988130D 00	-0.261592290D 00	-0.680449100D-01	0.999976250D 00
-0.300000000D 00	0.999998290D 00	-0.286592150D 00	-0.742308110D-01	0.999996590D 00
-0.325000000D 00	0.999999980D 00	-0.311592130D 00	-0.804167120D-01	0.999999600D 00
-0.350000000D 00	0.999999980D 00	-0.336592130D 00	-0.866026120D-01	0.999999960D 00
-0.375000000D 00	0.100000000D 01	-0.361592130D 00	-0.927885130D-01	0.100000000D 01
-0.400000000D 00	0.100000000D 01	-0.386592130D 00	-0.989744140D-01	0.100000000D 01
-0.425000000D 00	0.100000000D 01	-0.411592130D 00	-0.105160320D 00	0.100000000D 01
-0.450000000D 00	0.100000000D 01	-0.436592130D 00	-0.111346220D 00	0.100000000D 01
-0.475000000D 00	0.100000000D 01	-0.461592130D 00	-0.117532120D 00	0.100000000D 01
-0.500000000D 00	0.100000000D 01	-0.486592130D 00	-0.123718020D 00	0.100000000D 01
-0.525000000D 00	0.100000000D 01	-0.511592130D 00	-0.129903920D 00	0.100000000D 01
-0.550000000D 00	0.100000000D 01	-0.536592130D 00	-0.136089820D 00	0.100000000D 01
-0.575000000D 00	0.100000000D 01	-0.561592130D 00	-0.142275720D 00	0.100000000D 01
-0.600000000D 00	0.100000000D 01	-0.586592130D 00	-0.148461620D 00	0.100000000D 01
-0.625000000D 00	0.100000000D 01	-0.611592130D 00	-0.154647520D 00	0.100000000D 01
-0.650000000D 00	0.100000000D 01	-0.636592130D 00	-0.160833420D 00	0.100000000D 01
-0.675000000D 00	0.100000000D 01	-0.661592130D 00	-0.167019320D 00	0.100000000D 01
-0.700000000D 00	0.100000000D 01	-0.686592130D 00	-0.173205220D 00	0.100000000D 01
-0.725000000D 00	0.100000000D 01	-0.711592130D 00	-0.179391130D 00	0.100000000D 01
-0.750000000D 00	0.100000000D 01	-0.736592130D 00	-0.185577030D 00	0.100000000D 01
-0.775000000D 00	0.100000000D 01	-0.761592130D 00	-0.191762930D 00	0.100000000D 01
-0.800000000D 00	0.100000000D 01	-0.786592130D 00	-0.197948830D 00	0.100000000D 01
-0.825000000D 00	0.100000000D 01	-0.811592130D 00	-0.204134730D 00	0.100000000D 01
-0.850000000D 00	0.100000000D 01	-0.836592130D 00	-0.210320630D 00	0.100000000D 01
-0.875000000D 00	0.100000000D 01	-0.861592130D 00	-0.216506530D 00	0.100000000D 01
-0.900000000D 00	0.100000000D 01	-0.886592130D 00	-0.222692430D 00	0.100000000D 01
-0.925000000D 00	0.100000000D 01	-0.911592130D 00	-0.228876330D 00	0.100000000D 01
-0.950000000D 00	0.100000000D 01	-0.936592130D 00	-0.235064230D 00	0.100000000D 01
-0.975000000D 00	0.100000000D 01	-0.961592130D 00	-0.241250130D 00	0.100000000D 01
-0.100000000D 01	0.100000000D 01	-0.986592130D 00	-0.247436040D 00	0.100000000D 01

Figure B-3. Continued.

CONVERGENCE ATTAINED AFTER   3 ITERATIONS

RESULTS FOR X/C STATION 157   X = 0.202983410 01

JOUKOWSKI AIRFOIL/A=0/RN=.21/FREE TRANSITION/M=.05/CEDDY=.03/

ETA	U/UDEL	F	Y/C	(U/UDEL)**2
0.100000000 01	0.100000000 01	0.99375446D 00	0.49857225D 00	0.100000000 01
0.975000000 00	0.100000000 01	0.96875446D 00	0.486107950 00	0.100000000 01
0.950000000 00	0.100000000 01	0.94375446D 00	0.473643640 00	0.100000000 01
0.925000000 00	0.100000000 01	0.91875446D 00	0.461179330 00	0.100000000 01
0.900000000 00	0.100000000 01	0.89375446D 00	0.448715030 00	0.100000000 01
0.875000000 00	0.100000000 01	0.86875446D 00	0.436250720 00	0.100000000 01
0.850000000 00	0.100000000 01	0.84375446D 00	0.423786420 00	0.100000000 01
0.825000000 00	0.100000000 01	0.81875446D 00	0.411322110 00	0.100000000 01
0.800000000 00	0.100000000 01	0.79375446D 00	0.398857800 00	0.100000000 01
0.775000000 00	0.100000000 01	0.76875446D 00	0.386393500 00	0.100000000 01
0.750000000 00	0.100000000 01	0.74375446D 00	0.373929190 00	0.100000000 01
0.725000000 00	0.100000000 01	0.71875446D 00	0.361464880 00	0.100000000 01
0.700000000 00	0.100000000 01	0.69375446D 00	0.349000580 00	0.100000000 01
0.675000000 00	0.100000000 01	0.66875446D 00	0.336536270 00	0.100000000 01
0.650000000 00	0.100000000 01	0.64375446D 00.	0.324071960 00	0.100000000 01
0.625000000 00	0.100000000 01	0.61875446D 00	0.311607660 00	0.100000000 01
0.600000000 00	0.100000000 01	0.59375446D 00	0.299143350 00	0.100000000 01
0.575000000 00	0.100000000 01	0.56875446D 00	0.286679050 00	0.100000000 01
0.550000000 00	0.100000000 01	0.54375446D 00	0.274214740 00	0.100000000 01
0.525000000 00	0.100000000 01	0.51875446D 00	0.261750430 00	0.100000000 01
0.500000000 00	0.100000000 01	0.49375446D 00	0.249286130 00	0.100000000 01
0.475000000 00	0.100000000 01	0.46875446D 00	0.236821820 00	0.100000000 01
0.450000000 00	0.100000000 01	0.44375446D 00	0.224357510 00	0.100000000 01
0.425000000 00	0.100000000 01	0.41875446D 00	0.211893210 00	0.100000000 01
0.400000000 00	0.100000000 01	0.39375446D 00	0.199428900 00	0.100000000 01
0.375000000 00	0.100000000 01	0.36875446D 00	0.186964600 00	0.100000000 01
0.350000000 00	0.100000000 01	0.34375446D 00	0.174500290 00	0.100000000 01
0.325000000 00	0.999999999D 00	0.31875446D 00	0.162035980 00	0.999999990 00
0.300000000 00	0.999999992D 00	0.29375446D 00	0.149571680 00	0.999999840 00
0.275000000 00	0.999999926D 00	0.26875447D 00	0.137107370 00	0.999998520 00
0.250000000 00	0.999994367D 00	0.24375453D 00	0.124643060 00	0.999988550 00
0.225000000 00	0.999963670 00	0.21875495D 00	0.112178760 00	0.999927350 00
0.200000000 00	0.99981114D-01	0.19375730D 00	0.99714451D-01	0.999622320 00
0.175000000 00	0.999195080 00	0.16876811D 00	0.87250144D-01	0.998390820 00
0.150000000 00	0.997185200 00	0.143808920 00	0.74785838D-01	0.994378320 00
0.125000000 00	0.991916260 00	0.11893588D 00	0.62321532D-01	0.983697870 00
0.100000000 00	0.98091440D 00	0.94261356D-01	0.49867225D-01	0.962193060 00
0.750000000D-01	0.962900060 00	0.69949989D-01	0.373929190-01	0.92717757D 00
0.500000000D-01	0.94050808D 00	0.46154516D-01	0.249286130-01	0.884555450 00
0.250000000D-01	0.92112122D 00	0.22900051D-01	0.124643060-01	0.848464300 00
0.0	0.91336160D 00	0.0	0.0	0.83423774D 00
-0.250000000D-01	0.92112122D 00	-0.229000510-01	-0.124643060-01	0.848464300 00
-0.500000000D-01	0.94050808D 00	-0.461545160-01	-0.249286130-01	0.884555450 00
-0.750000000D-01	0.962900060 00	-0.69949989D-01	-0.373929190-01	0.92717757D 00
-0.100000000 00	0.98091440D 00	-0.94261356D-01	-0.498572250-01	0.962193060 00
-0.125000000 00	0.99191626D 00	-0.11893588D 00	-0.62321532D-01	0.983897870 00
-0.150000000 00	0.99718520D 00	-0.14380892D 00	-0.74785839D-01	0.994378320 00
-0.175000000 00	0.99919508D 00	-0.16876811D 00	-0.87250144D-01	0.998390820 00
-0.200000000 00	0.99981114D 00	-0.19375730D 00	-0.99714451D-01	0.999622320 00
-0.225000000 00	0.999963670 00	-0.21875495D 00	-0.112178760 00	0.999927350 00
-0.250000000 00	0.999994280 00	-0.24375453D 00	-0.124643060 00	0.999988550 00
-0.275000000 00	0.999999926D 00	-0.26875447D 00	-0.137107370 00	0.999998520 00
-0.300000000 00	0.999999920 00	-0.29375446D 00	-0.149571680 00	0.999999840 00
-0.325000000 00	0.999999999D 00	-0.31875446D 00	-0.162035980 00	0.999999990 00
-0.350000000 00	0.100000000 01	-0.34375446D 00	-0.174500290 00	0.100000000 01
-0.375000000 00	0.100000000 01	-0.36875446D 00	-0.186964600 00	0.100000000 01
-0.400000000 00	0.100000000 01	-0.39375446D 00	-0.199428900 00	0.100000000 01
-0.425000000 00	0.100000000 01	-0.41875446D 00	-0.211893210 00	0.100000000 01
-0.450000000 00	0.100000000 01	-0.44375446D 00	-0.224357510 00	0.100000000 01
-0.475000000 00	0.100000000 01	-0.46875446D 00	-0.236821820 00	0.100000000 01
-0.500000000 00	0.100000000 01	-0.49375446D 00	-0.249286130 00	0.100000000 01
-0.525000000 00	0.100000000 01	-0.51875446D 00	-0.261750430 00	0.100000000 01
-0.550000000 00	0.100000000 01	-0.54375446D 00	-0.274214740 00	0.100000000 01
-0.575000000 00	0.100000000 01	-0.56875446D 00	-0.286679050 00	0.100000000 01
-0.600000000 00	0.100000000 01	-0.59375446D 00	-0.299143350 00	0.100000000 01
-0.625000000 00	0.100000000 01	-0.61875446D 00	-0.311607660 00	0.100000000 01
-0.650000000 00	0.100000000 01	-0.64375446D 00	-0.324071960 00	0.100000000 01
-0.675000000 00	0.100000000 01	-0.66875446D 00	-0.336536270 00	0.100000000 01
-0.700000000 00	0.100000000 01	-0.69375446D 00	-0.349000580 00	0.100000000 01
-0.725000000 00	0.100000000 01	-0.71875446D 00	-0.361464880 00	0.100000000 01
-0.750000000 00	0.100000000 01	-0.74375446D 00	-0.373929190 00	0.100000000 01
-0.775000000 00	0.100000000 01	-0.76875446D 00	-0.386393500 00	0.100000000 01
-0.800000000 00	0.100000000 01	-0.79375446D 00	-0.398857800 00	0.100000000 01
-0.825000000 00	0.100000000 01	-0.81875446D 00	-0.411322110 00	0.100000000 01
-0.850000000 00	0.100000000 01	-0.84375446D 00	-0.423786420 00	0.100000000 01
-0.875000000 00	0.100000000 01	-0.86875446D 00	-0.436250720 00	0.100000000 01
-0.900000000 00	0.100000000 01	-0.89375446D 00	-0.448715030 00	0.100000000 01
-0.925000000 00	0.100000000 01	-0.91875446D 00	-0.461179330 00	0.100000000 01
-0.950000000 00	0.100000000 01	-0.94375446D 00	-0.473643640 00	0.100000000 01
-0.975000000 00	0.100000000 01	-0.96875446D 00	-0.486107950 00	0.100000000 01
-0.100000000 01	0.100000000 01	-0.99375446D 00	-0.49857225D 00	0.100000000 01

Figure B-3.   Continued.